Developing a cell surface display system for

C. necator H16

University of Sheffield

Department of Chemical and Biological Engineering

Supervisors: Dr. Tuck Seng Wong, Dr. Kang Lan Tee

A thesis submitted for the degree of Doctor of Philosophy

Melvin Mikuzi

15/10/21

The University Of Sheffield.

Acknowledgements

I would like to express my gratitude for the immeasurable amount of support provided by my family over the duration of this PhD. Without them, completion of this journey would not have been possible. I would also like to thank my girlfriend Emily Lambert for her support and encouragement.

I would also like to thank Dr. Wong as my primary supervisor, whose lab and expertise have made it possible for me to complete this work.

I would also like to give special thanks to Dr Kang Lan Tee with whom I worked with closely over the first 2 years of my PhD. She offered guidance support and was instrumental in teaching me several important skills both in and outside the lab that I am sure will help me in the future.

I would also like to thank many of the students in the Wong group who I got to interact with as part of my stay at Sheffield, specifically Robert and Valériane who provided support, friendship and scientific insight have most definitely had an invaluable effect on my work.

Declaration

This thesis and the data present in it is a product of original research conducted by me in the Department of Chemical and Biological Engineering, at The University of Sheffield. All sources of information presented in this work have been accordingly referenced. This thesis has never been previously submitted at this University or any other institution. Parts of this work take from my confirmation review submitted 15/10/18.

Contents

List of Figures

List of Tables

Summary

Carbon capture and utilisation has long since been a focal point of synthetic biology. Waste carbon can be utilised to manufacture fuel, chemicals, and other bioproducts. Using microorganisms as biorefineries for carbon utilisation is one of the ways that this can be achieved in synthetic biology. *Escherichia coli* is a model organism for these types of biological applications. It has been used as the scaffold for systems that demonstrate the ability of microorganisms to be used as biological tools. However, as our understanding of metabolic pathways and systems has increased, more organisms have been discovered to possess desirable traits that do not exist within *E. coli*, specifically those that could be implicated in efficient carbon capture and utilisation processes.

Cupriavidus necator, is an organism that has been the subject of interest due to its native metabolic qualities. In the context of using microorganisms as tools for carbon utilisation, *C. necator* H16 is superior to *E. coli* fundamentally because of the presence of some of these metabolic pathways. *C. necator* H16 is well known for its ability to metabolise carbon into polyhydroxy butyrate (PHB), a polymer that can be used to produce biodegradable bioplastics. The PHB is produced by *C. necator* H16 as a response to stress induced through nutrient deficient growing conditions. *C. necator* H16 is a prime candidate for "building" an organism that can utilise waste carbon to produce a bioproduct.

The final goal of this project alongside a collection of other work, is to use *C. necator* H16 as a biorefinery that can use many different carbon sources for growth and accumulation of PHB. It can become a modular framework for a system that can be changed dependent on the carbon feedstock, allowing it to degrade complex waste carbon, in a range of conditions, while still being able to metabolise the carbon into a high value product.

This work aims to develop such a cell surface display system for *C. necator* H16.

1. Introduction and assessment of literature

1.1. Carbon waste management

Carbon dioxide emissions from fossil fuels has been steadily increasing over the past 20 years and has become a rising concern due to the environmental impact of the greenhouse effect that is created by these emissions. As a result of this, many industrial, and commercial sectors have been tasked with reducing their carbon footprint. However, for many industries, the goals set by the government are challenging. With tight short-term targets and little room for large investment, the field of carbon capture has almost become a central part of bioprocessing and biotechnology.

Carbon capture and utilization methods are going to be necessary in combating this problem and reducing the overall carbon footprint and total carbon emissions. Some of these technologies have already generated interest in these industries as long-term solutions to greenhouse gas mitigation. Combining these systems also has the potential to create systems that can generate value out of the waste carbon that is generated by these industries, giving them more financial incentive to invest and utilise said solutions.

Carbon capture revolves around the concept that carbon waste streams can be used as feedstocks to produce other high value carbon-based products and is largely what the work we have pursued in this lab has revolved around.

As shown in ***Figure* 1**, the sheer amount of carbon waste that is generated by the US alone in a single year is astronomical, with several million tonnes of carbon being generated by transportation, agriculture, and energy generation. Due to the sheer enormity of these values, being able to employ carbon capture and utilization technologies will be invaluable in the future.

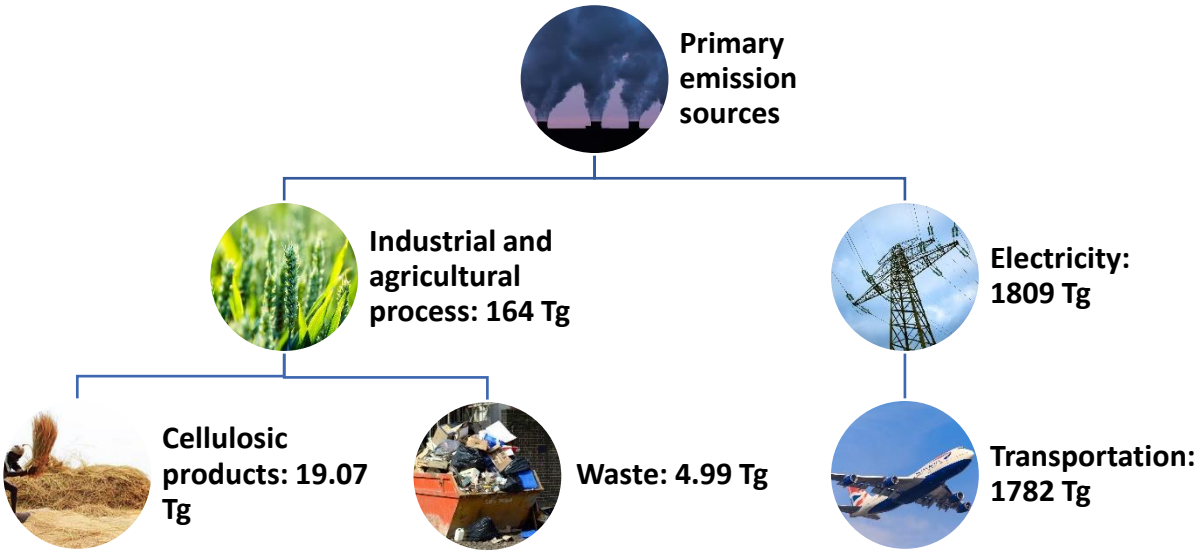

Figure 1 *Breakdown of US carbon emissions as one of the primary contributors to global carbon emissions in 2016. 1 Tg = 1 million tonnes. Figure formulated from data provided from* ("Gaseous Carbon Waste Streams Util.," 2019)

1.1.1. Plastics

Despite the value being a small percentage of total carbon emissions, a large amount of carbon waste is generated via the production of waste. As it stands, many of the carbon waste streams that contribute to this problem require specialised treatment, namely plastics. Plastics are a common carbon-based waste product that is generated on a large scale. As such, a substantial amount of research has been spent elucidating methods that can either allow for the efficient recycling of plastic-based products or, optimizing the production of biodegradable analogues that can be used in place of current plastics that do not lend themselves towards such processes.

According to some of the most recent statistics regarding the production of plastic, nearly 350 million tons of plastic was produced globally in 2018 (Association of Plastics manufacturers, 2018). As the utilisation of plastics increases, there is a proportionate growth in the production of plastic waste. Experts cite that 26 billion tons of plastic waste will have been generated by the year 2050 and a significant proportion of this will end up in landfills (Jambeck *et al.*, 2015). To prevent some of these plastics entering and disrupting ecological environments, it is imperative that methods are developed to combat the production and processing of these plastics.

This can be directly observed by looking at the way petroleum-based plastics have been integrated into several different processes and products. The main drawback of these plastics is their environmental impact. The lack of biodegradability and their toxicity within systems that cannot process them makes these plastics severely problematic in tandem with the fact that they are being produced and disposed of in such high quantities. Biodegradable plastics combat many of the issues that are posed by petrochemical based plastics, and these can often be produced using renewable carbon sources.

A closer look at the different types of commonly used plastics illustrates their prevalence within industrial and commercial markets. Plastics have evolved to become synonymous with many of these industries. As the implications of having this plastic waste enter the environment began to become clear, a move towards developing systems to recycle plastics was made. As a result, many of the plastics we now utilise are recyclable (***Table 1***).

Table 1 *Brief summary of some of the most common plastics produced and used. Specialised use cases are highlighted as well as important characteristics of each type of plastic. The recyclability and biodegradability of the plastics is also shown*

Name	Comments	Recyclable	Biodegradable
Acrylic	This strong, plastic is very transparent, and is often utilised in optical devices.	Yes	No
Polycarbonate	Extremely high strength and transparency allows it to be used in both industrial and optical solutions.	Yes	Yes
Polyethylene	This plastic has low-density and high-density variants.	Yes	Some polyethylene films are biodegradable, but can take decades to do so
Polyethylene Terephthalate	Most widely used plastic globally, often used for producing beverage bottles.	Yes	No
Polyvinyl chloride	Frequently used in construction for plumbing, insulation.	No	No
Acrylonitrile-Butadiene-Styrene	Often used as a substrate in injection moulding due to its low melting temperature. Very popular for 3D printing.	Yes	No
Polypropylene	Used for a wide variety of applications and products.	Yes	No

	due to its chemical resistance, elasticity, toughness, and fatigue resistance. Can function as a plastic and a fibre.		
Polystyrene	Commonly associated with packaging protection.	Yes, but is not commonly recycled due to the lack of investment in the equipment required	No
Polylactic acid	Often used to package food products.	Yes	Yes, but not easily done due to the high melting point
Acetal, (polyoxymethylene)	Used in applications where high stiffness and low co-efficient of friction is required. Frequently used in the automotive industry and for high performance components.	Yes	No
Nylon	Fibre used in the production of many clothing products.	Yes	No

While carbon dioxide is a pertinent contributor to carbon waste, there are many other areas in which carbon waste is introduced. A large percentage of waste carbon is sequestered in land and in soils, while smaller amounts are released from non-biogenic processes. This demonstrates the large reserves of untapped carbon sources that are all potential feedstocks to produce biofuels and chemicals. Carbon capture systems that have been integrated into industrial processes that produce high volumes of carbon dioxide are effective at capturing carbon, but still require large amounts of infrastructure, energy, and money for them to function. Processes such as post combustion carbon capture, and oxyfuel (Spigarelli and Kawatra, 2013) are all useful tools for preventing carbon dioxide from entering the atmosphere, however, the carbon is processed and then needs to be transported and then geo-sequestered. Each step of the process will have its own carbon output and largely, the processes are only applicable to very specific types of carbon waste streams.

While all this carbon is liberated, many have come to see that utilising this carbon and repurposing it into high value products is a means of economically addressing carbon dioxide emissions both directly (carbon capture systems that utilize carbon dioxide released into the atmosphere) and indirectly (using waste carbon to produce high value products, reducing the cost of the measures put in place for carbon capture and utilisation.

The use of modular biological systems through the advent of synthetic biology and biotechnology, is proving to be a method that can seamlessly integrate its way into the current carbon capture infrastructure, but with significant reductions in cost and carbon footprint.

Bacteria and other microorganisms can effectively be used as a means of metabolising carbon dioxide and other waste carbon into useful products. In doing this, integrating a bio-based carbon utilisation system into a carbon waste stream can become lucrative. As is clear from the reports, there is a large amount of carbon that can be provided for such systems. Consequently, it becomes obvious that there is a need for the development of a methodology that can provide a means of efficient carbon utilisation.

1.1.2. Cellulosic waste

A separate but equally important carbon waste stream is cellulosic waste. This type of carbonic waste poses a significantly lower issue regarding its threat to the environment, it can be seen as a huge potential feedstock to produce energy. This can be facilitated by combustion, or fermentation of the feedstock into other biofuels and products.

Paper, wood, and crop residues are the primary constituents of cellulosic waste in our society, and the production of this type of waste is estimated to be near 900 million tonnes per year for the EU alone. (Searle & Malins, 2013) Due to the nature of these products, these waste streams often find themselves naturally being allocated towards other uses particularly in agriculture, or in repurposing the waste into new products. Examples include using sawdust from wood milling to produce animal bedding and fibreboard. These types of biodegradable wastes can also easily be returned to nature and play a key role in environmental sustainability.

Due to these facts, it is important to note that if a significant portion of this waste is funnelled into other waste processing streams, there could be downstream effects on industry and the environment. However, with that in mind, analysis of the current usage shows us that about 25% of the current production of cellulosic waste is available to use for new endeavours such as renewable energy projects.

Table 2 *Present and future production and distribution of waste.* (Searle & Malins, 2013)

Category	**Subcategory**	**Current availability (Mtonnes/yr)**	**2030 Availability (Mtonnes/yr)**
Waste	Paper	17.5	12.3
	Wood	8	5.6
	Food and garden	37.6	26.3
Crop residues		122	139
Forestry residues		40	40

Sum	225	223

1.1.3. Using microbial systems for carbon recycling

To combat some of the issues faced by the growing problem of the accumulating carbon waste, the use of microbial systems has been employed for their natural capability to turn different types of carbon sources into a variety of different carbon substrates into a variety of metabolites. Most of these metabolites can then go on to facilitate the growth of the organism, but others can be engineered to produce specific products.

When it comes to the specific usage of cellulosic waste utilisation as a feedstock for microorganisms, a popular methodology employs the mesophilic wood fungus *Trichoderma reesei*, an organism well characterized for high secretion yield of cellulolytic enzymes. These enzymes exist primarily as 3 different components of a system that breaks down the complex cellulose crystalline system. The enzymes are cellobiohydrolases (CBH) endoglucanases, and beta glucosidases. A collection of enzymes is used to break down cellulose as the different enzymes contain different affinities for polymers of different size. They also are different in their ability to degrade cellulose either from the distal ends of a chain or their ability to make cleavages in the middle of the polymer.

These enzymes can exist in different forms depending on the organism that utilises the metabolic pathway. In terms of organism that have been isolated for use in biofuel production from cellulosic waste, we can see secreted cellulolytic enzymes from organisms like *H. jecorina* have been engineered to function at higher temperatures. (Goedegebuur, et al., 2017)

Of course, many of the existing CBH systems that exist in nature may also perform these processes with more complex systems such as the bifunctional CelA protein of *Caldicellulosiruptor bescii.* This system employs a processive endoglucanase, two family 3 carbohydrate-binding modules (CBM3), and a C-terminal exo-β-1,4-glucanase domain all in a single protein complex. This complex is then secreted into the media as a means of degrading extracellular cellulose. However, there are some drawbacks to localising these enzymes to a specific system, as free enzymes can work in a synergistic fashion, to effectively break down the crystalline structure of cellulose by being able to break down the parts with the highest affinity for their specific substrates.

1.1.4. Production of bioethanol

One of the most established and characterised organisms used in the process of producing biofuel is *Zymomonas mobilis*. *Z. mobilis* is a gram-negative organism is well known for its production of bioethanol under several detrimental environments. The organism has an unusually high tolerance for ethanol during the fermentation stage, allowing for higher yields to be obtained (Antoni, Zverlov and Schwarz, 2007).

The preferred substrates for this organism are glucose, fructose, and the disaccharide of the former, sucrose. These sugars can enter the Entner-Doudoroff pathway (a pathway implicated in the metabolism of pyruvate using glucose as the primary metabolite), and are metabolised into pyruvate, and ultimately ethanol and carbon dioxide. Some work has been done to try and expand the substrate range of this organism outside of that of these few hexose sugars, with varying degrees of success (Sarkar *et al.*, 2020). Similar work has also been done to try and overcome the problems that come with the production of inhibitive compounds produced in lignocellulosic lysate such as furfural and aliphatic acids (Wang *et al.*, 2018), Chang et al., 2018, K. Zhang et al., 2019, Jönsson et al., 2013)

Another common organism used to produce bioethanol is *Saccharomyces cerevisiae.* This yeast has been used for the fermentation of ethanol in for human consumption. This likely was the most logical organism to be used in the production of ethanol for use as a biofuel. Yeasts like *S. cerevisiae* offer a different range of benefits over other bacterial systems for bioethanol production such as Z. *mobilis* include its high pH tolerance, and a lower susceptibility to contamination (Lee *et al.*, 2010). This can be invaluable in saving money and allowing biofuel production to become more financially viable as a means of carbon capture.

Much like *Z. mobilis,* there has been significant effort put towards the optimisation of yeast systems to produce bioethanol. One of the primary ways that this has been done is by expanding the number of strains that can be used for this process. Studies found that a wide array of other yeasts can overcome the different challenges faced when it comes to using *S. cerevisiae*(Mohd Azhar *et al.*, 2017). These include issues such as the inability of the organisms to metabolise pentose sugars, tolerance of high

temperatures and the inhibitive nature of growing the cells in high concentrations of ethanol (Mohd Azhar *et al.*, 2017).

Consolidative bioprocessing is another system that currently exists as a means of producing biofuels from recalcitrant cellulose. The bacteria *Clostridium thermocellum* is one of the best organisms used in this area due to its cellulolytic nature, and efficient processing of sugars into ethanol (Akinosho *et al.*, 2014). However, there are a few limitations posed by this organism when it comes to ethanol production. Examples include low yield, and an inability to be cultured at high temperatures, and the cells relatively low tolerance of ethanol in the extracellular environment(Akinosho *et al.*, 2014). As such, some of these issues have also been synthetically improved through engineering key rate limiting enzymes such as and PDC (Pyruvate decarboxylase) (Kannuchamy, Mukund and Saleena, 2016) to either function at higher temperatures or introducing new recombinant proteins such as ADH (alcohol dehydrogenase) to increase the tolerance of ethanol (Tian *et al.*, 2019).

Many of the pathways for biofuel production have been engineered to allow the use of cellulosic waste as a carbon waste stream to be used as a feedstock, however, regarding carbon recycling, there are still other methods that can be utilised for processing other carbon waste streams, not necessarily into valuable products. An excellent example of how this may work in practice is by shifting the focus away from biofuels. There is a propensity to associate biofuel production with cellulosic waste streams; however, microorganisms can also be used as a means of targeting different carbon sources such as plastics and even carbon dioxide produced from industrial processes (see ***Figure* 2**).

Studies have shown that several organisms have evolved to be able to degrade plastics such as polyethylene due to its presence in different environments. These have been isolated from landfill sites (Orr, Hadar and Sivan, 2004) , marine environments (Harshvardhan and Jha, 2013), and the digestive system of complex organisms such as the waxworm that occupy soil that contain polyethylene films (Yang *et al.*, 2015). However, this is still a relatively new area of work and as such, while many organisms have been identified as being capable of degrading some of these plastics, further analysis shows that a limited number of enzymes are implicated in the process. As far as we know, the degradation of complex plastics such as that of polyethylene films is facilitated by several peroxidases

and potentially some laccase homologue proteins. However, while we know that these enzymes are required for the degradation, their mechanism for the process are yet to be elucidated. It is likely that the generation of radicals and reactive oxygen species plays a crucial role in polyethylene degradation seeing as UV radiation is known to catalyse this process.

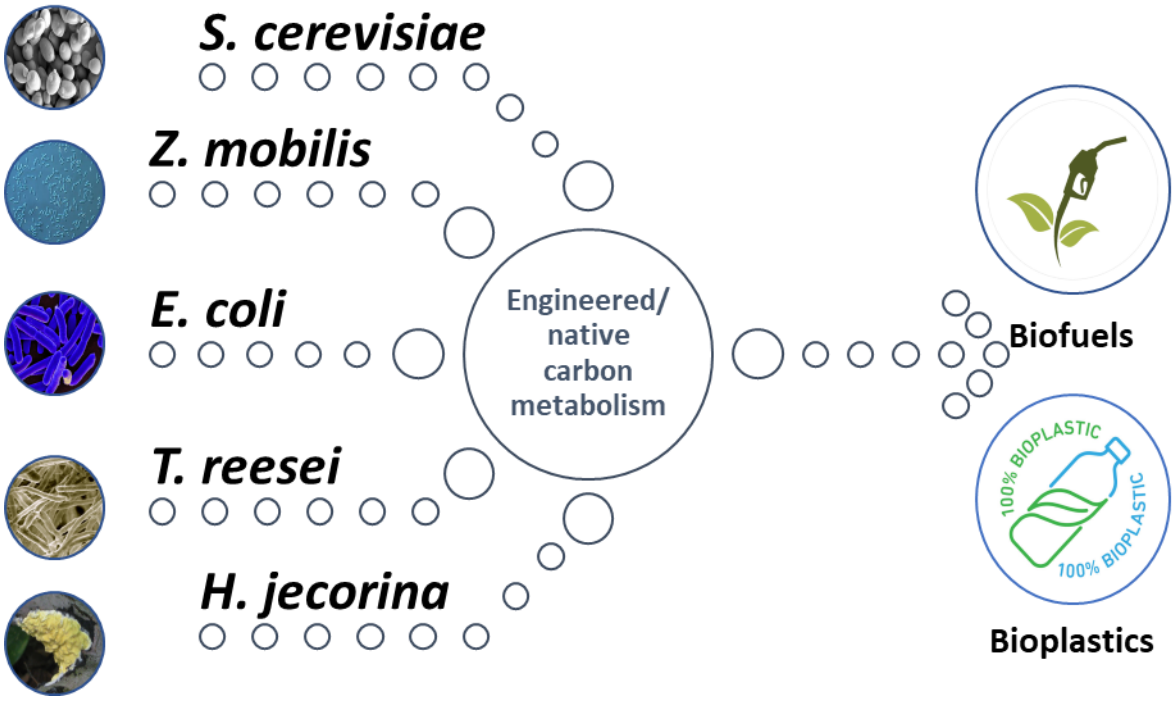

Figure 2 *Many organisms have been isolated and engineered to take advantage of the fact that they can be used as a means of recycling carbon from a wide variety of carbon sources and repurposing them into high value products such as bioplastics and biofuels. Each system has a range of metabolic tools and preferred conditions that allow for a wide range of carbon utilization to be facilitated by biological processes.*

Because many different plastics are introduced to the environment in a similar way, we can observe similar patterns in which a multitude of different organisms evolve pathways to facilitate in the degradation and valorisation of many of these waste products. However, due to our rudimentary understanding of the way in which these systems work, it is a challenging prospect to see how we are going to integrate the use of these microorganisms into systems that allow for the controlled and rapid recycling or degradation of waste plastics. As it stands, increasing the enzymatic efficiency requires a two-pronged approach to overcome the resilient cross linked crystalline structure of plastics, while also using other methods such as directed evolution to improve the performance of the enzymes.

That in mind, the challenges that are faced here in the removal of normal plastics does mean that there is a clear demand to produce bioplastics that lend themselves to biological degradation.

1.2. Cupriavidus necator

To tackle the aforementioned problems, the ideology behind much of our labs' work revolves around the overarching goal of producing a microbial system which is capable of degrading a range of carbon waste streams. This carbon can then be repurposed towards renewable energy systems, or can directly combat the issue of plastic waste, by producing bioplastic precursors. At the heart of a system like this would be a modular biorefinery, an organism equipped with all the necessary tools to systematically and autonomously do all of these tasks when provided with complex mixed waste streams, allowing for minimal input from human beings. To achieve a system like this requires a great deal of critical analysis assessing the different microbial candidates, seeing what they each bring to the table, and *Cupriavidus necator* stands out as a great option for several key reasons.

1.2.1. History

Cupriavidus necator was first discovered in the early 1900's when several different bacteria had been discovered for their innate ability to utilise hydrogen as an energy source. Later, the first isolates of the organism were cultured in 1962 when the growth characteristics of the then *Hydrogenomonas eutropha* where being characterised. As early as this, it was identified that the organism could grow using carbon dioxide as its primary carbon source, and that the viability of growth was heavily influenced by the presence of ferrous iron (Repaske, 1962). This early work would then go on to pave the way to understand the functionality of iron in the nickel-iron hydrogenases that give the organism its lithotrophic abilities (Repaske, 1962).

As more information was divulged about the inner workings of the organism, the nomenclature of the needed to evolve to make it more distinct from the other hydrogen lithotrophs that were coming to light in the mid to late 20th century. Here the Hydrogenomonas genus was challenged by Mandel et. al, as it was argued that the autotrophic growth using H_2 was no longer sufficient to allow for us to distinguish clearly between the then 56 existing strains of bacteria (Davis *et al.*, 1969). It was here that the new name alcaligenes eutropha was given to the organism, with a more formal definition of the morphology,

and clearly defined distinguishing features, namely the pigmentation and flagellar arrangement. This paper also formalised the genus *Pseudomonas*(Davis *et al.*, 1969).

Further investigation into other phenotypical attributes of the organisms had its name again be changed into Ralstonia eutropha (Yabuuchi *et al.*, 1995). However, this was found to be redundant due to the fact Ralstonia eutropha biologically identical to an existing species *C. necator* H16.

1.2.2. Metabolism

One of the key distinctions about *C. necator* H16 that makes it such an apt scaffold for a system such as this is its capability to naturally metabolise a variety of carbon sources, while simultaneously functioning as a chemolithoautotroph. It can grow on mixtures of H_2 and CO_2 or, on other sugar sources. It can then utilise CO_2 by integrating it into the Calvin–Benson–Bassham (CBB) cycle. This synergises with the idea that we would like to create an autonomous system that functions in a range of environments.

C. necator H16 is an attractive chassis for metabolic engineering for carbon bioconversion to high value metabolites. As more studies have been conducted, it has continued to grow as one of the most advanced genetic systems for this purpose (Müller *et al.*, 2013).

However, the most critical of the metabolic features of *C. necator* H16 is the native biosynthetic pathway to produce poly[(R)-3 hydroxybutyrate] (PHB) (see **Figure 3**), a carbon dense molecule that is stored intracellularly in granular form. This is a high value polymer that can be used to produce bioplastics. There have been reports that cite titres of accumulated PHB that exceeded 70% of the total biomass by dry weight (Mravec *et al.*, 2016). This is facilitated by the redirecting carbon flux from the central carbon metabolism into polyhydroxy alkanoate (PHA) synthesis pathway. The PHB production of *C necator* H16 is a highlight of the organism because it leads quite smoothly into the functionality that is necessary to create a working microbial biorefinery.

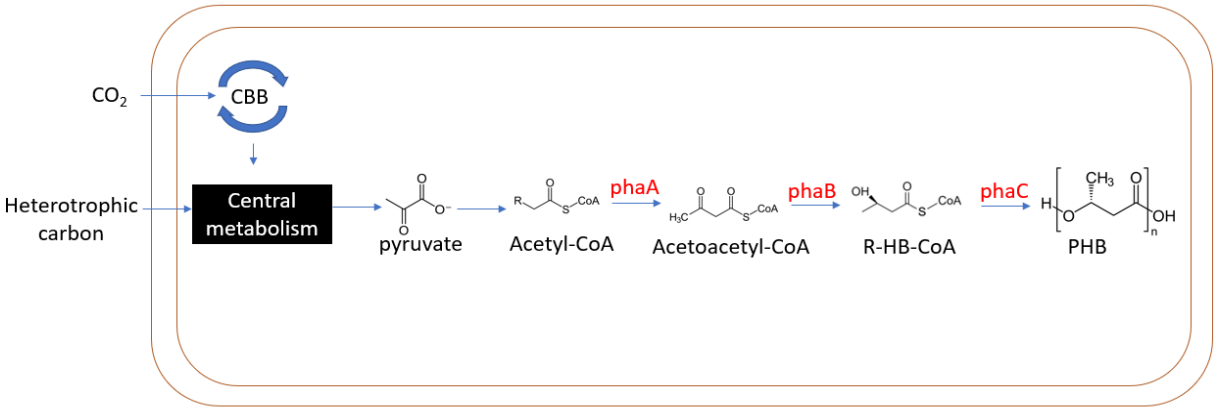

Figure 3 *Carbon flux from both CO_2 and heterotrophic carbon sources (gluconate, formate, etc) into PHB facilitated by the PHA synthase enzymes phaA, phaB, and phaC.*

The organism can utilise an extensive variety of carbon sources such as starch (Haas, Jin and Zepf, 2008) and fatty acids (Riedel *et al.*, 2014). In addition to this, *C. necator H16* is capable of utilising carbon dioxide as a primary carbon source. Here, carbon dioxide and formate can enter the CBB cycle. The carbon dioxide is fixed via 4 different hydrogenases and RuBisCo (ribulose-1,5-bisphosphate carboxylase). The hydrogenases' role is to catalyse the oxidation of hydrogen to generate electrons and form [H]+ ions. These enzymes also have differing subcellular localisation with the existence of the membrane bound hydrogenase being found in the inner membrane and the others being found in the cytosol. The membrane bound is responsible for the delivery of the liberated protons of the electron transport chain of *C. necator* H16 as well as the B-Type cytochrome, which facilitates the process of energy production. Meanwhile the soluble hydrogenase is responsible for delivery of [H]+ ions and electrons to NAD+ for the formation of NADH which is utilised in a wide array of biological processes. The third hydrogenase plays a role in the detection of [H]+ and is implicated in the regulation and expression of the previous two hydrogenases. The final hydrogenase Hyd4 remains largely uncharacterised with its function yet to be fully elucidated (Li *et al.*, 2020).

However, despite this fascinating capability of *C. necator* H16 to utilise CO_2 as a carbon source, it is incapable of using many common carbohydrates and sugars. The most notable of these is the inability to metabolise glucose. However, there have been reports detailing the organisms' ability to metabolise some sugars that can easily be incorporated into the central carbon metabolism such as fructose,

gluconate and xylose (Alagesan, Minton and Malys, 2018). It is interesting to note that the key factor preventing the organism from utilising glucose as a carbon source is not in fact a lack of the molecular machinery but because the organism does not have a means of assimilating glucose at a rate that is high enough to support growth (Sichwart *et al.*, 2011). The necessary transporters are present within the genome of *C. necator H16 but* are not expressed enough to allow glucose to be used as a means of reliable growth (Orita *et al.*, 2012).

When thinking about how *C. necator* H16 can be exploited given these native metabolic systems, PHB is a key metabolite as this product is a prerequisite molecule to different types of new age bioplastics. Several publications have investigated the integration of PHAs into standard plastic manufacturing, but to understand how this is possible, we must take a short look at the molecular structure of PHB and understand how it can be used as a plastic.

1.2.3. PHB

The monomer units of any PHA are classified based on the number of carbon atoms present on the primary carbon chain that makes up the repeating monomer. The length and structure of the monomer determines the polymer properties, as such, this information is used when targeting specific properties of the polymer. A short-chain length PHA (scl-PHA) comprises of 3–5 carbon atoms. The scl-PHA materials have thermoplastic properties like that of polypropylene

The properties of PHB allow it to be used in a variety of different settings. Its biocompatibility and biodegradability allow the plastic to be used for many different biomedical applications such as tissue engineering scaffolds, controlled release of drugs, sutures, and other structural supports in the human body. This is partly since that it degrades *in vivo* to d-3-hydroxybutyric acid, a normal constituent of human blood. These properties also make it particularly useful for encapsulation of agricultural products such as fertilizer, or as means of packaging food. The biodegradable nature of PHB also lends itself to being a great replacement for plastics used for disposable items such as bags, bottles, and film packaging.

The PHB produced directly from *C. necator* H16 is naturally quite stiff and crystalline. To expand the application of the PHB, it is often co polymerized with other monomers that alter the mechanical and thermal properties. The most common copolymer used is 3 hydroxyvalarate, which is incorporated into PHB to create a plastic that has a lower melting temperature, which is more flexible and less brittle. The resulting copolymer P(3HB-co-3HV) lends itself to easier injection moulding, extrusion, and other already existing plastic manufacturing methods.

1.3. Cell surface display in nature and synthetic biology

Extracellular surface display of proteins is an important feature of single celled organisms. In mammalian cells, such proteins mediate many key processes. These include signal transduction, the maintenance of membrane integrity, and adhesion (Pizzaro-Cerda & Cossart, 2006). In bacteria, many membrane-bound proteins are implicated in similar processes. The family of outer membrane proteins (OMPs) in gram negative bacteria, have been characterised as important proteins that interface with the extracellular environment. Proteins such as OmpA, OmpC and OmpF and their homologues have been found to be present in high concentrations in the cell membrane of *E. coli*, and other gram-negative organism, suggesting they are involved in many processes (Uemura & Mizushima, 1975). These outer membrane proteins are involved in the translocation of a range of small hydrophobic molecules as well as mediating virulence and acting as adhesion molecules. Many of these proteins have also been identified as receptors for bacteriophages (Morona, et al., 1984).

Many synthetic systems have been developed that attempt to introduce new metabolic capabilities to the cells via the extracellular display of proteins. This has allowed for new methodologies to be explored for the development of other systems. The first real application of cell surface display was to create peptide screening libraries to identify antigenic epitopes for use in vaccine development (Westerlund-Wikström, 2000). Systems such as these later paved the way for the more sophisticated system. It became possible to transport specific antigens on non-pathogenic carriers, exposing them to the immune system in a non-hazardous format (Rutherford and Mourez, 2006). For many years, this was the intended goal of many engineered cell surface display systems. However, as time has progressed, more uses have been found for this technology (Lee, Choi and Xu, 2003).

Cell surface display (CSD) systems have found their use in bioremediation, as biocatalysts, and as molecular tools for basic research. Such systems have been developed for more organisms, that support larger proteins, and as a result, CSD has become commonplace in the study and development of biological systems.

1.3.1. Application in industry

Using cells as enzyme scaffolds has proven to be a powerful tool in synthetic biology. Due to the current drive to utilise more carbon neutral sources of energy, there have been significant steps forward in using biotechnology to achieve these means. CSD systems are being used in this area through the cell meditated degradation of lignocellulosic mass. Lignocellulosic materials have been identified as a cheap, environmentally friendly carbon feedstock that can be used for the synthesis of bio-based chemicals, precursors, and liquid biofuels (Pal and Paul, 2008) ,(Vinet and Zhedanov, 2010b). The main issue is that lignocellulosic matter is difficult to degrade efficiently without the use of expensive chemical processes. Enzymatic process can be employed for the saccharification and fermentation of the biomass, but current technologies utilise large amounts of enzyme, while also taking a significantly long time. Cellulase displaying yeast strains have been developed as whole cell biocatalysts for the degradation and fermentation of lignocellulosic biomass. There have been forays into using different glycosidic enzymes to enable the formation of different biofuels. These enzymes can be displayed and anchored using α-agglutinin. By developing co-displaying systems, the complex procedure required for cellulose degradation can be made a simpler, and faster process (Chen, 2017).

Rising environmental concerns have led to an increasing demand for sustainable systems that are able to keep waste and pollution production at a minimum. There are tangible failings in some of the current systems put in place for the removal of dangerous waste contaminants such as heavy metals. We have long since been aware of many proteins capable of binding heavy metals and CSD offers a means of using those enzymes as a means of removal. This exact strategy was employed by (Kotrba *et al.*, 1999) when they utilised *E. coli* as a host for extracellularly displayed metallothionein, anchored to the membrane via the LamB protein. This paved the way for others to develop sophisticated systems for the bioaccumulation of heavy metals (Valls and Delorenzo, 2002) (Bae *et al.*, 2000).

Similar reports have been made where yeasts have been used as the host cell for the display of laccases (Fishilevich *et al.*, 2009). Laccases have been shown to have high biochemical activity when it comes to catalysing the treatment of waste products and organic molecules that are often resistant to standard degradative measures. After discovering their capability to degrade many of these substrates, work was

done to find a way to introduce it to wastewater management due to high catalytic efficiency and simple regeneration and reuse.

1.3.2. Anchoring proteins

The membranous surface of bacteria is a dynamic and complex environment. The membrane also plays in a crucial role in maintaining cell viability (Silhavy, Kahne and Walker, 2010). Many of the proteins found in the outer membrane are responsible for the transport of essential molecules and nutrients (Wimley, 2003) (Tommassen, 2010). The membrane also acts as a means of separating harmful extracellular molecules from diffusing into the bacteria. For this reason, it is important to ensure that when designing a cell surface display system, the integrity of the membrane is maintained. This is one of the many critical aspects that need to be considered when choosing an anchoring motif and anchored protein.

Anchoring motifs can originate from many sources, but in most cases, they are developed from other membrane bound proteins (Shi and Wen Su W, 2001; Rice, 2006; Rutherford and Mourez, 2006). However, these proteins are implicated in different cellular functions. This means that proteins fused to these anchoring motifs may end up having the adverse effects on the protein's functionality. When they start to populate the membrane in high concentrations. Altering the composition of the membrane in this way can become detrimental to the survival of the cell.

It is important that the anchoring motif not only allows the fused protein to be stably inserted into the membrane but must also be able to mediate the translocation of the fused protein from the cytoplasm to the membrane. Because the target protein is not natively found within the cell, it is important that the bacteria is able to identify the anchoring motif as a translocation signal. This will then allow the passage of the fusion protein into the periplasmic space, where it can then be inserted into the outer membrane through the correct molecular apparatus (Mori and Ito, 2001).

The anchoring motif must also be stable when fused to its passenger protein. This would be demonstrated by maintaining its structure after being expressed and transported. There have been reports of systems where the fusion protein does show signs of degradation after expression (M. Shimazu, Mulchandani and Chen, 2001; van Bloois *et al.*, 2011). This is often because the fusion is prone to protease attack, and once expressed, it is rapidly broken down before it gets translocated to the

membrane (Li *et al.*, 2009). This is done by carefully assessing the method in which the fusion construct is put together. There are instances in which carriers and fusions will show large differences in stability due to the location in which the two proteins are put together.

Over the past several years, many different anchoring motifs have been used to achieve all the traits, while still conveying the ability to display recombinant proteins on the surface of different organisms. This has been achieved to some degree in a whole host of bacteria, using many different CSD systems. **Table 3** highlights some of the more notable systems that have been developed, alongside the different functions the displays have been used for.

Table 3 The multitude of display systems that have been employed over several years to achieve cell surface display.

Anchor	Origin	Comments	Ref.
AIDA-I	*E. coli*	Member of the immunoglobulin A1 protease like autotransporters. Widely used anchoring motif.	(Lattemann *et al.*, 2000)
InpN	*P. syringae*	Protein implicated in the extracellular crystallization of ice, popular choice display of larger proteins	(M. Shimazu, Mulchandani and Chen, 2001)
FadL	*E. coli*	Outer membrane protein used for binding of long chain fatty acids	(Lee *et al.*, 2004)
PgsA	*B. subtilis*	A part of a complex, PGA, which contains a subunit, PgsA, that stabilizes it within the membrane.	(Narita *et al.*, 2006)
OmpC	*E. coli*	Early use of outer membrane proteins for cell surface display.	(Xu and Lee, 1999)
OmpX	*E. coli*	Demonstration of one of the many uses for cell surface display as a peptide screening methodology.	(Rice, 2006)
OprF	*P. aeruginosa*	At the time of its conception, this anchoring motif supported the largest protein, at a size of 44.9 kDa	(Lee, Lee and Park, 2005)
CWB_b (truncated CwlB)	*B. subtilis*	These were used to demonstrate how cell surface display can be used for	(Kuroda and Sekiguchi, 1991)

		cell wall localization of a recombinant protein.	
BclA	*B. anthracis*	Demonstration of an exosporal protein being used as an anchoring motif in a gram-negative bacterium.	(Park *et al.*, 2013)
Lpp-OmpA hybrid	*E. coli*	An early, and prolific cell surface display motif that largely pioneered bacterial cell surface display	(Georgiou *et al.*, 1996)
LamB	*E. coli*	Displaying metallothionein, capable of bioaccumulation of heavy metals. Early example of how cell surface display can be used for bioremediation.	(Kotrba *et al.*, 1999)
OmpS	*E. coli*	Cell surface display system was used as another peptide screening system.	(Lång *et al.*, 2000)
Msp1	*Magnetospirillum magneticum*	Development of a cell surface display system for an organism that contains other desired properties. In this case, magnetostatic bacteria.	(Tanaka *et al.*, 2008)
Wza-Lpp hybrid	*V. anguillarum/ E. coli*	Novel development of a cell surface display system for *V. anguillarum*	(Yang *et al.*, 2008)
FhuA	*E. coli*	First instance of phage receptors being utilized as cell surface display anchors	(Etz *et al.*, 2001)

FnBPB	*S. aureus*	Using the ubiquitous cell wall immobilization mechanism for the display of active enzymes	(Strauss and Götz, 1996)
FimH	*E. coli*	Display using a different type of extracellular protein, contrary to the many lipoproteins and OMPs used in other experiments.	(Pallesen *et al.*, 1995)
Flagella	*E. coli/S. enterica subsp.*	Early example of how cell surface display can be used for vaccine development	(Westerlund-Wikström, 2000)
EspP/EstA	*E. coli*	Used for high throughput sorting of an anticalin library. These are small single chained binding proteins derived from a family of proteins that bind hydrophobic molecules.	(Binder *et al.*, 2010)

1.3.3. Ice nucleation protein as an anchoring motif

Many anchoring motifs have been developed for use in cell surface display systems. One specific system that is of interest to this project is the ice nucleation protein (INP) from *Pseudomonas syringae.* This protein has been used in several instances to mediate the display of recombinant proteins on the surface of gram-negative organisms.

The first known report of ice nucleation activity was reported by (Chafee, Maignien and Simmons, 2015). *P. syringae* is a bacterium that resides on plant surfaces without harming the plant itself. However, when water freezes on the plant surfaces, the ice crystals formed can damage the plant cell and the *P. syringae* utilize the expelled biomass as a source of nutrients. To promote freezing, this particular species of bacteria has membrane proteins protruding into extracellular space that position water molecules in a particular orientation that increases the propensity for ice crystals to form.

The gene encoding the INP has been identified in a multitude of strains of *P. syringae*. The homologues that have been cloned and characterised include inaK, inaV, and inaZ. As of 2016, the mechanism of translocation is not known for this protein (Zhang *et al.*, 2016). The gene used in this work is from the inaK variant, isolated from *Pseudomonas syringae* KCTC1832. This domain has several asparagine, threonine, and serine residues which facilitate the potential coupling to the mannan-phosphatidylinositol group in the outer membrane through N-glycan or O-glycan linkages. The rest of the protein consists of a CRD (central repeating domain) of an octapeptide A-G-Y-G-S-T-L-T motif. This repeating sequence is responsible for the ice nucleation activity. The remainder of the protein is the C-terminal domain (Li *et al.*, 2012).

InpN is the N-terminal sequence from inaK that covers the first 179 amino acids, and despite the fact it is very likely implicated in the translocation of the full INP to the membrane, it shares no homology with any known signal sequence, and as such cannot be associated with any secretory/translational proteins.

There have been many studies in which INP has been used as the basis for an anchoring motif. However, there are small differences in the way these experiments were designed and approached. There have

also been reports of differing degrees of success when using constructs that utilise different parts and combinations of INP (see **Figure 4**).

1.3.3.1. Translocation of INP-passenger fusions

Across several studies (Jeong, Yoo and Kim, 2001; Nicchi *et al.*, 2021), 2 different constructs are often used to display the investigated surface protein (this surface protein changes depending on the study). Construct 1 utilises only the N-terminal domain from different INP variants fused to the N terminus of the passenger protein. This alone acts as the anchoring motif. For construct 2, both the N and the C terminal domain from INP variants are used to create the anchoring motif (Jeong, Yoo and Kim, 2001; Nicchi *et al.*, 2021).

In the study conducted by (Li, Gyun Kang and Joon Cha, 2004), GFP was used as a passenger protein, and the two different constructs were investigated: the N terminal domain fusion, and the N and C terminal fusion .

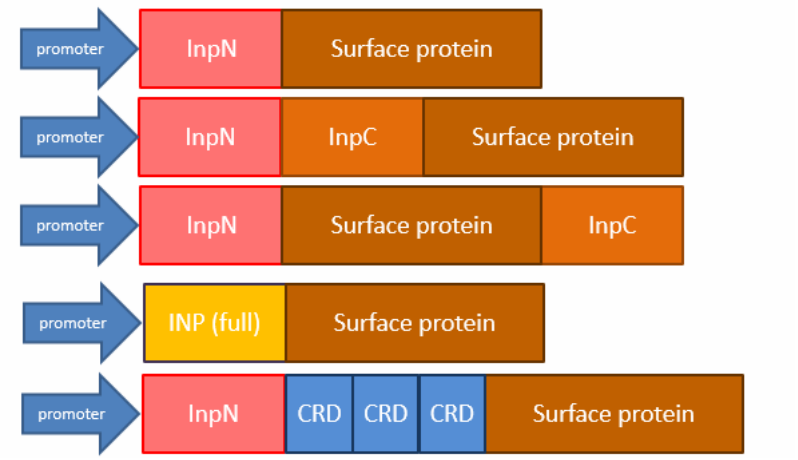

Figure 4 *Different potential construct designs for the fusion proteins. This approach can be applied to many different anchoring motifs.*

They observed that the amount of GFP translocated to the membrane, increases in the stationary phase. This suggests that it does take time for large amounts of protein to be translocated to the cell surface. They also highlight protein expression as a rate limiting step. It is insinuated that high rates of transcription can cause the translocation pathway to be inhibited (Li, Gyun Kang and Joon Cha, 2004).

Li et. al stated that between the expression and the secretion/translocation of the recombinant protein, the secretion/translocation is the slower of the 2 processes (Li, Gyun Kang and Joon Cha, 2004). As such, high expression and transcription will lead to an overload and decrease in efficiency of the translocation step. This in turn will lead to inhibited growth rate. Using 0.1 mM IPTG as opposed to 1 mM helps balance the flux between the two processes. There was an >3-fold increase in membrane fluorescence when the 0.1 mM IPTG concentration was used for induction. It will therefore be important to look at different concentrations of our own inducer to ensure that we can increase the amount of protein being translocated to the membrane when using our own construct.

1.3.3.2. Varying expression efficiency with construct design

Another point that was highlighted in the Li study, was the difference in expression efficiency between the two anchoring motifs (Li, Gyun Kang and Joon Cha, 2004). The amount of fluorescence observed in the InpN-GFP construct, is higher compared to the InpNC/GFP construct. However, when they assessed the comparative fluorescence from in the respective membrane fractions is almost identical. This further confirms the possibility that the rate limiting step is the translocation of the fusion protein (Li, Gyun Kang and Joon Cha, 2004).

Immunolabelling assays were used to assess whether the GFP was on the surface of the intact cells. This gave conclusive results in that the InpNC/GFP fusion showed slightly higher amounts of staining immunolabelling, indicating the presence of more GFP on the surface. However, the other variant InpN-GFP, was also very efficient in its cell surface expression. This informs us that the simpler construct containing only the N terminal domain, may be favoured for our own experiments (Li, Gyun Kang and Joon Cha, 2004).

1.3.3.3. INP-passenger fusion stability

The Li study talks about the stability of the two constructs relative to one another (Li, Gyun Kang and Joon Cha, 2004). In brief, the construct is not very stable and is proteolyzed heavily, resulting in very little of the full fusion being present. However, once in the membrane, the fusion protein is more stable, and they observe an increased amount in its full form in the membrane. This holds true for both variants.

However, they found that the InpNC-GFP construct showed lower concentrations of the protein present in the membrane (Li, Gyun Kang and Joon Cha, 2004).

The N terminal domain is the domain that is susceptible to protease attack whereas the C terminal is less so. This is inferred by an assessment of the products of the proteolysis. In the InpN-GFP construct, the degradation products had molecular weights that corresponded to InpN and GFP. However, in the InpNC-GFP construct, the molecular weight corresponds to InpN and InpC-GFP, suggesting the cleavage is happening at the interface of InpN and whatever is adjacently fused.

Similar reports have been made in many other papers, where the passenger protein, describing weak stability of the InpN-passenger construct. This will be important to look out for.

The INP system will be investigated in this project as a potential candidate for cell surface display in *C. necator* H16. The observations made in these papers should give valuable insight into how to correctly design the construct for expression, and how to measure and assess the efficacy of expression and translocation.

1.3.4. BclA protein

The BclA protein comes from the gram-positive *Bacillus anthracis* spore. The spore formed by this bacterium has a series of spherical shells that all differ in composition. The inner most shell contains the spore's genetic material. This inner core is surrounded by a cortex, composed of a complex mesh peptidoglycan. The cortex is then surrounded by a protein layer called the coat (**Figure 5**). This coat has several interesting features such as its ability to expand in response to germination, and protection from microbial predation (Driks, 2009). The coat is covered by the outermost layer, the exosporium. The exosporium is a proteinaceous shell that surrounds the coat, separated by a gap called the interspace. The contents of the interspace have not yet been elucidated.

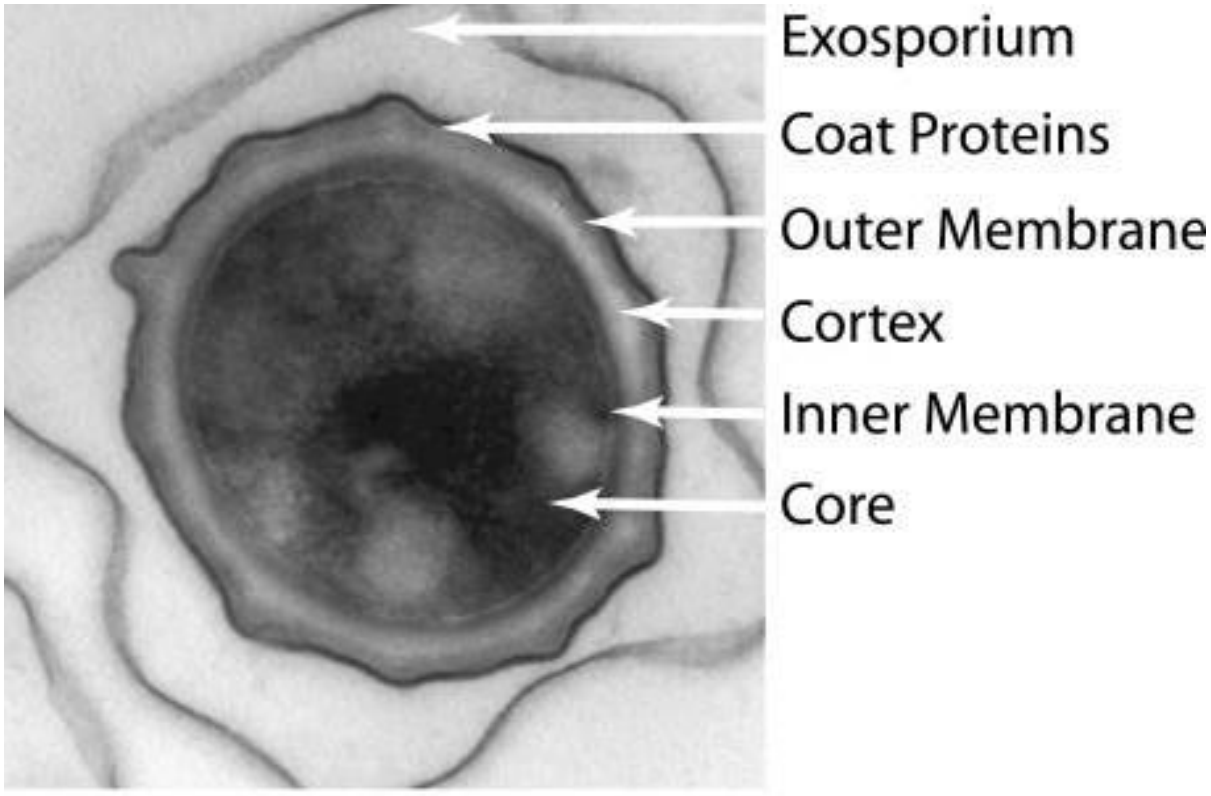

Figure 5 *Structure of Bacillus anthracis spore. Figure taken from* (Liu et al., 2004).

In the exosporium, the most abundant protein that projects into the extracellular space, is BclA, the protein of interest. BclA is the main constituent of a hair like nap on the outermost surface of the spores. This extracellular glycoprotein plays a prevalent role in the virulence and survival of the spores (Sylvestre, Couture-Tosi and Mock, 2002).

BclA has a simple structure consisting of 3 main domains, the N-terminal domain (NTD), the central repeating domain (CRD) and the C-terminal domain (CTD). The NTD is what can be exploited to confer membrane affinity (Lequette *et al.*, 2011). There is also the CRD which is a repeating unit for a collagen like structure. Within the NTD, there is consensus sequence that may be responsible for membrane association. This is a heavily hydrophobic sequence, potentially allowing for anchoring within the hydrophobic regions of the membrane (Lequette *et al.*, 2011).

In *Bacillus anthracis* spores, the BclA glycoprotein is translocated via a set of proteins that are implicated in the translocation process (ExsF complex and BxpB). Their exact mechanism of function is not known, but knockout mutants show no exosporium formation. It may be possible that homologues of these proteins exist in gram negative bacteria, but that much has not been made clear by current literature (Sylvestre, Couture-Tosi and Mock, 2005).

A paper in 2013 detailed how recombinant proteins were displayed on the surface of *E. coli* using specific domains of this exosporal protein as an anchoring motif. BclA was investigated as an anchoring motif. The N – terminal domain of the BclA protein was fused to the C terminal domain of their carrier protein. This was done in hopes that a cell surface display system that would be able to accommodate larger proteins on the extracellular surface. Their study looked at the display of endoxylanase and P450 (Park *et al.*, 2013).

Many studies have detailed the native translocon systems that exist within gram negative organisms. The two systems that are very abundantly documented are the sec and tat system (Thomas *et al.*, 2001). The sec translocase has been established as responsible for the translocation of proteins into the periplasmic space in their unfolded form (Mori and Ito, 2001; Beckwith, 2013). This is facilitated by a signal peptide on the target protein. However, the BclAN peptide sequence is not the same as the native signal sequence. This has led to speculation as to how BclAN facilitates the translocation of recombinant protein to the extracellular surface.

Because BclA has only been used as an anchoring motif in one study, it is difficult to assess the different aspects and potential pitfalls of the system. However, sequences within BclA have been identified that

trigger the incorporation of the protein into the exosporium layer of the spores. This study illustrates that the expression of BclA happens first within the cytoplasm of the mother cell, before incorporation into the spore. However, after this step the N terminal domain is cleaved from the full protein for the BclA protein to form the exosporium. Given this information, it becomes increasingly unclear how this anchoring motif can function as such in *E. coli* (Thompson and Stewart, 2008).

There is little existing bioinformatic analysis that on the mechanism in which the BclAN anchoring motif functions. No homogeneity has been found between the BclAN domain and other ubiquitous membrane binding domains in gram negative bacteria. Sequence alignments between BclAN and outer membrane proteins from the organism also show no homology.

While the mechanism of function is not understood, it may still be applicable to *C. necator* H16. As such, it will be investigated as a potential anchoring motif. By illustrating its ability to anchor proteins in a different gram-negative organism, more light can be shed on how the system works.

1.4. Beta glucosidase from *Thermobifida Fusca YX* Tfu0937

Beta glucosidases are glycosidic enzymes capable of hydrolysing glycosidic bonds in carbohydrates and sugars. There are other organic substrates that can also be hydrolysed by the enzyme. One of these substrates, p-nitrophenyl- β-D-glucopyranoside (pNPG), will be used for the assessment of beta glucosidase activity. When hydrolysed, two compounds are released, p-nitrophenol, and β-D-glucuronic acid. By adding a solution of pNPG to cells displaying the beta glucosidase, the p-nitrophenol produced is easily measured by spectrophotometry (absorbs well at 405 nm), giving an indication of how much beta glucosidase has been translocated to the membrane in those cells (Spiridonov and Wilson, 2001). In its native state, the Tfu0937 beta glucosidase is responsible for the degradation of cellobiose into glucose (see **Figure 6**).

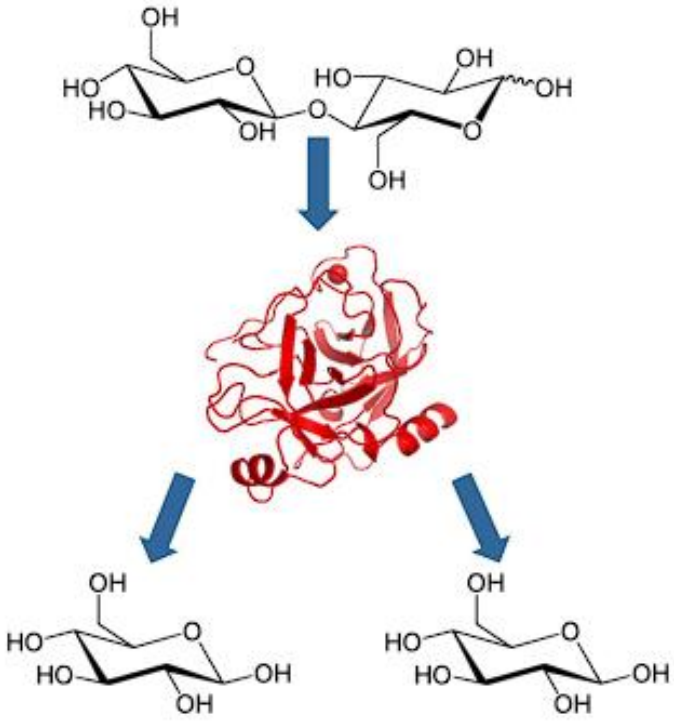

Figure 6 *Basic schematic showing the hydrolytic cleavage of cellobiose facilitated by Tfu0937 (red protein)*

1.5. Research aims

A biotechnological advent that could be implicated in the process of carbon capture and utilisation is cell surface display. CSD has become an essential part of many research areas, such as drug discovery and vaccine development. Phage display systems have been used in the past to display recombinant proteins, but there has been a shift towards more complex bacterial display systems capable of displaying larger proteins. Bacterial surface display in *E. coli* has been shown to be an efficient way of introducing new functionality to cells.

By using bacteria as a means of displaying enzymes that can be used for the degradation and metabolism of different carbon sources, it may become possible to effectively manage these carbon waste streams more efficiently.

The main aim of this project is to contribute 3 new molecular tools for use in *Cupriavidus necator*. *E. coli* is a good host for many synthetic systems due to our understanding of the organism and its genome. However, there are several limitations in using *E. coli* for some of the more practical applications of bacteria in an industrial sense. These stem primarily from the fact that *E. coli* doesn't natively have the metabolic systems that are desirable for commercial purposes. While engineering them into *E. coli* is possible, that brings with it a whole host of problems such as metabolic regulation which only serve to increase the amount of time it takes to take from proof of concepts that are frequently demonstrated in literature, into real biobased solutions that are applied in the real world.

By developing tools that allow us to delve into the more intricate workings of *C. necator* H16, we will be able to use it in place of other organisms which are not capable of the same metabolic functionalities. This will serve to open a new door in the possibilities for biocatalysis, bioremediation, and other biological industrial processes, specifically repurposing waste carbon into valuable PHB (polyhydroxybutyrate) (Priefert and Steinbüchel, 1992).

To do this, the primary aim of this project is to integrate new biotechnological advances, specifically CSD into *C. necator* H16. This will be done by achieving the following goals.

- Develop a cell surface display system for *C. necator* H16.
- Develop assay(s) to easily assess if the display system is working
- Demonstrate the functionality of cell surface display by using the displayed protein to mediate cell growth in cellobiose.

2. Beta glucosidase assay development

2.1. Introduction

Beta glucosidases are a class of enzymes used in the degradation and metabolism of cellulose. They are often found and expressed as part of a multitude of other cellulases that all work together to facilitate the degradation of cellulose down to monomeric glucose molecules that can often be used as a carbon source for an organism. Beta glucosidase (BGL) from Thermobifida fusca YX (Tfu0937) is an enzyme that has been used extensively in other works as a reporter enzyme that can be easily expressed and monitored, but those papers look specifically at Tfu0937 that has been expressed and is freely suspended either in the cytosol, periplasmic space or the extracellular space. There are very few papers that use Tfu0937 as a reporter as a membrane bound protein. This is in part to the sheer size of the enzyme. At 53.4 kDa, the number of known display systems that exist that would be capable of displaying such a large protein is low, and completely non-existent when looking at display systems in *C. necator* H16. I intend to utilise beta glucosidase not only as a reporter enzyme for cell surface display, but also as a means of facilitating the growth of *C. necator H16* using cellobiose.

To do this, an assay was developed and optimized to measure the amount of activity that is present on the surface of the *C. necator* H16 cells. This process was done in incremental stages to see the effects of different parameters that changed the interaction between Tfu0937 that was present on the cell, and the extracellular substrate, *p*NPG (4-Nitrophenyl-β-D- glucopyranoside) and later, cellobiose. Similar endeavours have been made using *E. coli* (Tanaka *et al.*, 2011), but as previously explained, there is an important novelty in shifting the scaffold to *C. necator* H16.

The basis of the assay revolves around subjecting cells that are thought to be displaying Tfu0937 and then introducing the colourless *p*NPG to the extracellular environment of these cells. Given there is adequate display and activity of the Tfu0937, the *p*NPG is broken down into 4-nitrophenol and β-D-glucopyranoside. After the reaction is complete, addition of a basic reagent deprotonates the 4-nitrphenol, turning it into a bright yellow metabolite that absorbs very well at the wavelength of 405

nm. The amount of 4-nitrophenol produced is then measured via a spectrophotometric method and used to quantify the amount of Tfu0937 present.

This chapter's purpose is to detail exactly how the assay was developed and optimized, rationalising all the different methods used to get the most reliable data using this system.

2.2. Materials and methods

2.2.1. Strains

Bacterial strains of *E. coli* DH5α obtained from Novagen. The *C. necator* H16 used extensively in this work was kindly donated to our lab by Dr. Steinbuchel's group and are used in perpetuity for the remainder of all chapters.

2.2.2. NB media and plate preparation

NB media was used for routine cultivation of *C. necator H16* cultures. Per 1 L, mix: 5 g peptone (Foremedium, UK), 1 g Beef extract (Sigma Aldrich, UK), 2 g Yeast extract (Foremedium, UK), 5 g NaCl (Foremedium, UK), 15 g Agar (Foremedium, UK, used to prepare plates). Sterilise by autoclaving.

2.2.3. 2TY media and plate preparation

2TY media was used for routine cultivation of *E. coli* DH5α. Per 1 L mix 16 g Tryptone (Foremedium, UK), 10 g Yeast extract (Foremedium, UK), 5 g NaCl (Foremedium, UK), ad 15 g of agar (Foremedium UK, used to prepare plates)

2.2.4. MSM media preparation

MSM media was used for routine cultivation and protein expression of *C. necator* H16 To 1 L of media 6.74 g Na_2HPO_4, 1.50 g KH_2PO_4, 1 g NH_4Cl, 0.20 g $MgSO_4 \cdot 7H_2O$ (400 µL from a 0.5 g/mL stock), 20 mg $CaCl_2 \cdot 2H_2O$ (80 µL from a 0.25g/mL stock), 1.20 mg Fe (III)NH_4-Citrate (4.8 µL from a 0.25 g/mL stock), 10 g sodium gluconate, 0.1 mL SL6 (Trace elements solution)

To prepare SL6

Per 1 L: 10 mg $ZnSO_4 \cdot 7H_2O$, 3 mg MnCl2 • 4H2O, 30 mg H_3BO_3. 20 mg $CoCl_2 \cdot 6H_2O$, 1 mg $CuCl_2 \cdot 2H_2O$, 2 mg $NiCl_2 \cdot 6H_2O$ 3 mg $Na_2MoO_2 \cdot 2H_2O$, sterilised 0.2 µm Molecular cloning of pBBR1c-His-BclAN-Tfu0937

2.2.5. Agarose gel

0.5 g (1% gel) or 0.35 g (0.7% gel) agarose (Lonza, UK) 50 mL TBE buffer, 2 µL EtBr, (Merck, Germany). Add the agarose to 50 mL of TBE buffer in a 250 mL cylindrical flask and microwave until the agarose dissolves. Allow to cool to 50 °C before adding EtBr. Swirl to dissolve EtBr and pour into an appropriate gel casing,

2.2.6. Cultivation of *C. necator* H16

Unless stated otherwise, *C. necator* H16 was cultivated at 30 °C, 250 rpm, in MSM media supplemented with 1% gluconate ,0.5% cellobiose or NB media. Ensure all cultures are supplemented with gentamicin (10 µg/mL working concentration), and cultures containing pPJ5'c.rbs-His-BclAN-Tfu0937/ pBBR1c-His-BclAN-Tfu0937 and pPJ5'c.rbs-Tfu0937/ pBBR1c-Tfu0937 are supplemented with chloramphenicol (25 µg/mL working concentration)

2.2.7. Cultivation of *E. coli* DH5α

Unless stated otherwise all cultures of *E. coli* DH5α were cultivated at 37 °C and 250 rpm, in 2TY media. Ensure all cultures are supplemented with gentamicin (10 µg/mL working concentration), and cultures containing pPJ5'c.rbs-His-BclAN-Tfu0937/ pBBR1c-His-BclAN-Tfu0937 and pPJ5'c.rbs-Tfu0937/ pBBR1c-Tfu0937 are supplemented with chloramphenicol (25 µg/mL working concentration)

2.2.8. Molecular cloning of pBBR1c and $P_{j5[A1A3C2]}$ (Pj5) constructs

2.2.8.1. Plasmid isolation

The DNA sequences encoding the *E. coli* osmotically inducible protein Y (OsmY; GenBank: AUY30809.1), the *Thermobifida fusca* YX β-glucosidase (Tfu0937; GenBank: AAZ54975.1), were codon-optimized for protein expression in *E. coli* and synthesized by GenScript (Piscataway, USA). OsmY, the secretory carrier, was fused to the N-terminus of Tfu0937 and cloned into a pET24a(+) vector using NdeI and EcoRI sites. The resulting plasmid was used for protein engineering in this study.

E. coli DH5α was used for the molecular cloning of the pBBR1c-InpN-Tfu0937. Using the QIAprep Miniprep kit was used for the isolation of pET24a(+)OsmY-Tfu0937. *E. coli* DH5α was cultivated in 5 mL of 2TY media containing the appropriate antibiotic (Kanamycin, Applichem, UK) overnight. Cells were harvested by centrifugation of the 5 mL of overnight culture and 10000 rpm for 1 minute. The media is aspirated, and the cell pellet is suspended in 250 µL of Solution 1. Subsequently, 250 µL of solution 2 is added to initiate cell lysis. The tubes are gently inverted for no more than 5 minutes, at which point 350 µL of solution 3 is added. The tube is inverted several times until a white flocculent appears. The sample is then centrifuged at 13000 rpm for 10 minutes. The supernatant is transferred to a spin column to bind the DNA and centrifuged at 10000 rpm for 1 minute. Once the solution has eluted from the tube, the DNA is washed with 750 µL of HBC buffer 2 times. The tube is then washed with 700 µL ethanol and left to stand at 50 °C to remove the residual ethanol. The DNA was then eluted in 50 µL of elution buffer by centrifugation at 13000 rpm for 2 minutes. The concentration of DNA was then quantified on the NanoDrop 1000 spectrophotometer (Sartorius).

2.2.8.2. PCR amplification of Tfu0937, incorporation of XhoI, NdeI, and BamHI restriction sites.

To amplify the Tfu0937 DNA fragment, the following PCR reaction mixes were prepared

Table 4 *Components and concentrations used for PCR amplification of Tfu0937 gene fragment*

Component	**Stock concentration**	**Volume (µL)**
ddH_2O	-	33
Q5 buffer	5x	10
dNTPs	10 mM	1
pET24a(+)OsmY-Tfu0937	100 ng/ µL	0.5
Forward primer	20 µM	2.5
Reverse primer	20 µM	2.5
Q5 DNA polymerase	2 U/µL	0.5
Total reaction volume		50

Table 5 *Primer sequences used for amplification of Tfu0937*

Primer	**Oligonucleotide sequences**
Tfu0937-XhoI	5’ ACTGCTCGAGTTACTCTTGACCAAAAATACCGCCATTAC 3’
BamH1 – Tfu0937	5’ ATCGGGATCCACCAGCCAAAGCACCACC 3’
NdeI – Tfu0937	5’ ACTGCATATGACCAGCCAAAGCACCACC 3’

Table 6 *PCR program for the amplification of Tfu0937 fragments*

Stage	**Temperature (°C)**	**Time (s)**
Initial denaturation	98	30
Denaturation	98	12
Annealing	72	30
Extension	72	44
Final extension	72	120
Holding	4	-

Repeat denaturation →extension 30 times. The appropriate primers were added to create the following constructs NdeI-Tfu0937-XhoI, BamH1-Tfu0937-XhoI.

2.2.8.3. PCR/DNA fragment purification

A NucleoSpin® Gel and PCR Clean-up Kit (Germany) were used to carry out purification of PCR products. PCR products are loaded onto a 1% agarose gel. Sample is run for 40 minutes at 90 V and 400 mA. Gel is visualised using a transilluminator at 302 nm or using a GenoSmart VWR gel documentation system, and the desired band is removed using a clean scalpel. 200 µL of NT1 buffer was added for each 100 mg agarose gel. The sample is incubated at 50 °C for 10 minutes and then vortexed until the gel had completely dissolved. 700 µL of the solution is transferred to the spin column and centrifuged for 30 s at 10000g. The flow through is discarded and the remaining solution is

transferred to the tube. This process is repeated until all the solution has been run through the column. The column was washed twice with 700 µL of NT3 buffer for 60 s. The empty tube was centrifuged for 2 minutes, and the flowthrough discarded. The DNA was eluted with 30 µL of elution buffer, and the DNA concentration measured on the NanoDrop 1000 spectrophotometer (Sarotrius)

2.2.8.4. Preparation of pBBR1c vectors and $P_{j5[A1A3C2]}$ vectors

E. coli DH5α containing pBBR1c-His-BclAN-GFP, pBBR1c-InpN-GFP, and $P_{j5[A1A3C2]}$.-OsmY-Tfu0937 were used to isolate their respective plasmid using the aforementioned plasmid isolation protocol. The following protein digestion mixtures were prepared.

Restriction enzymes, NdeI, XhoI, and BamHI were sourced from New England Biolabs

Table 7 Components of stock concentrations for the restriction digestion of plasmids for pBBR1c and $P_{j5[A1A3C2]}$ backbone vectors.

Component	**Stock concentration**	**Volume (µL)**
Water	-	31.9
Cutsmart	10x	5
pBBR1c-His-BclAN-GFP	90ng/µL	11.1
NdeI	20000 U/mL	1
XhoI	20000 U/mL	1
Final concentration		50

Component	**Stock concentration**	**Volume (µL)**
Water	-	30
Cutsmart	10x	5
pBBR1c-His-BclAN-GFP	100ng/µL	10
BamHI	100000 U/mL	1
XhoI	20000 U/mL	1

Final concentration		50

Component	**Stock concentration**	**Volume (µL)**
Water	-	28.88
Cutsmart	10x	5
pBBR1c-InpN-TGP	67ng/µL	14.92
BamHI	100000 U/mL	0.2
XhoI	20000 U/mL	1
Final concentration		50

Component	**Stock concentration**	**Volume (µL)**
Water	-	30
Cutsmart	10x	5
$P_{j5[A1A3C2]}$-OsmY-Tfu0937	100ng/µL	10
BamHI	100000 U/mL	1
XhoI	20000 U/mL	1
Final concentration		50

Component	**Stock concentration**	**Volume (µL)**
Water	-	30
Cutsmart	10x	5
$P_{j5[A1A3C2]}$-OsmY-Tfu0937	100ng/µL	10
NdeI	20000 U/mL	1
XhoI	20000 U/mL	1
Final concentration		50

The pBBR1c vectors were then purified using the DNA fragment protocol. The target vectors were pBBR1c-His-BclAN-, pBBR1c-InpN-, pBBR1c-. The same treatment was applied to the Tfu0937 fragments purified from the PCR preparation.

2.2.8.5. Ligation of the Tfu0937 fragments to the pBBR1c backbones

The following mixtures were prepared to ligate the Tfu0937 fragments to the pBBR1c vector backbones.

Table 8 Components for the ligation mixture used for the ligation of the pBBR1c or $P_{j5[A1A3C2]}$ *backbone*

Component	**Stock concertation**	**Volume (µL)**
ddH_2O	-	7.29
T4 DNA ligase buffer	5x	4
Vector	8 ng/µL	5.88
Tfu0937 insert	21 ng/µL	1.83
T4 DNA ligase	1 U/µL	1
Final volume		20

Incubate the reaction mixture at 16 C overnight.

2.2.9. Plasmid maps

Plasmid map for pET-24(+)OsmY-Tfu0937

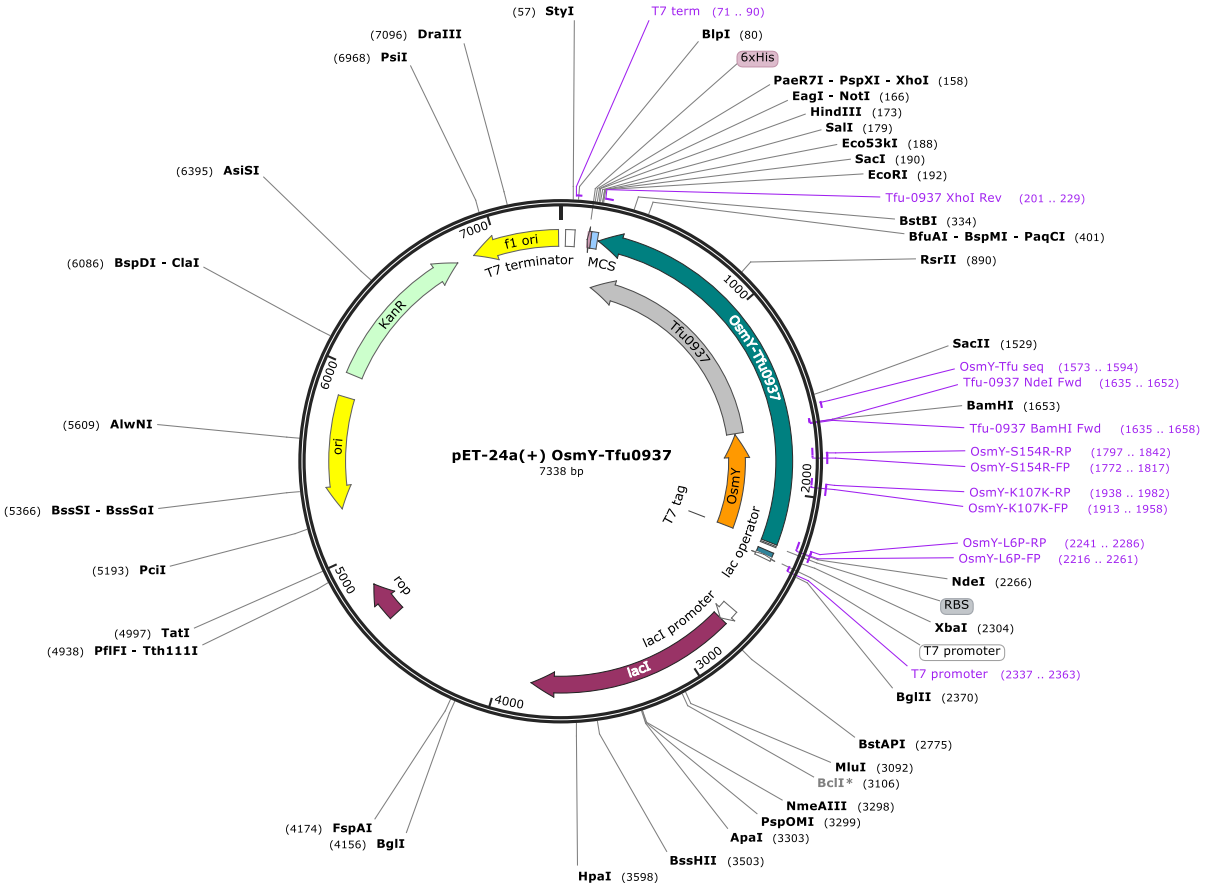

Plasmid map for pBBR1c-His-BclAN-TGP

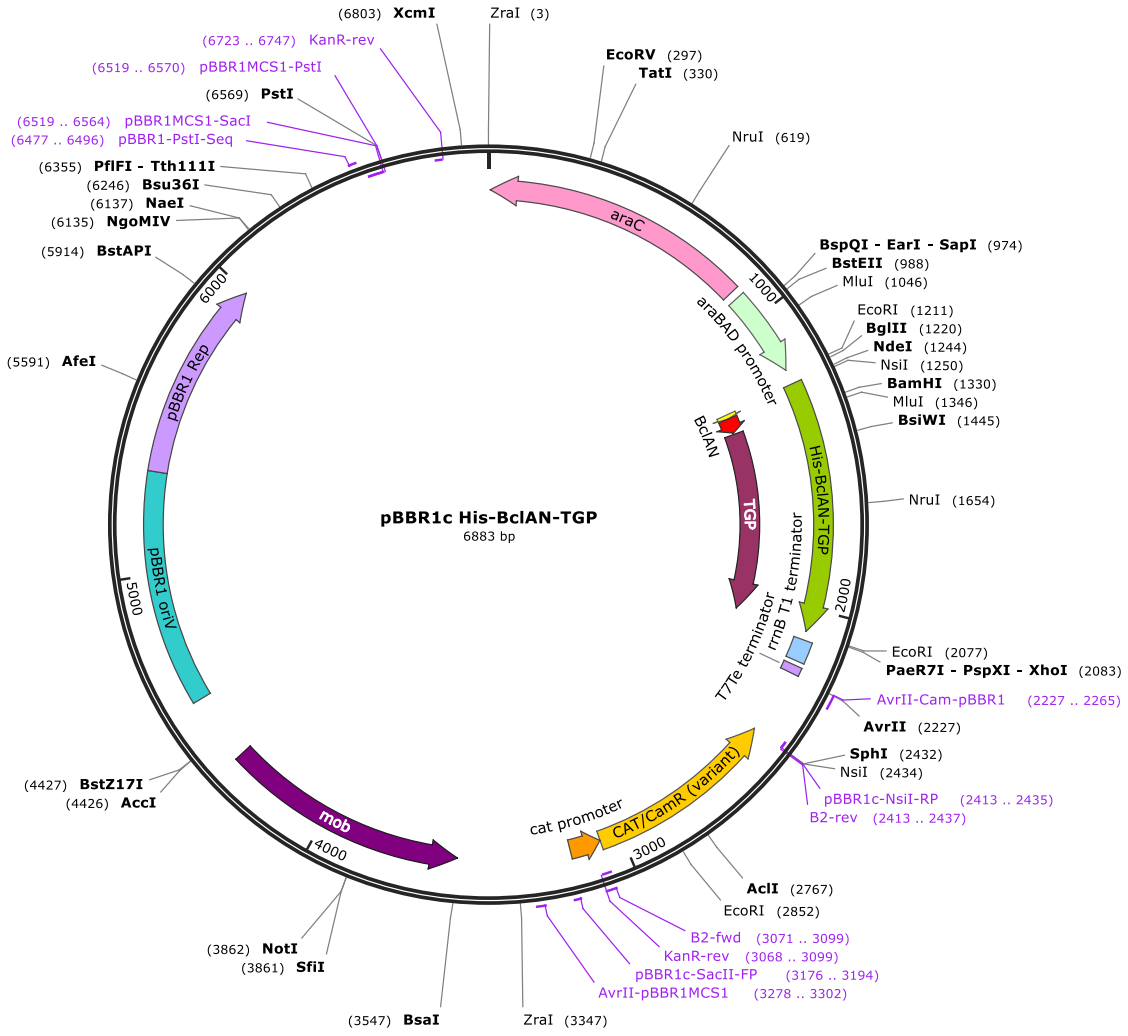

Plasmid map for pBBR1c-His-BclAN-Tfu0937

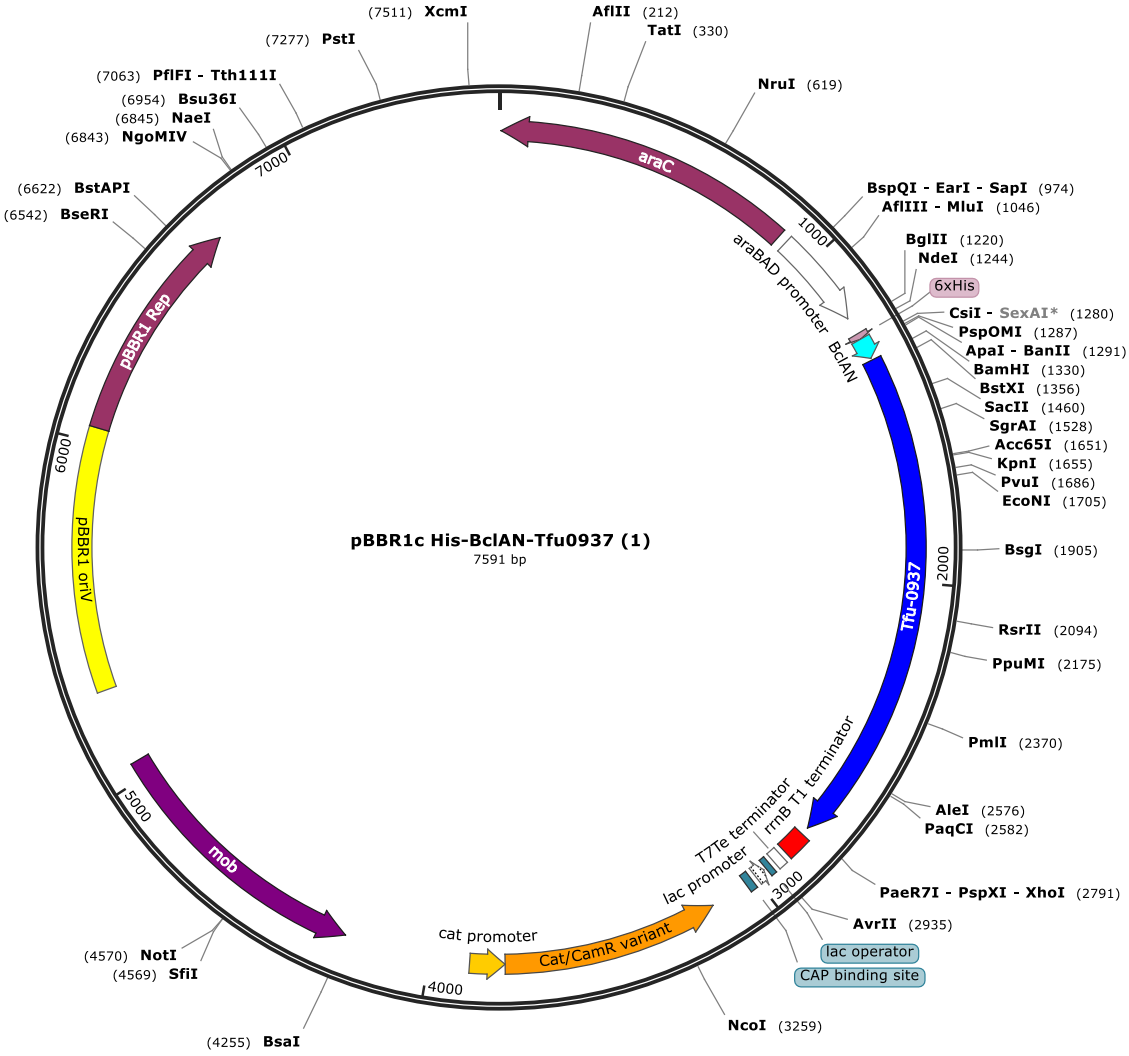

Plasmid map for pBBR1c-Tfu0937

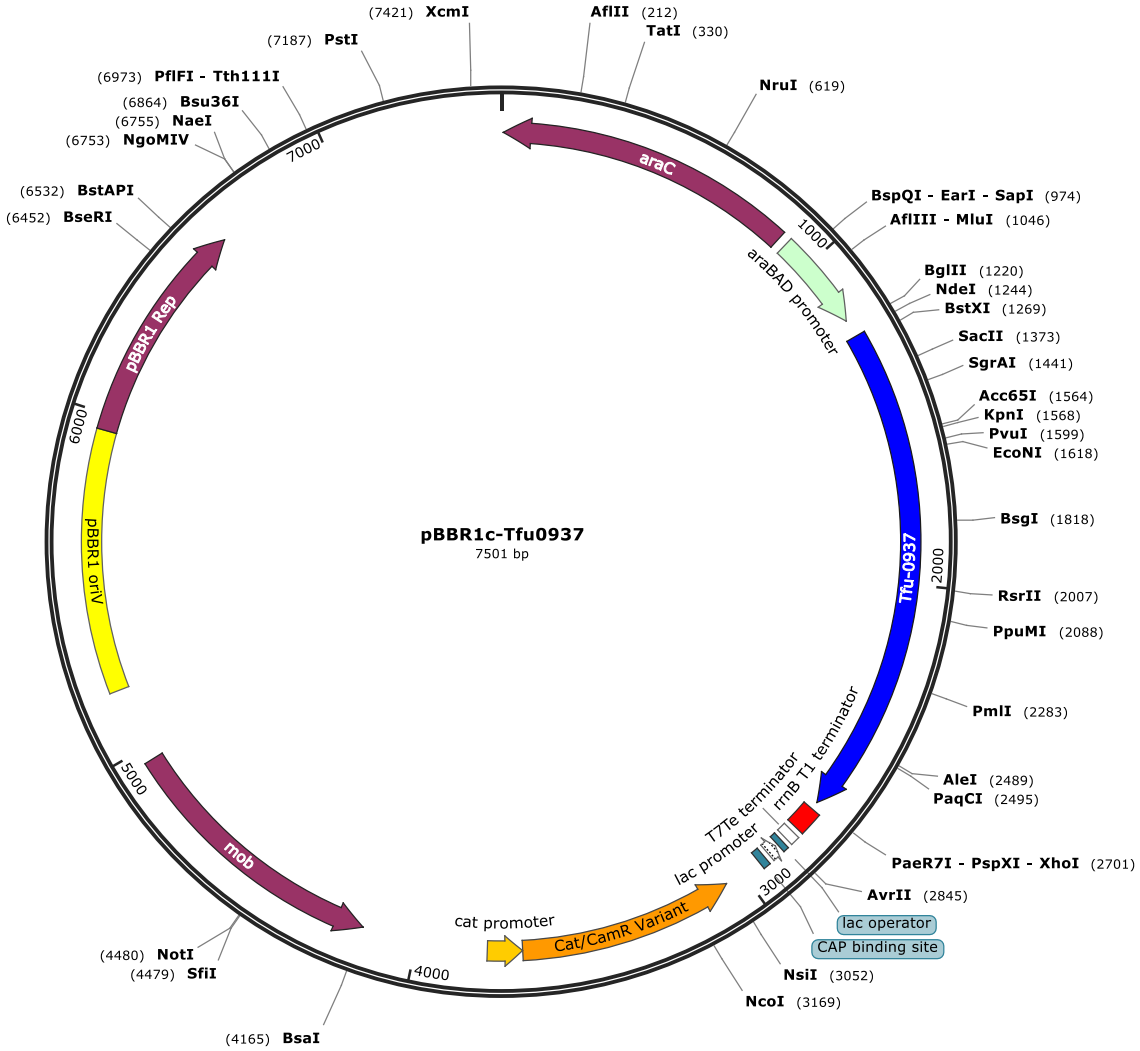

Plasmid map for pBBR1c-InpN-Tfu0937

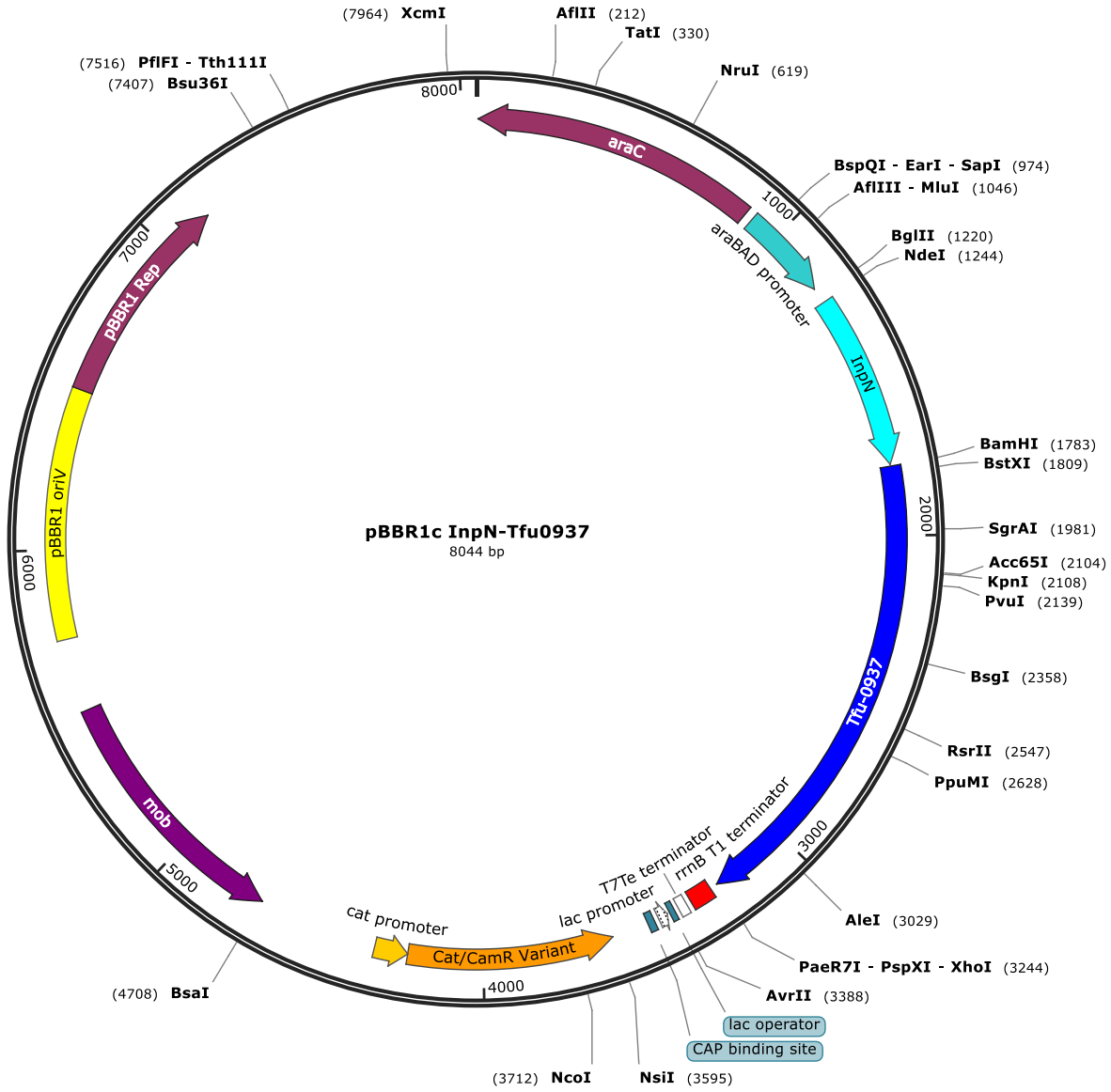

Plasmid map for $P_{j5[A1A3C2]}$-His-BclAN-Tfu0937

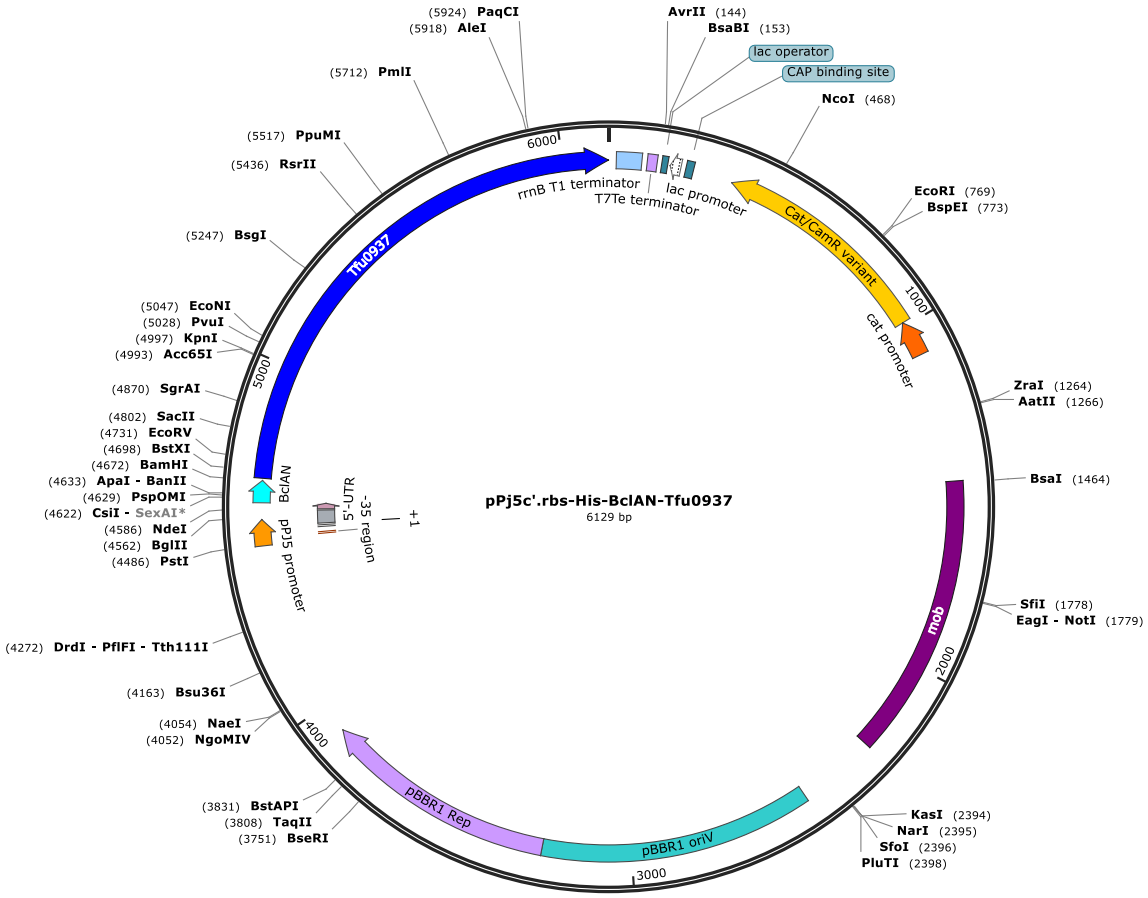

Plasmid map $P_{j5[A1A3C2]}$ -Tfu0937

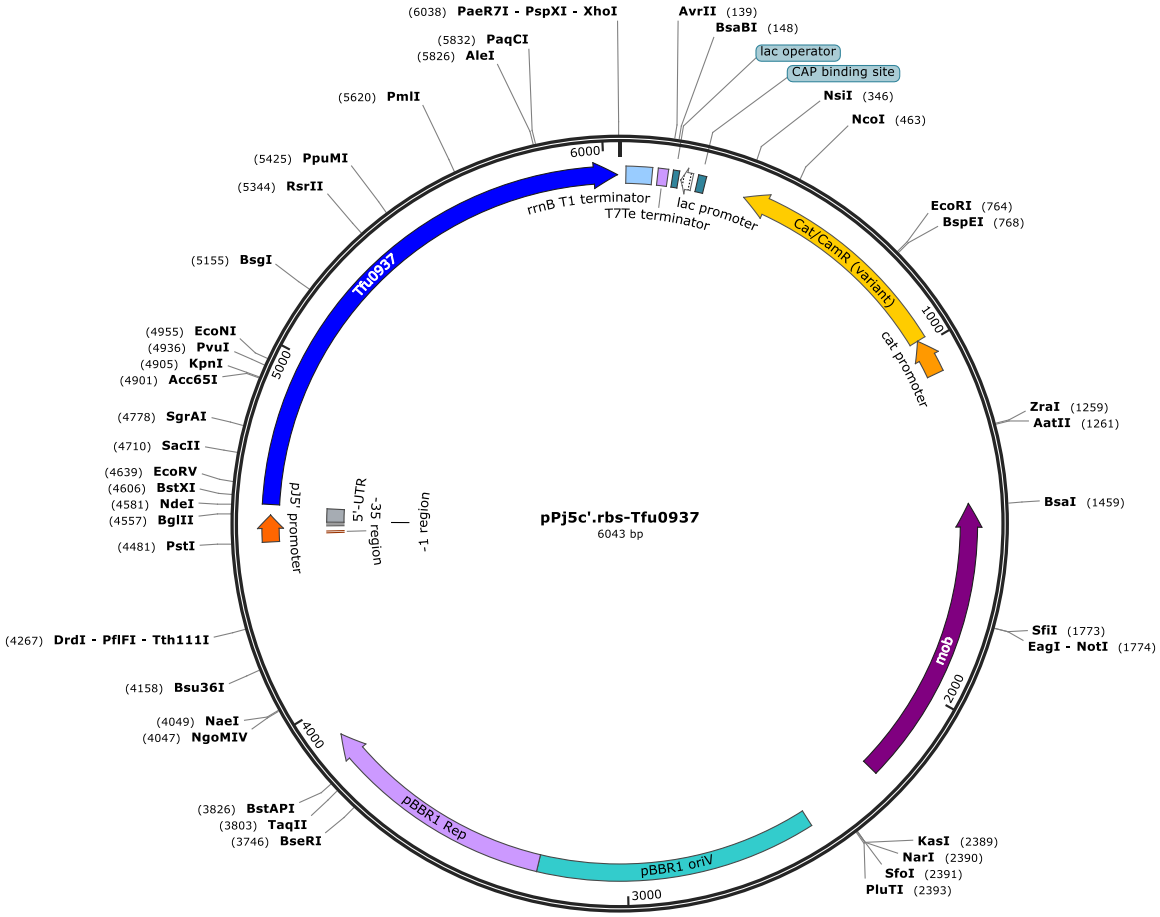

2.2.10. Chemical transformation of pBBR1c constructs into *E. coli* DH5α

Transformation of ligation products and other plasmids was conducted as follows. A 5 mL O/N culture of *E. coli* DH5α was cultivated in 2TY. The following day, inoculate 5 mL of fresh 2TY with 50 µL of O/N culture. Cultivate the cells to an OD_{600} of 0.5-0.6. Transfer 1 mL of culture per transformant to a sterile 1.5 mL Eppendorf. Centrifuge the cells for 2 minutes at 2800 rpm. Remove the supernatant and resuspend in 500 µL of cold, sterile $CaCl_2$. Centrifuge the cells at 2800 rpm, before resuspending the cells in a fresh 500 µL of cold sterile $CaCl_2$. Incubate the cells for 30 minutes on ice. After the incubation, add 5 µL of plasmid to the treated cells. Mix and incubate on ice for 30 minutes. Heat shock the cells

at 42 °C, for 1 minute. Add 800 µL of prewarmed 2TY to the cells and grow them for 1 hour. Centrifuge the cells at 2800 rpm for 2 minutes, remove 1.1 mL of media and resuspend the remaining cells in 200 µL 2TY, and plat on NB agar supplemented with the appropriate antibiotic (chloramphenicol for pBBR1c strains). Plasmids were sequences

2.2.11. Electroporation of pBBR1c or $P_{j5[A1A3C2]}$ constructs into *C. necator* H16

Prepare cooling the following: Pre chilled 2-mm electroporation cuvettes, Pre chilled 2 mL centrifuge tube,2 mL centrifuge tube, Cold, sterile, 0.2 M sucrose (Sigma Aldrich, UK), Cold sterile 50 mM $CaCl_2$, DNA to be transformed, Pre chill centrifuge

Streak out *C. necator* H16 cells from glycerol stock onto NB-gentamicin plate and incubate at 30 °C, transfer single colony to 5 mL of MSM-gen in a falcon tube and cultivate at 30 °C until OD_{600} Measure OD600 ¬of cells and transfer culture to incubate on ice for 5 minutes. Aliquot 2 mL of culture into a 2 mL centrifuge tube and centrifuge at 10000 g, 4 °C for 1 minute Remove supernatant by pipetting and resuspend the cell pellets with 1 mL of pre chilled 50 mM $CaCl_2$ Incubate samples on ice for 15 minutes Centrifuge the samples at 10000 g, 4 °C for 11 minute and remove the supernatant Wash cells twice with 1 mL of 0.2 M sucrose (centrifuge 10000 g, 4 °C for 1 minute between washes, remove supernatant by pipetting) Resuspend cells in 400 µL of ice cold 0.2 M sucrose. Transfer 200 µL to a fresh tube. Add DNA (0.1-1 µg) to each tube before transferring the mixture to the pre chilled cuvettes. Tap cuvette gently to remove air bubbles and wipe cuvette dry. Electroporate using 2.3 kV and return sample to ice. Add 1 mL of NB media to electroporated cells. Transfer all cells from the cuvettes to a fresh 2 mL centrifuge tube. Incubate cells at 30°C, 250 rpm, for 2 hours. Plate cells on an NB agar plate with necessary antibiotics

2.2.12. Expression of Tfu0937 fusion proteins & Tfu0937 in *C. necator* H16

A 5 mL culture of *C. necator* H16 harbouring the appropriate plasmids was cultivated O/N in MSM supplemented with 1% gluconate. The cells were then sub-cultured into a 5-25 mL of fresh MSM to an

OD_{600} of 0.4-0.6 unless stated otherwise. 25 µL of arabinose is added to the cells (0.1% working concentration unless stated otherwise).

2.2.13. SDS- PAGE gel analysis of protein expression in *C. necator* H16

In 5 mL of MSM supplemented with 1% sodium gluconate, grow pre-cultures of ReH16 cells transformed with: pPJ5'c.rbs-His-BclAN-Tfu0937/pBBR1c-His-BclAN-Tfu0937pPJ5'c.rbs-Tfu0937/pBBR1c-Tfu0937/pBBR1c-InpN-Tfu0937, or No plasmid Ensure all cultures are supplemented with gentamicin (10 µg/mL working concentration), and cultures containing pPJ5'c.rbs-His-BclAN-Tfu0937/ pBBR1c-His-BclAN-Tfu0937 and pPJ5'c.rbs-Tfu0937/ pBBR1c-Tfu0937 are supplemented with chloramphenicol (25 µg/mL working concentration) . Cultivate the pre-cultures for 24 hours. Sub-culture the precultures into 5 mL of MSM supplemented with 1% gluconate, in a 50 mL falcon tube to an OD_{600} of 0.2. For tubes inoculated with pBBR1c strains, cells are cultivated to an OD_{600} of 0.4-0.6 before the addition of 25 µL of 20% arabinose, this induces the cells at a working concentration of 0.1% arabinose. Cultivate over the course of 24 hours, removing 1 mL of culture for gel samples. Collect the cells and sonicate 15 seconds on, 45 seconds off for 10 cycles before

10% SDS gels were prepared in two parts, a stacking gel and a resolving gel. Resolving gels were composed of, 4.1 mL dd H_2O, 3.3 mL 30% acrylamide (Severn biotech, UK), 2.5 mL 0.5 M Tris-HCl (pH 8.8) (Tris base, Fluka, Germany, HCl Sigma Aldrich, UK.), and 0.1 mL SDS (VWR, UK) (10% w/v). The addition of 5 µL TEMED (Applichem, UK) and 50 µL 10% APS (Applichem, UK) was performed prior to pouring the gel. A layer of ddH2O was added on the top of the resolving gel, and the gel was allowed to solidify for 45 minutes The stacking gel was prepared using 4.1 mL ddH_2O, 3.3 mL 30% acrylamide, 2.5 mL 0.5 M Tris-HCl (pH 6.8), and 0.1 mL SDS (10% w/v). 10 µL TEMED and 50 µL of 10% APS were added before the gel was poured to initiate the setting. The DDI H2O layer was drained and, the stacking gel was poured on top, and the comb was placed into the assembled gel cassette.

2.2.14. Measuring whole cell Tfu0937 activity

Reagents

Reaction buffer: 0.2 M sodium acetate (Alfa Aesar, UK), pH 4.8. 100 mL of reaction buffer is prepared by mixing 59 mL 0.2 M sodium acetate, and 41 mL 0.2 M acetic acid (VWR, UK).

NaOH glycine buffer pH 10.8: 15 g of glycine (Sigma Aldrich, UK) dissolved in 300 mL of milliQ water. Adjust to pH 10.8 with NaOH (Sigma Aldrich, UK) pellets. Bring volume to 500 mL with milliQ water.

*p*NPG solution: Dissolve 80 mg of *p*NPG (Sigma. Aldrich, UK) in 50 mL of reaction buffer. Pre-heat *p*NPG solution to 50 °C (10-15 minutes).

Pre-heat the plate shaker to 50 °C.

Protocol

Take a sample from 150 µL from the culture, dilute it to an OD_{600} of 0.1 and aliquot 1 mL of the diluted culture into an Eppendorf tube. Label this tube “Tube 1”. Repeat this step in a second tube and label it second tube “Tube 2”. Centrifuge Tube 1 at 10 000 g, 1 min at RT. Transfer the supernatant from Tube 1 to a fresh tube labelled Tube 3 for subsequent assay. Resuspend the cells in Tube 1 in 1 mL µL of fresh MSM. Aliquot each assay sample into 3 wells (50 µL per well) in a 96 well plate.

50 µL from Tube 1 (Cells only)	50 µL from Tube 1 (Cells only)	50 µL from Tube 1 (Cells only)
50 µL from Tube 2 (Culture)	50 µL from Tube 2 (Culture)	50 µL from Tube 2 (Culture)
50 µL from Tube 3 (Spent media)	50 µL from Tube 3 (Spent media)	50 µL from Tube 3 (Spent media)

Figure 7 *Schematic showing the distribution of sample placement in a 96 well plate for the whole cell beta glucosidase assay*

Using a multichannel pipette, add 50 µL of *p*NPG solution to the each well. Incubate at 50 °C for 15 minutes with shaking at 750 rpm. While the incubation is happening, measure and record the OD_{600} of the samples in Tube 1 and Tube 2. After the incubation is complete add 100 µL of sodium hydroxide-glycine buffer to each well. Shake samples for 5 seconds in the plate reader before measuring the absorbance of the samples at 405 nm.

Repeat steps for all cultures.

2.3. Results and Discussion

The beta glucosidase assay was identified as the primary method of data collection in this work. The assay functions by assessing the amount of enzymatic activity seen from Tfu0937. This enzyme originates from *Thermobifida fusca YX*. The assay was designed to monitor the activity of extracellular Tfu0937, with further processing to distinguish between membrane bound and free enzyme. The intention of these exploratory experiments was to isolate potential issues that we might have optimised the pre-existing protocol in place for measuring free Tfu0937, versus membrane bound Tfu0937. To begin, the different display systems were expressed using standard protein expression protocol and cultivated in NB media.

2.3.1. NB cultivation

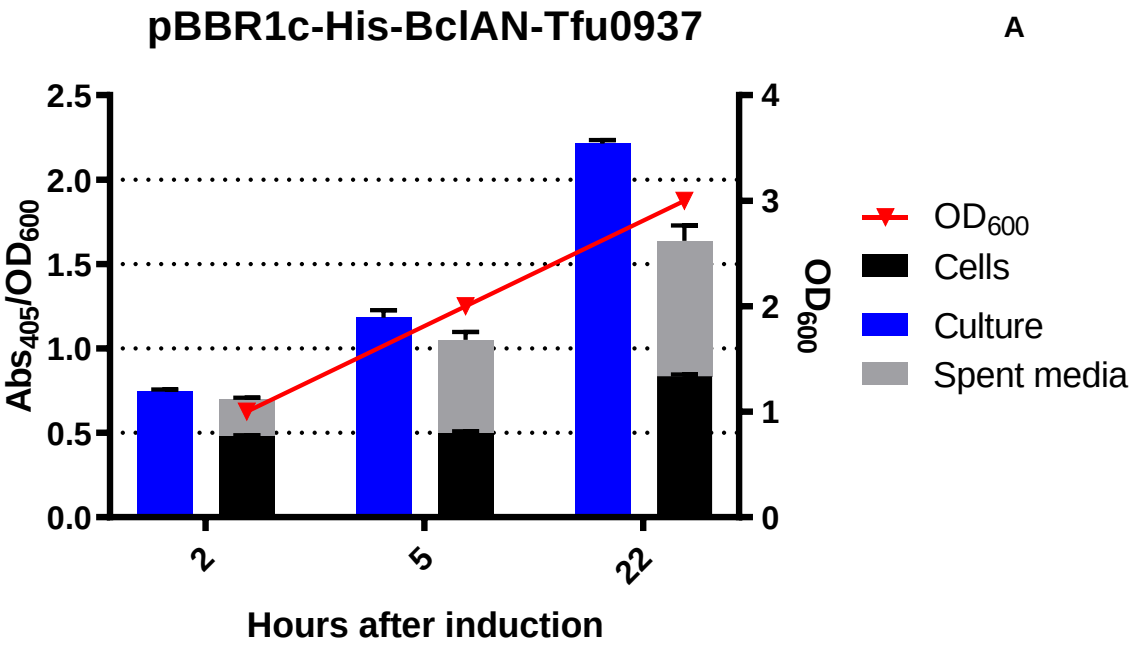

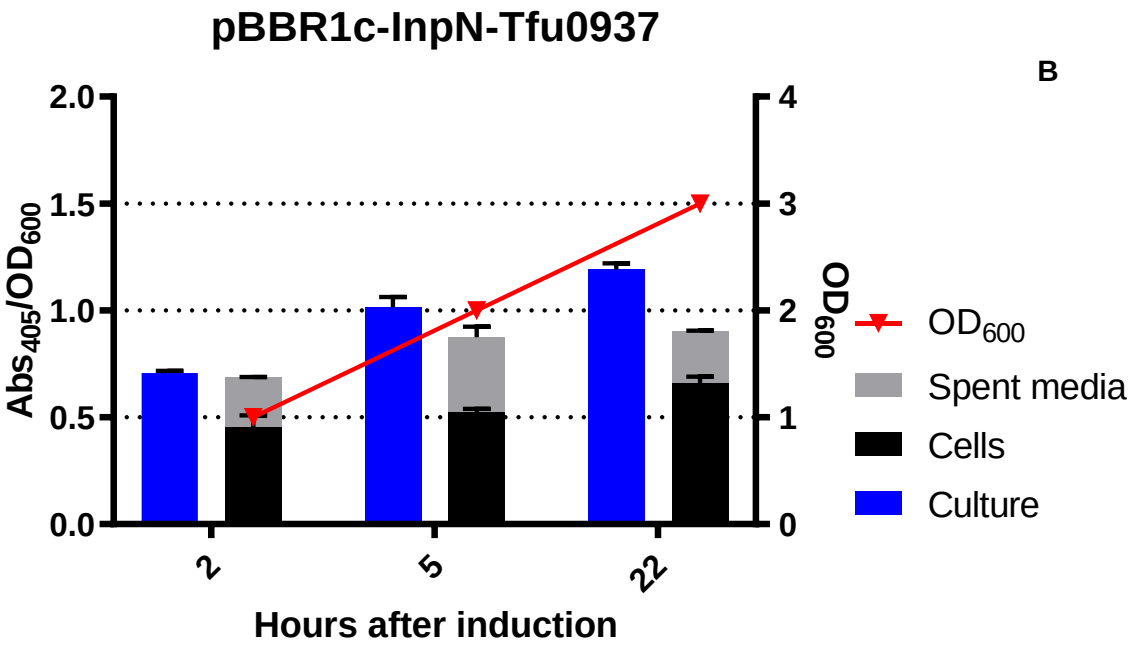

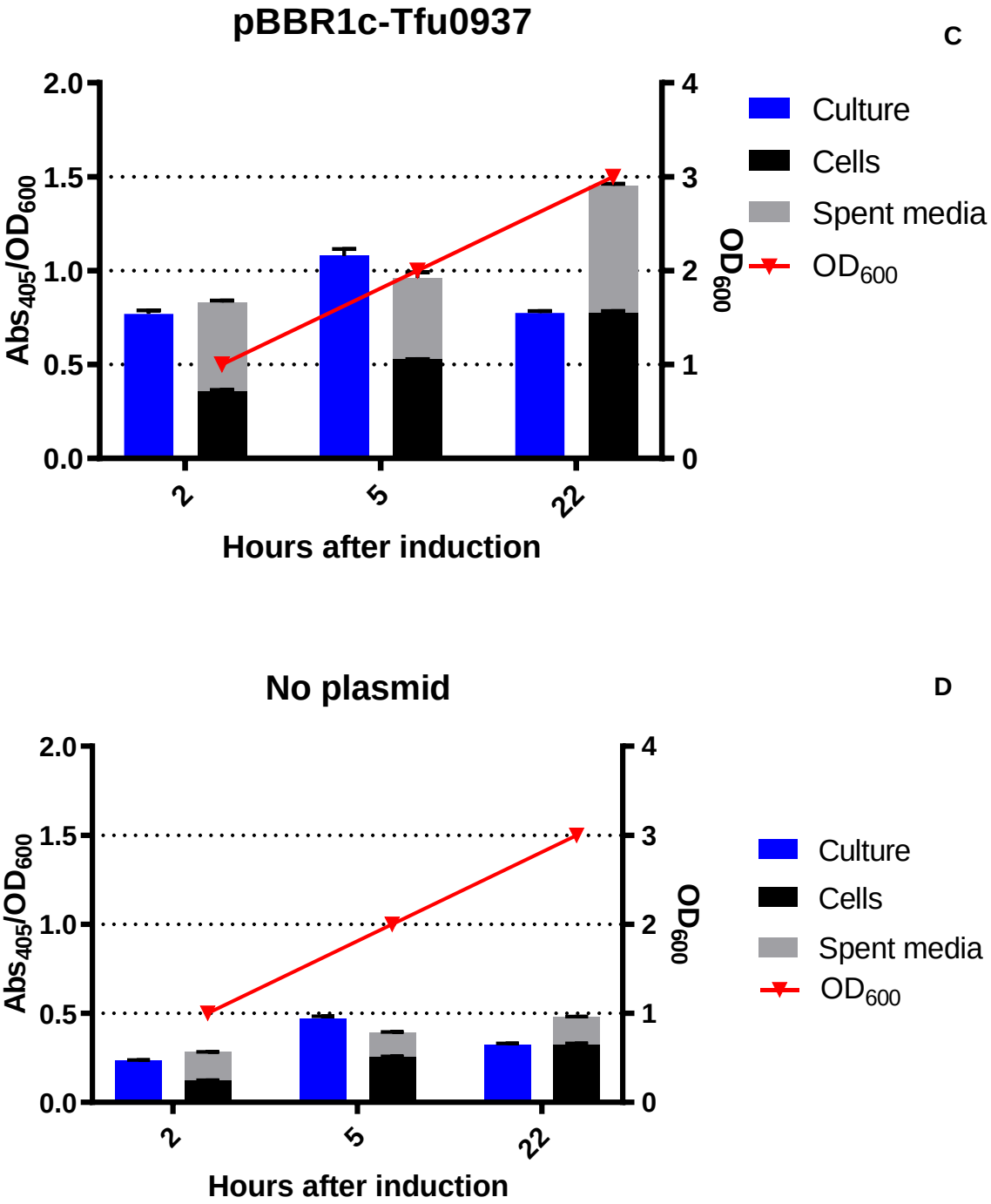

Figure 8 *Activity profiles of A: pBBR1c-BclAN-Tfu0937, B: pBBR1c-InpN-Tfu0937, C: pBBR1c-Tfu0937, and D: WT C. necator H16 cells with no plasmid. Activity measured across the approximately 1 day at points which were thought to represent the lag, exponential and stationary phase. Red line marks the change in* OD_{600} *over the course of the cultivation.*

The aim of the experiment was to assess the amount of displayed protein at each of the different growth stages of *C. necator* H16 expressing either BclAN-Tfu0937, InpN-Tfu0937, and Tfu0937. The data suggested there was a gradual accumulation of Tfu0937 activity on all the strains expressing Tfu0937, regardless of if it was fused to an anchoring motif or not. Following **Figure 8**, and looking first at pBBR1c-BclAN-Tfu0937, we can see the total amount of activity between 2 and 5 hours showed an increase, but it was clear that this was due to an accumulation of extracellular Tfu0937 and not cell bound Tfu0937 (black bar). Between the 5-22 hours after induction, there was an increase in both the cell bound and extracellular Tfu0937. suggesting that the expression of the BclAN-Tfu0937 fusion protein is following a typical increase during the cultivation, but that the display of the protein is slower than the rate of production.

When analysing the production in the InpN-Tfu0937 system, we could see that the trend in activity similar to that of the BclAN-Tfu0937 system. The only exception is that the accumulation of extracellular Tfu0937 is lower than that of the BclAN-Tfu0937 system. This could hint at possible lack of stability within the BclAN system, or perhaps excess intracellular Tfu0937 is leaking into the media because of over expression and cell death over the course of the cultivation. This theory is further supported by the idea that the over-expression of a membrane bound protein may lead to loss of cell viability (Wagner *et al.*, 2007). While not as extreme, the same phenomenon may be present in these systems.

The control system that was designed for this assay was the expression of Tfu0937 by itself to see if any activity would be present in any of the areas that were being tested (membrane/extracellular space). Here clear activity was seen in the both membrane and the spent media, showing a very similar activity profile to that of BclAN-Tfu0937. This was the case for the cell associated activity as well as the accumulation of Tfu0937 in the media. When assessing the data from the cells harbouring no plasmid, there was visible activity in the fractions albeit significantly less.

This made it clear that there were some potential shortfalls in the way this data set was being obtained. The first issue was that using NB as the culture medium was causing unnecessary problems as its straw colour was present in all parts of the assay. This meant that the yellow colour produced by the 4-

nitrophenol, was being interfered with during the assay. This could potentially explain the high amounts of assumed activity within the spent media, but also would be causing issues with readings across all the different assays. The fact that the cells were also growing at different rates meant that the change in colour of the media would not be identical across all the cultures. So, the first step for optimising the assay was to move out of the NB media system and into a colourless and clear media, that would not result in these issues. As it were, *C. necator* H16 is often cultivated in MSM for a multitude of experiments, with its only potential drawback being the extended growth period due to the increased concentration of carbon source.

2.3.2. MSM media supplemented with 1% gluconate

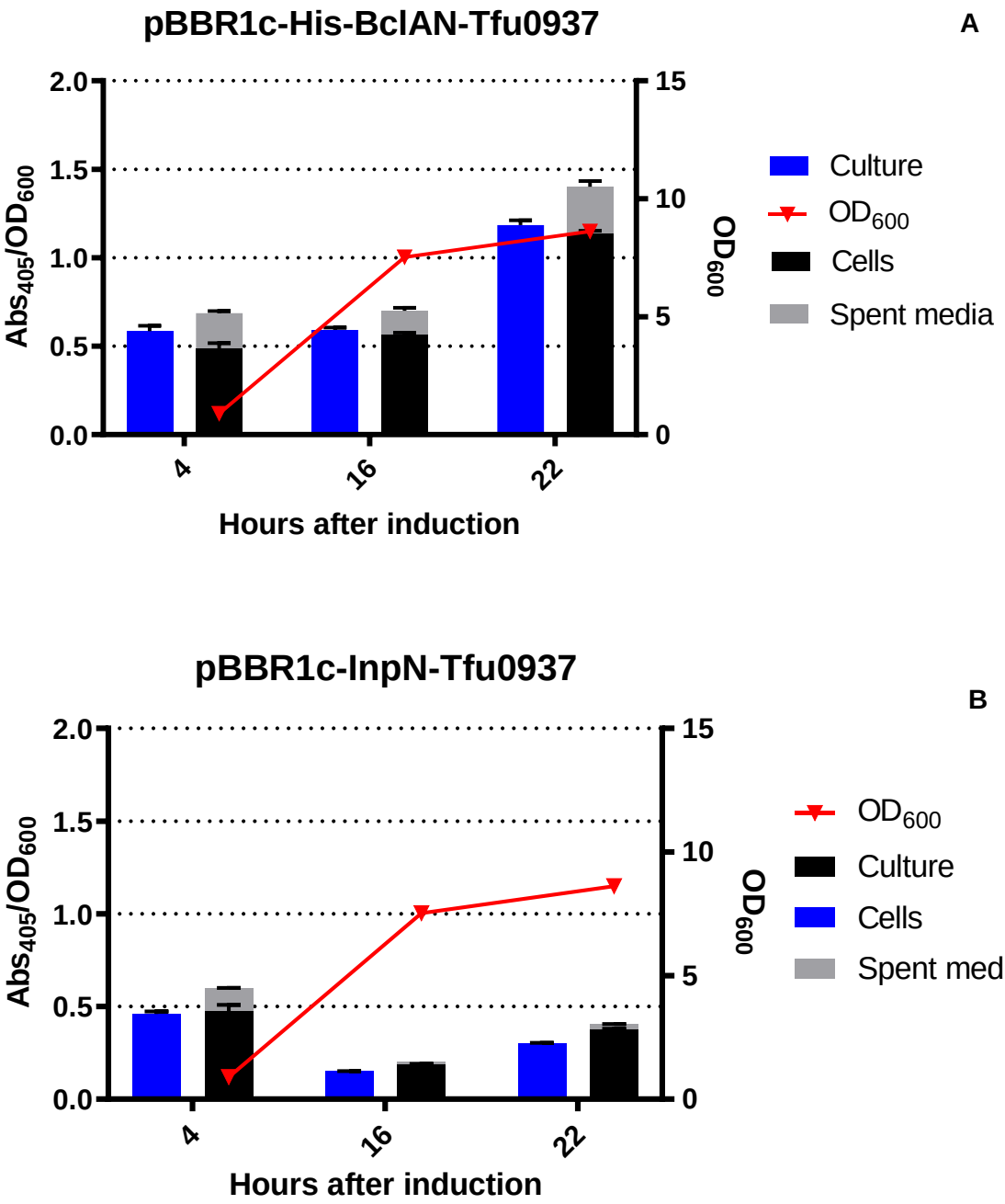

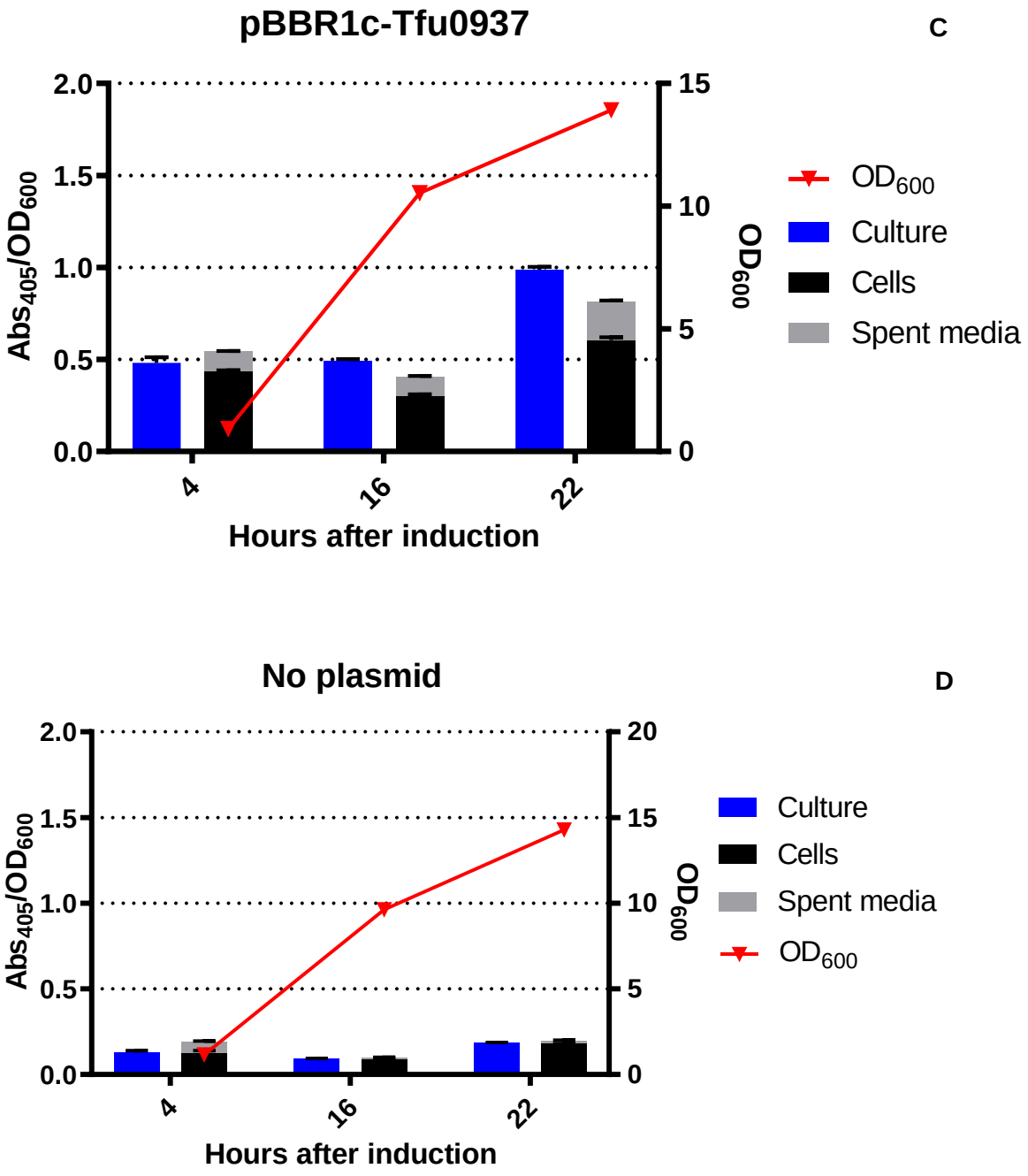

Figure 9 *First set of biological repeats using the pBBR1c- strains when cultivation the cells in MSM supplemented with 1% gluconate.*

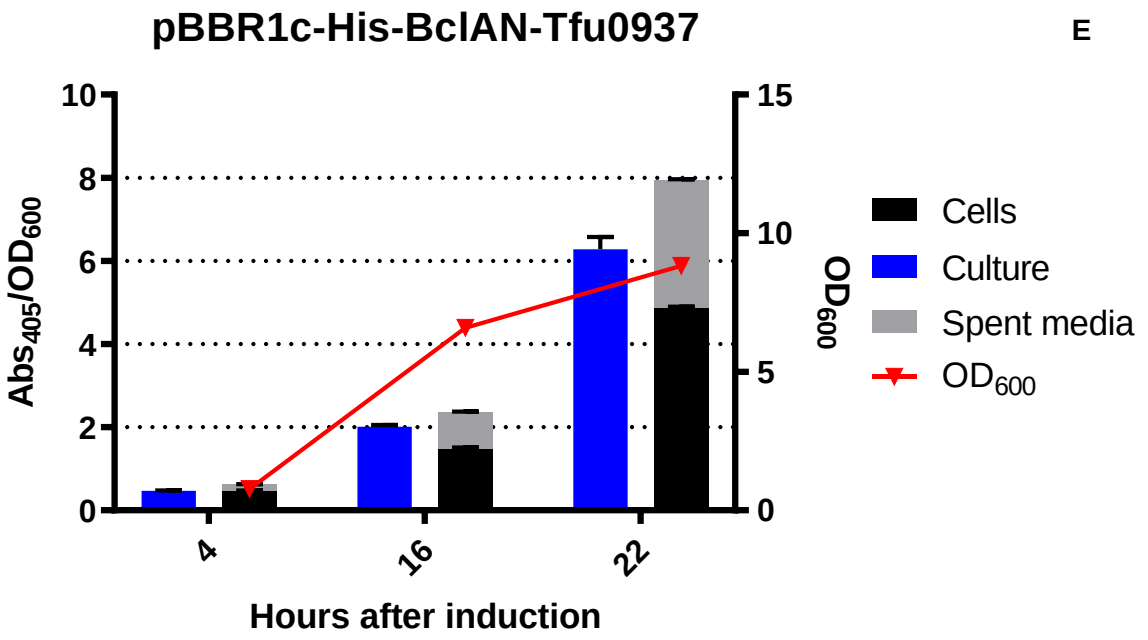
pBBR1c-His-BclAN-Tfu0937
E
Abs405/OD600
OD600
Cells
Culture
Spent media
OD600
Hours after induction
0
2
4
6
8
10
0
5
10
15
4
16
22

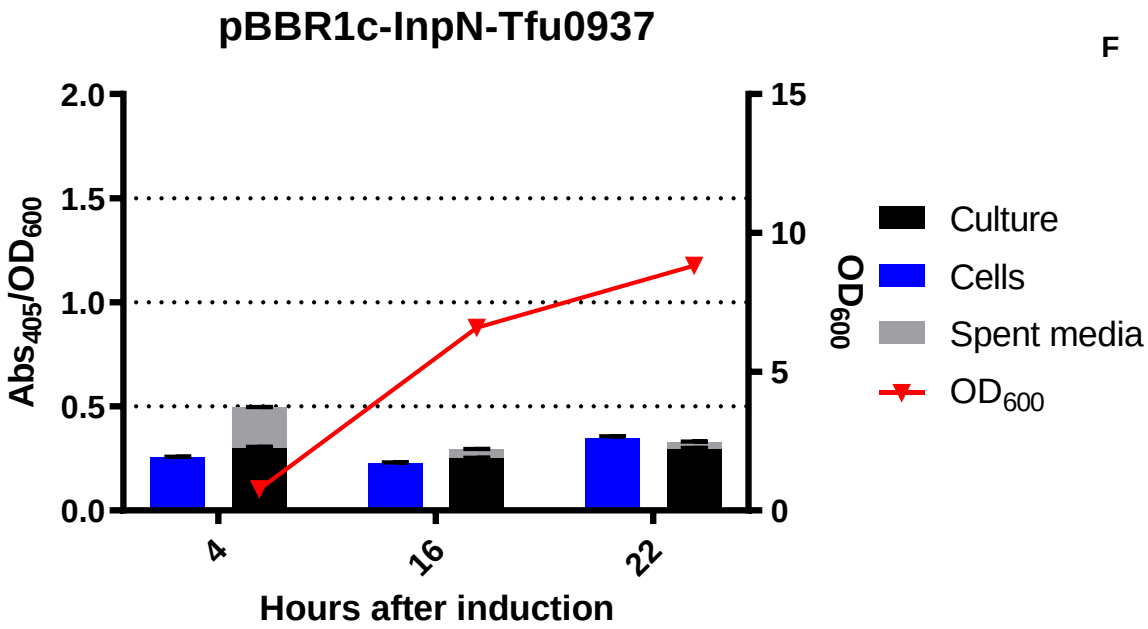
pBBR1c-InpN-Tfu0937
F
Abs405/OD600
OD600
Culture
Cells
Spent media
OD600
Hours after induction
0.0
0.5
1.0
1.5
2.0
0
5
10
15
4
16
22

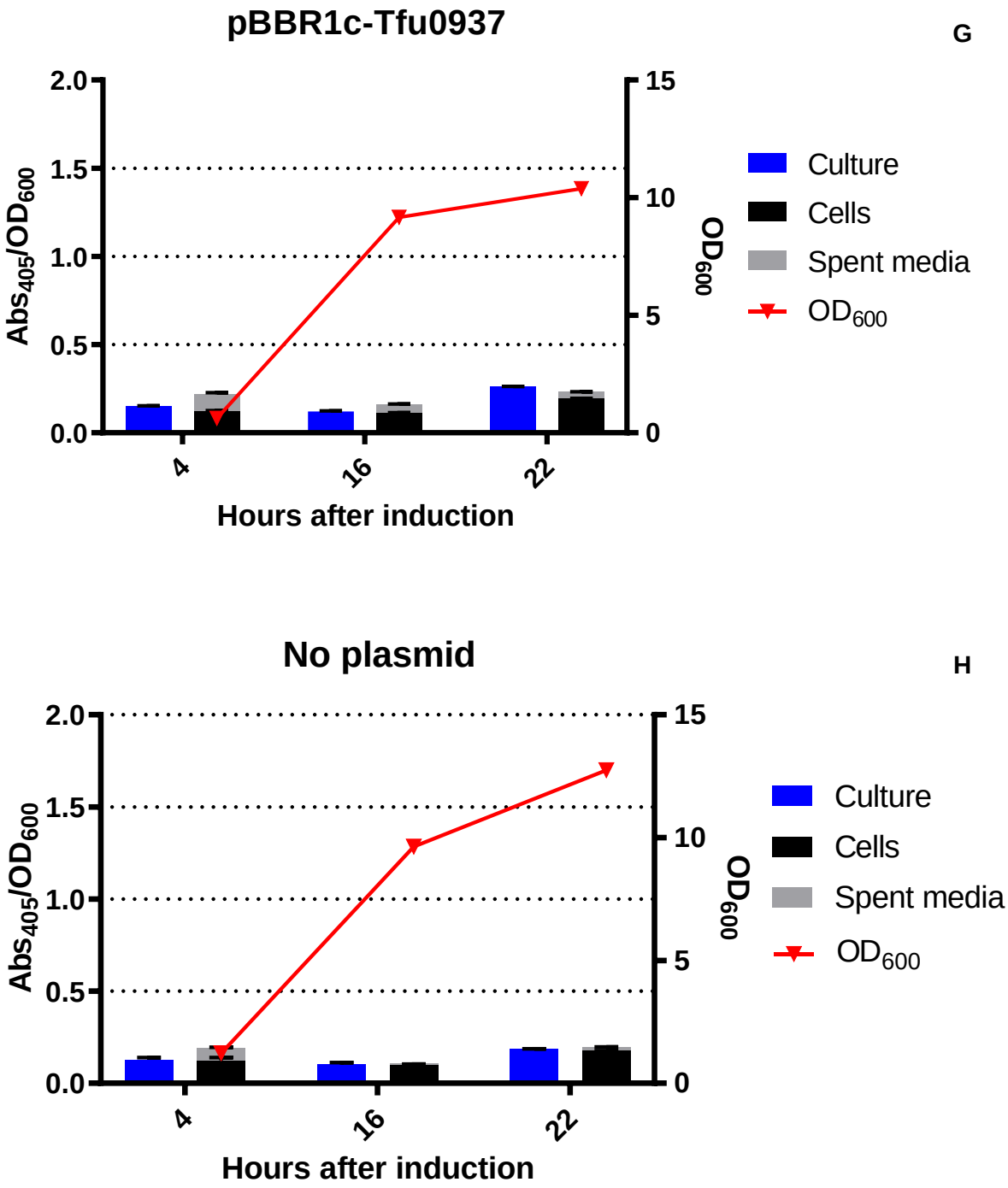

Figure 10 *Second set of biological repeats using the pBBR1c- strains when cultivation the cells in MSM supplemented with 1% gluconate.*

The data here illustrated in **Figure 9** and **Figure 10** some key differences and similarities between the two experiments. The first issue was a 3-fold difference in activity between the two BclAN cultivations, with the increase being observed in the second cultivation. The InpN shows unusual activity profile in the first cultivation, suggesting a loss of activity of ~40% in the first cultivation, however this is not

present in the second cultivation. Overall activity in the cells expressing Tfu0937 show a difference in activity of 50% between these 2 experiments, with the more activity being present in the first experiment.

It was noted that the cells in some of these experiments would take a particularly long time to grow (8 hours) from OD_{600} 0.2 to 0.4. This suggested that the cells were likely still in the very early log phase, if not the lag phase when induced. This effect was extrapolated for all the previous repeats and gave a potential rationale for the inconsistency of the activity profiles.

The Tfu0937 cells have less fluctuations in the amount of activity per cell, which is also concomitant with the consistent growth rate of the cells. The BclAN cells show more inconsistent activity, alongside inconsistent growth. It has already been put forward that the expression of any protein that interferes with the outer membrane can influence the cell viability, however it is not clear if the lowered cell growth is due to the loss of cell viability or because more cellular resources are being directed towards synthesis and translocation of the Tfu0937 fusion.

When approaching the assessment of data holistically, it seems that it is more likely that the cells are growing less when they produce more protein as is shown by the inverse proportionality between activity per cell and the OD_{600} after 24 hours.

Given the current scope of understanding of the system, it was agreed that the best course of action was to optimise the expression system to get the best activity profile. The first of these issues was the unusually low and fluctuating activity of the pBBR1c-InpN system.

2.4. INP fusion instability

One of the key issues with the data gathered during the cultivation experiments is that the INP-Tfu0937 fusion appeared to be losing activity after 16 hours after the induction of the protein. This was indicative of potential issues with stability of the fusion protein. To investigate this further, SDS gel analysis of the whole cell lysate was done to investigate if the protein was still intact in the later stages of the cultivation

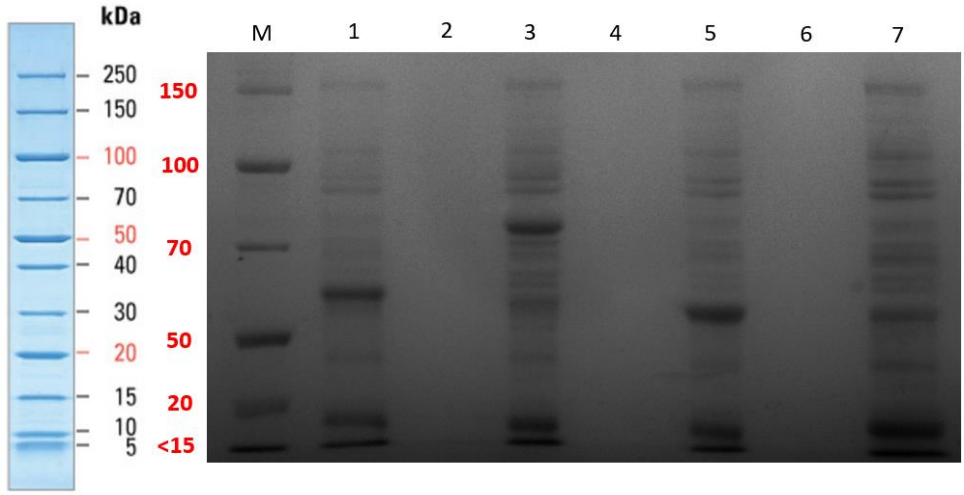

Figure 11 *Samples taken at 4 hours after induction. Lane M: Marker, Lane 1: pBBR1c-BclAN Tfu0937 whole cell lysate, Lane 2 pBBR1c-His-BclAN-Tfu0937 culture supernatant, Lane 3 pBBR1c-InpN-Tfu0937 whole cell lysate, Lane 4: pBBR1c InpN-Tfu0937 culture supernatant, Lane 5: pBBR1c-Tfu0937 whole cell lysate. Lane 6 pBBR1c-Tfu0937 culture supernatant. Lane 7: WT no plasmid, whole cell lysate. The concentration of cells loaded into the wells was between* OD_{600} *15. MW of His-BclAN-Tfu0937 fragment 57.4 kDa, InpN Tfu0937 fragment- 72.4 kDa, Tfu0937 fragment-53.4 kDa*

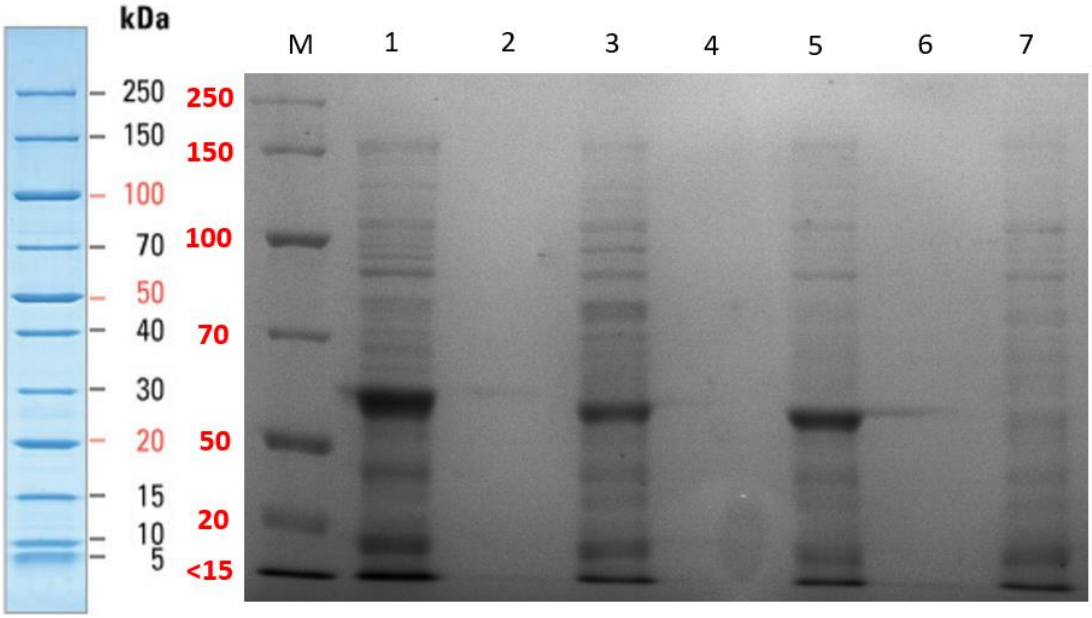

Figure 12 *Samples taken at 20 hours after induction. Lane M: Marker, Lane 1: pBBR1c-BclAN Tfu0937 whole cell lysate, Lane 2 pBBR1c-His-BclAN-Tfu0937 culture supernatant, Lane 3 pBBR1c-InpN-Tfu0937 whole cell lysate, Lane 4: pBBR1c InpN-Tfu0937 culture supernatant, Lane 5: pBBR1c-Tfu0937 whole cell lysate. Lane 6 pBBR1c-Tfu0937 culture supernatant. Lane 7: WT no plasmid, whole cell lysate. The concentration of cells loaded into the wells was between* OD_{600} *15. MW of His-BclAN-Tfu0937 fragment 57.4 kDa, InpN Tfu0937 fragment- 72.4 kDa, Tfu0937 fragment-53.4 kDa*

The gel images in **Figure 11** and **Figure 12** showed degradation of the fusion protein, with a distinct loss in the 72 kDa band (InpN-Tfu0937) in the 20-hour sample. This was something that had been previously reported in other publications (Li, Gyun Kang and Joon Cha, 2004) that had used the InpN system, however, it was reported to primarily affect the cytosolic protein fraction. The fusion was said to have much higher stability once integrated with the membrane. However, this may be evidence enough that the system is unstable in the later stages of the cultivation. One other observation that can be made from this gel is the lack of the INP fragment that should theoretically be present if only the domain between the N terminal domain of the INP and the Tfu0937 is prone to protease attack. One possible explanation for this is that it is more likely to be targeted for proteolysis by cytosolic proteases because of the presence of the domain, and its size may make it more amenable for degradation. Tfu0937 on the other hand would remain a fully folded protein even after its separation from the InpN domain, making it less likely to be degraded. Experiments using this system were largely postponed until much later when some new considerations were made regarding the time for which the complex was stable.

2.5. Optimising the expression conditions for His-BclAN-Tfu0937

To understand why there could be large amounts of variation in expression between experiments, a brief analysis of different factors affecting protein expression was done. The following factors were all considered as potential reasons for unusual expression patterns.

2.5.1. Strength" of the promoter

The araP_{BAD} promoter used in this system is tightly regulated. There have been no results showing any basal expression in cells that contain the plasmid but have not been induced. It is unlikely that this has anything to do with the inconsistent protein expression profile.

2.5.2. Stability of the cloned protein

If BclAN-Tfu0937 or just Tfu0937 were unstable, then there would not be instances where the protein accumulates in high levels in the membrane as observed in the repeated experiments of expression analysis. The protein has also been confirmed to accumulate in the cells though protein SDS gel analysis

2.5.3. Stability of the gene

Gene was confirmed to be stable and remained present in the cells through PCR. The gene of interest Tfu0937 was amplified in both the BclAN-Tfu0937 and the pBBR1c-Tfu0937 variant. There was clear banding in the PCR indicating presence of both genes in their respective cells. This is further combated using antibiotics throughout the duration of the induction. Antibiotics ensure that there is minimal survival of any bacteria not harbouring the plasmid. It must be noted however that the *C. necator* cells do show slight resistance the working concentration of chloramphenicol used in the beta glucosidase assay. Despite this, it is still unlikely that this alone would be responsible for large fluctuations in protein expression.

2.5.4. Metabolic state of the cell

This pertains particularly to the growth phase in which the cells are induced. Literature states that induction at low OD_{600} may lead to attenuated growth. Studies have shown that inducing in the early log phase causes the cells that are being actively induced to be slowed in growth. The cells which can dedicate more of their resources to growth begin to proliferate more than those expressing protein. This is made even worse by the fact that $araP_{BAD}$ and many common regulated expression systems utilize high affinity active transport of inducer. The variable levels of the regulatory proteins involved in this transport result in a very steep induction curve. This leads to an all-or-none induction of an increasing number of cells rather than a homogeneous increase in all cells. Reports of this have shown that at concentrations of 10^{-4} µg/mL of arabinose (equivalent to 0.2%), the highest degree of variation in expression heterogeneity is observed (see **Figure 13**).

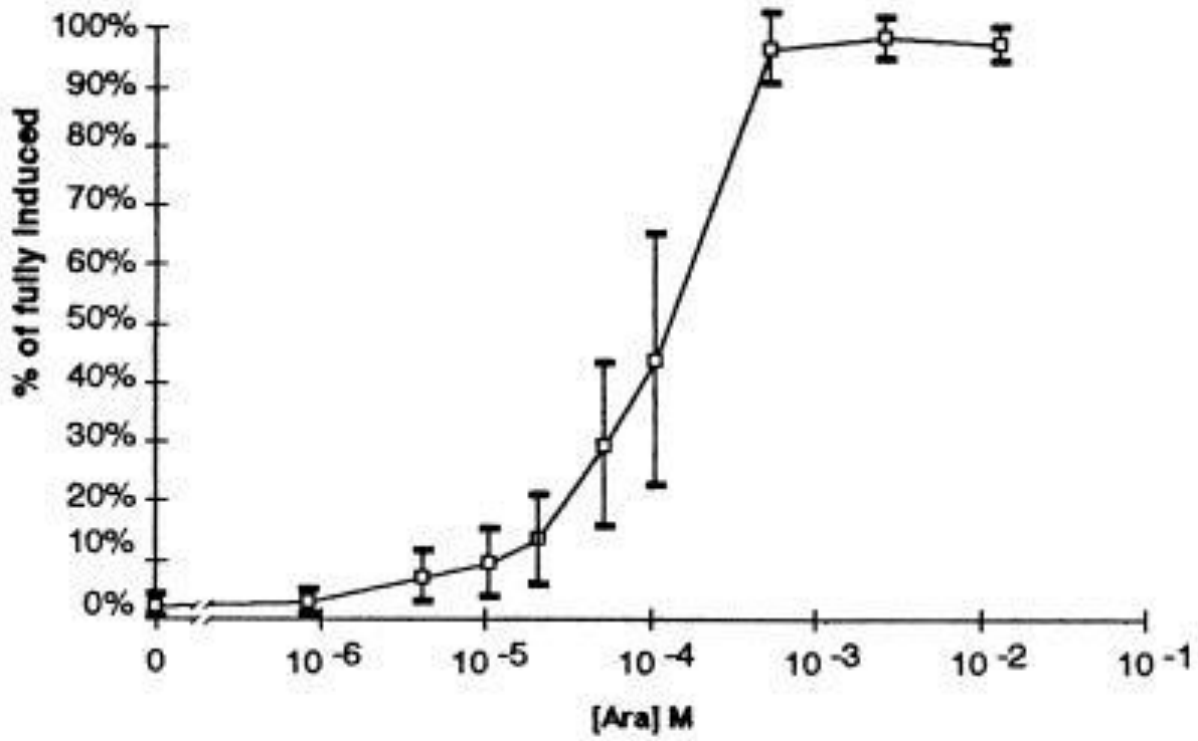

Figure 13 *Dependence of GFP levels on inducer concentration. Cultures were grown in the presence of the indicated concentrations of arabinose for 5 hrs. Fluorescence was measured on suspensions of intact cells. Figure from Siegele DA, Hu JC* (Siegele and Hu, 1997).

The activity of the cells was measured five times across a series of biological repeats, to see the extent of the activity fluctuations. While a relatively consistent growth rate and activity was observed in the pBBR1c-Tfu0937 strain, the most striking result was that the pBBR1c-His-BclAN-Tfu0937 strain had much more erratic activity.

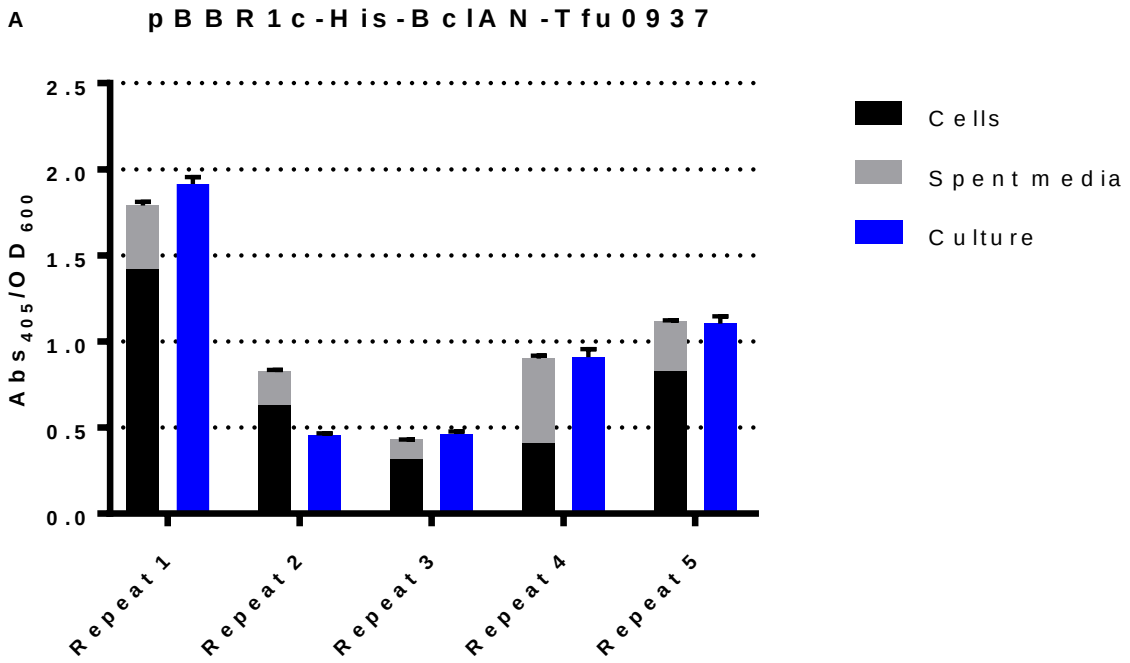

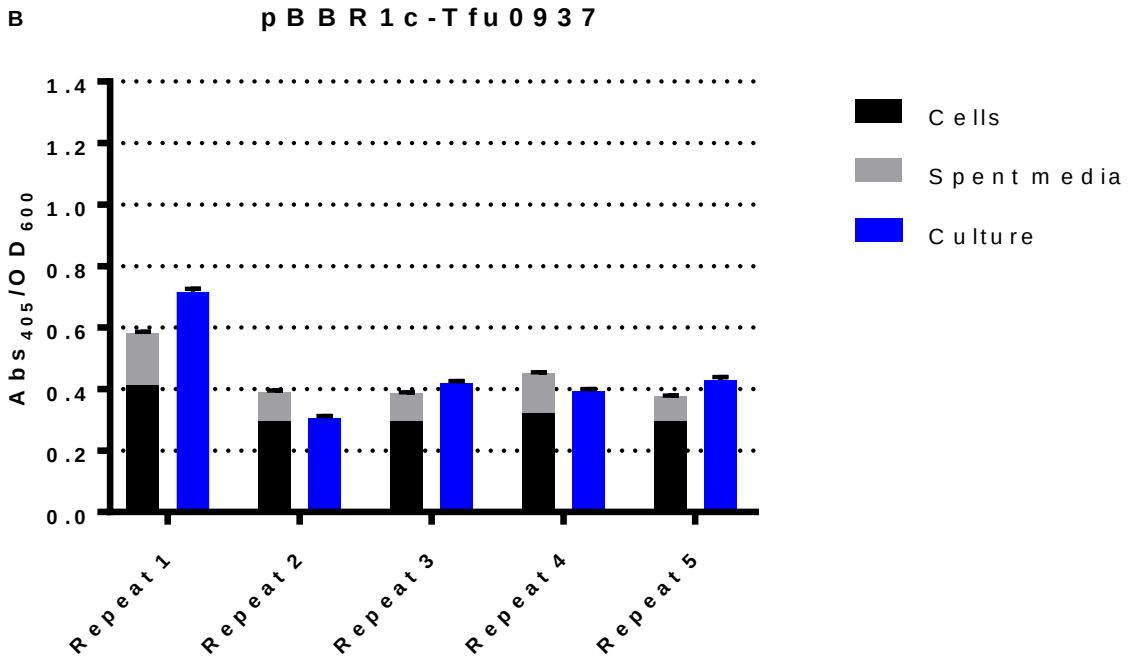

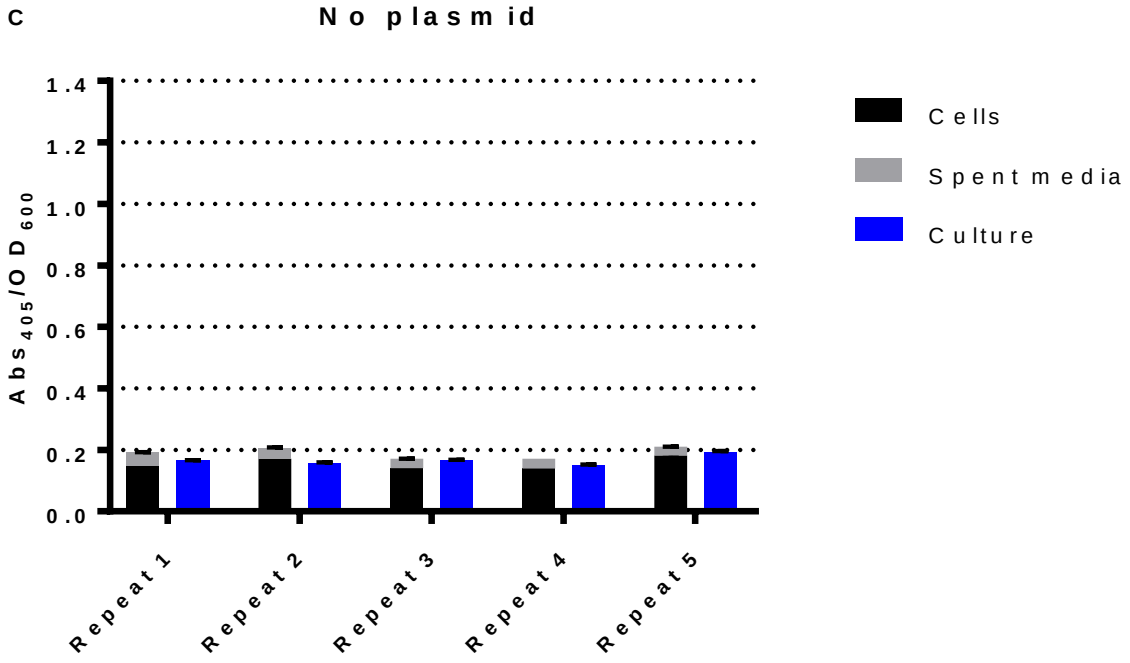

Figure 14 *Relative activities of cells when the beta glucosidase was repeated 5 times to assess the variation in expression. Strains pBBR1c-His-BclAN-Tfu0937(panel A) and pBBR1c-Tfu0937(panel B) were tested 5 a total of 5 times. All cultures were cultivated and expressed in MSM, excluding repeat 4. The pre culture for repeat 4 was prepared in NB media, but expression was conducted in MSM.*

Table 9 *The different parameters of the repeated beta glucosidase assays. Repeat number 4* (marked with a star) is a repeat where the pre cultures were grown for 10 hours in NB as opposed to 36-40 hours in MSM.*

Anchoring Motif	Repeat number	Duration pre-culture growth (hours)	Time between T_0 and T_i (hours)	OD of pre-culture	OD_{600} at T_0	OD_{600} at T_i	OD_{600} after 24 hours induction
BclAN	1	36	5.5	11.52	0.147	0.225	2.84
No motif	1	36	5.5	12.66	0.142	0.253	5.84
No plasmid	1	36	5.5	14.50	0.240	0.434	12.16
BclAN	2	40	5	14.67	0.187	0.262	6.08
No motif	2	40	5	14.20	0.196	0.236	9.56
No plasmid	2	40	5	13.71	0.217	0.438	12.59
BclAN	3	38	5.5	9.09	0.264	0.363	12.61
No motif	3	38	5.5	11.69	0.246	0.319	9.76
No plasmid	3	38	5.5	13.12	0.245	0.356	12.67
BclAN	4*	10	3	3.246	0.271	0.590	10.60
No motif	4*	10	3	3.574	0.245	0.492	9.81
No plasmid	4*	10	3	3.550	0.344	0.619	11.81
BclAN	5	40	8	12.97	0.218	0.307	5.48
No motif	5	40	8	13.22	0.209	0.397	9.01
No plasmid	5	40	8	13.32	0.230	0.436	10.42

The protocol stated that the cells must be induced at an OD_{600} of 0.4, however, due to time constraints, this was not always possible as the cells were taking exceptionally long to grow. This often led to inductions of between 0.2 and 0.3. In previous experiments, the cells would take close to 4 hours to grow from OD_{600} of 0.2 to 0.4. For this set of experiments longer periods of growth, and still not reaching the optimal OD_{600} of 0.4. This was believed to have played a major part in the inconsistencies seen in the activity values across the repeats.

In Repeat 1, there was very slow growth with the cells reaching a low OD_{600} of 2.84 after 24 hours of induction. Similarly, the pBBR1c-Tfu0937 cells only reached a growth of 5.96. When we look at the corresponding activity graphs, these were the most active cells (see **Figure 14**).

In the repeats 2 and 3, there are more cells after 24 hours of induction, but less activity per cell. There seems to be a correlation between growth rate and activity. If the growth rate is low, the cells are more active.

The activity of the pBBR1c-Tfu0937 cells is quite consistent across repeats 2, 3, and 4. This corresponds with the relatively similar OD_{600} at 24 hours after induction for each repeat. These were 9.56, 9.76, 9.81 respectively. The consistent growth correlates with consistent levels of activity per cell.

There seems to be slower growth when the cells are induced earlier. The growth rates, growth phase, and OD_{600} at time of harvest, all seem to play a vital role in determining the final activity of the cells. The next step was to look at the effects of inducing at different OD_{600} would have. The results from this work illustrated the potentially large consequences for not executing these areas of the protocol consistently.

The pBBR1c-Tfu0937 cells had a low range of activity. However, the pBBR1c-His-BclAN-Tfu0937 cells showed higher fluctuations in activity between repeats. The difference in activity could not be clearly correlated to anything other than the fact that the cells may have been in different growth stages when induced, leading to different expression profiles.

2.6. Investigating plasmid stability

Another potential reason for inconsistent expression was plasmid stability. To assess this, a PCR was performed on the induced pBBR1c-His-BclAN-Tfu0937 cells, and pBBR1c-Tfu0937 cells to see if either plasmid was losing stability during the expression (see **Figure 15**).

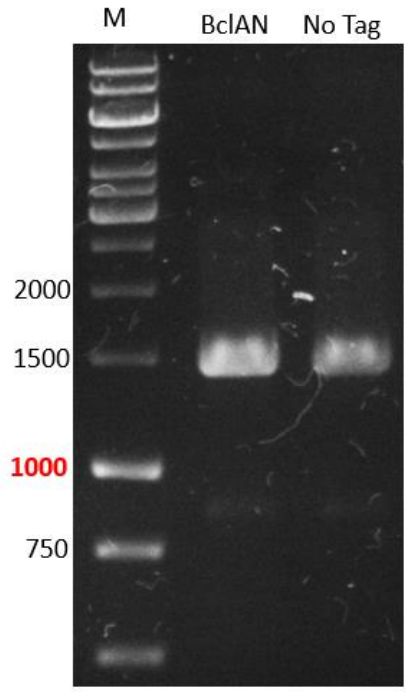

Figure 15 *PCR image confirming the presence of the plasmid in the culture after 24 hours of induction.*

The PCR amplified the His-BclAN-Tfu0937 gene sequence from the pBBR1c-His-BclAN-Tfu0937 cells and the Tfu0937 gene sequence in the pBBR1c -Tfu0937 cells. Their respective sizes are 1536 bp and 1455 bp. Cells were showing presence of the plasmid 24 hours after expression.

The previous experiments illustrated that inducing at varying OD_{600} values can influence the expression of *C. necator* harbouring the pBBR1c-His-BclAN-Tfu0937 plasmid.

2.6.1. Induction profiling

The aims of this experiment were to investigate the effect of inducing at an OD_{600} of 0.4, 0.9, 1.6, and 5. The following information was ascertained from this data.

- The best performing induction OD_{600}
- Relationship between growth and activity
- Effect of inducing with different arabinose concentrations (0.2%, 0.1%, 0.02%)

2.6.1.1. OD_{600} of 0.4

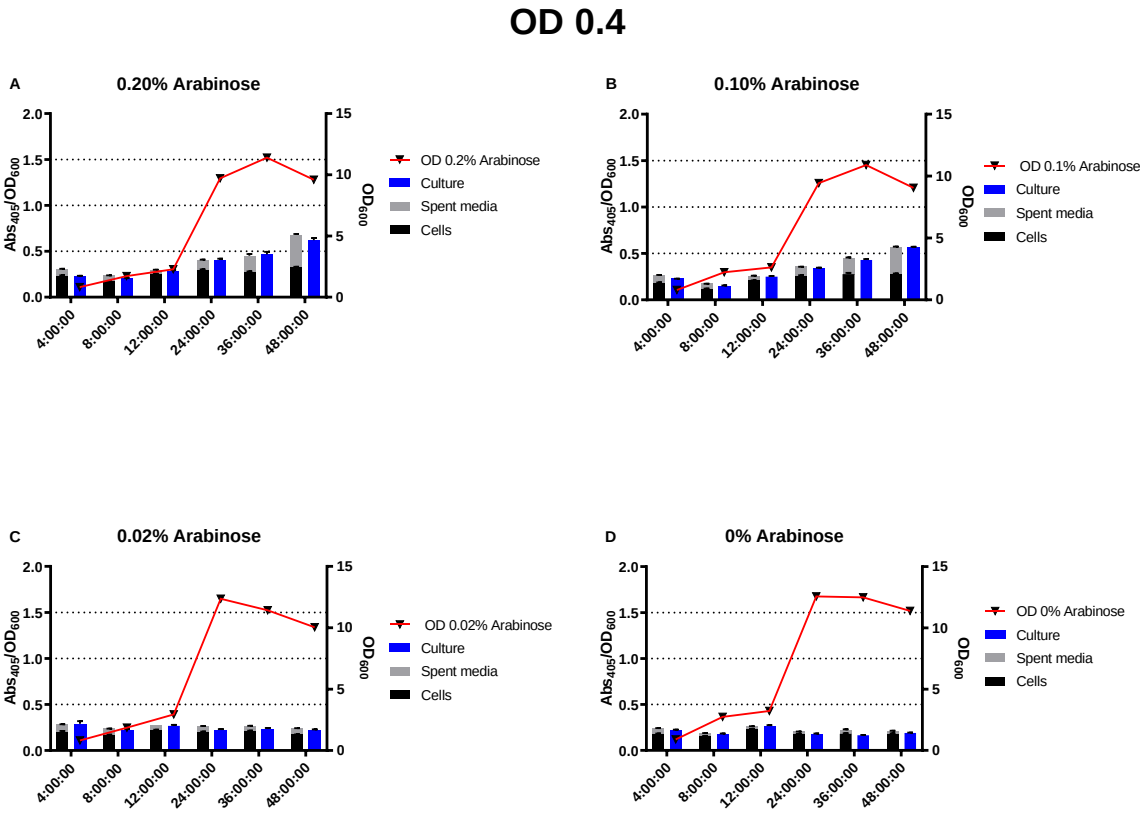

Figure 16 *Growth curves for cells after induction at an OD_{600} of 0.4. On the same graphs, the relative activities of the cells have been shown at different time points after induction.*

The activity of the cells in this experiment is most accurately represented by the cells only. These are the cells that have been washed before being assayed (see **Figure 16**). All activity in this sample is likely only going to be as a direct result of extracellularly displayed Tfu0937. The first important piece of information is that induction at higher concentrations does lead to more activity per cell. However,

the difference between using 0.2% arabinose and 0.1% is minimal. There is slightly more activity in the spent media after 48 hours of induction in the 0.2, but this can be attributed to the lower cell density, indicating higher cell death at this time point (see **Figure 16**).

2.6.1.2. OD_{600} of 0.9

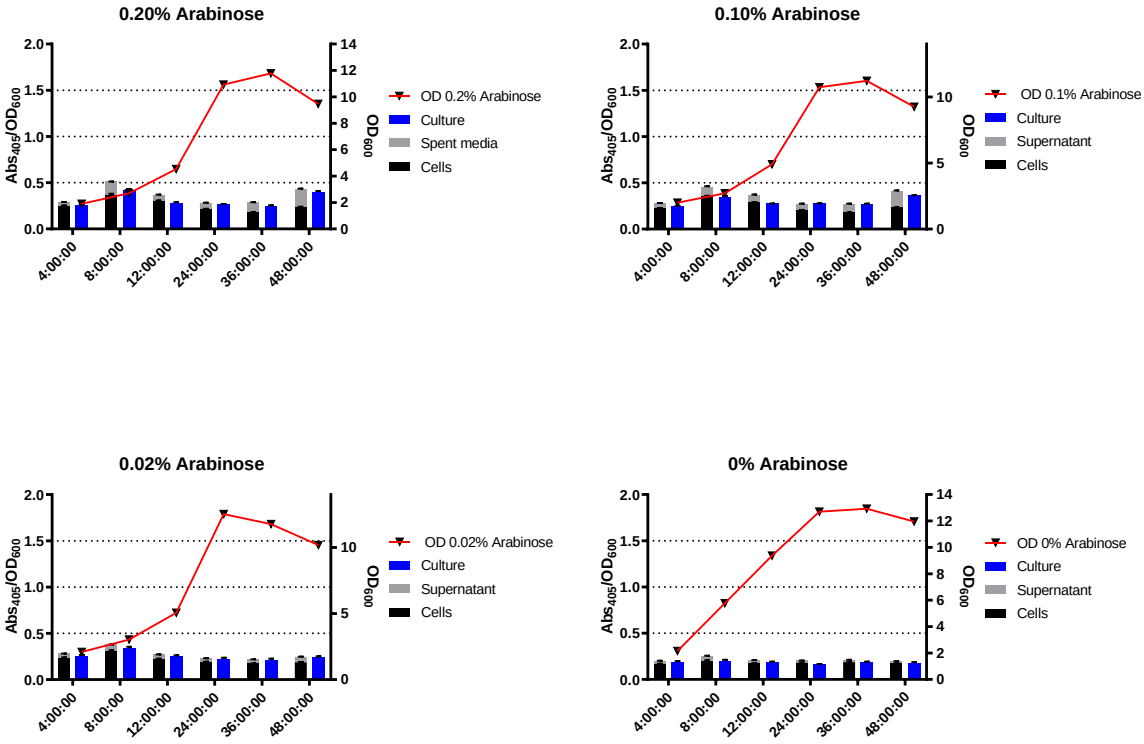

Figure 17 *Growth curves for cells after induction at an OD_{600} of 0.9. On the same graphs, the relative activities of the cells have been shown at different time points after induction. Graphs for the induction at 0.02% and 0% are not shown due to their similarity to the data presented for the induction at OD_{600} of 0.4.*

The activity per cell value for cells seems to fluctuate throughout the duration of the experiment. In the OD_{600} 0.4 induction, the activity per cell value hovers around 0.25-0.3. When induced at an OD_{600} of 0.9, this value is in the range of 0.20-0.25, with a peak at 0.35 at the 8-hour time point.

The maximal activity per cell for each induction OD_{600} was reached at separate times. When induced at OD_{600} = 0.9 it was at 8 hours post induction, and for induction at OD_{600} = 0.4, it was 48 hours post induction. This is an interesting phenomenon that does not particularly correlate to the growth of the cells. It appears that the translocation and expression of the protein are separate bottlenecks. It is not clear which of these then influences the growth of the cells or vice versa (see **Figure 17**).

A complicated issue being faced with this data is the reduction in total activity, i.e., activity in the culture after 8 hours, a trend that continues until 24 hours after induction. This indicates a loss of enzymatic activity, which can either stem from denaturation of the enzyme, or loss/degradation of the enzyme, neither of which seem to likely possibilities.

2.6.1.3. OD_{600} of 1.6

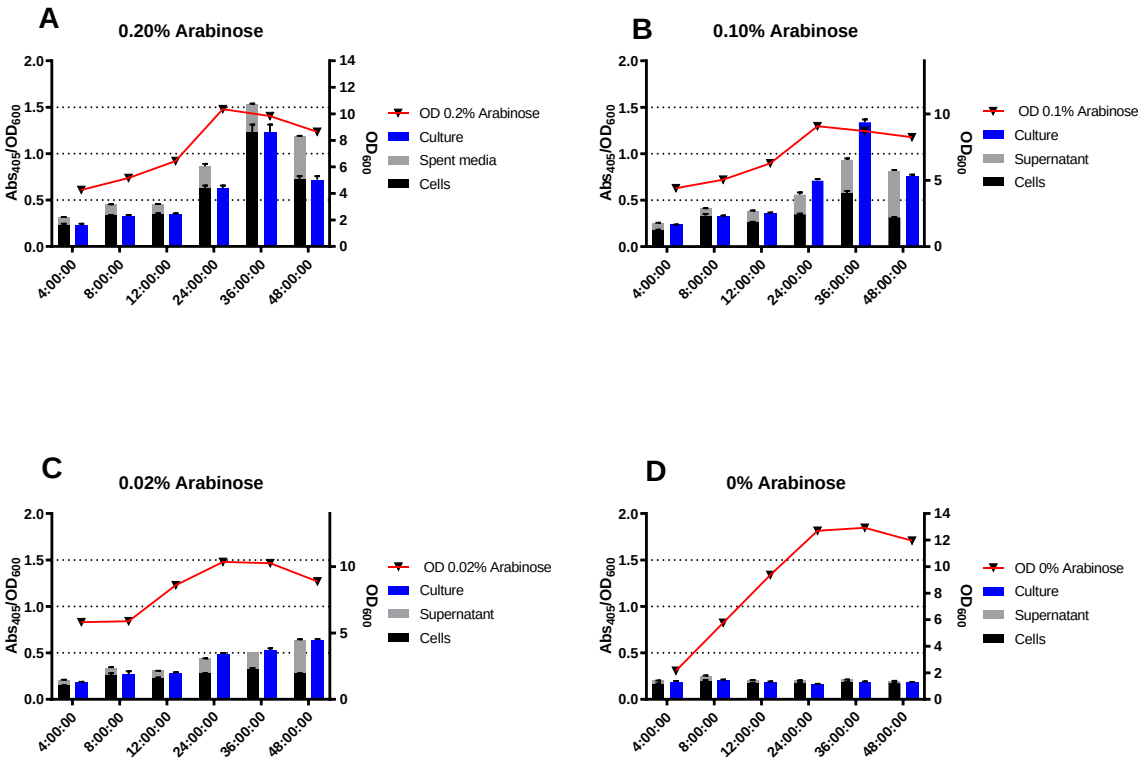

Figure 18 *Growth curves for cells after induction at an OD_{600} of 1.6. On the same graphs, the relative activities of the cells have been shown at different time points after induction. Graphs for the induction at 0.02% and 0% included here to show the difference in activity at 36 hours. Activity from the cells in ppanels A and B show stagnation in activity between 8 and 24 hours, with a decline in activity between 8 and 16 hours. Unwashed cells show similar trend, but with no decline between 8-16 hours. Instead, there is steady increase between 8-16, with sharp increase at 24 hours.*

The growth rates and growth patterns of the cells change dependent on when the cells were induced. When induced at OD_{600} = 1.6, there is an extended lag phase in the early stages of growth. This is illustrated by the slow growth rate between the first 36 hours of expression in panel A and B (0.2% and 0.1% induction).

Between 24-36 hours, the highest values of activity per cell is reached, but a strange issue is noted when this occurs. The summation of the cells and the media is not equivalent to the culture. Given that these

samples are prepared by separating their constituents, it seems unlikely that it is possible for them not to summate. In the 0.1% induction sample there is another issue with the data. After 48 hours, the activity appears to decrease in the culture (see **Figure 18**).

Induction at OD_{600} of 1.6 seems to be the optimal condition as it yielded the highest activity per cell. Using an arabinose concentration of 0.1% also yields the highest activity, but it is still almost identical to that of the 0.2%.

2.6.1.4. OD_{600} of 5

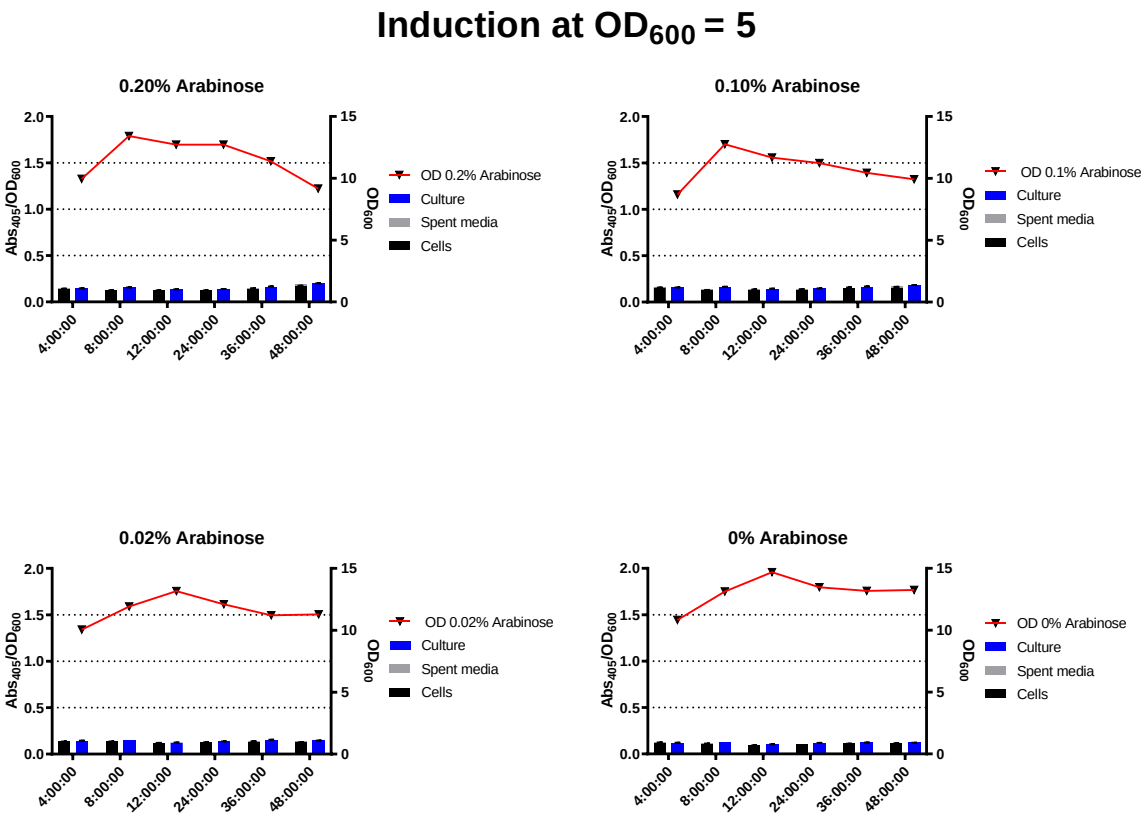

Figure 19 *Growth curves for cells after induction at an OD_{600} of 5. On the same graphs, the relative activities of the cells have been shown at different time points after induction. All graphs shared very similar values. Only negative control and 0.2% induction are shown as 0.1% and 0.02% induction showed similarly low levels of activity.*

The induction of the cells at such a high OD_{600} was only detrimental to the activity. As shown by the activity levels at 0.2% compared to that of the control, the expression was significantly reduced. This data also suggests that even though cells were dying and lysing, nothing was being released into the media, further proving that the expression was suboptimal. One of the methodologies employed to

resolve the problem with the inconsistent activity was to try and optimise the expression conditions for the protein. As previously addressed, optimising expression is an important part of developing a functioning display system. Optimising the expression plays a vital role in making sure the translocation machinery does not become inundated with protein. Excessive protein expression of a protein destined for the membrane can limit the translocation of other proteins required for viability. This process can also lead to destabilisation of the membrane due to the high concentration of components present in the membrane that do not contribute to its stability (see **Figure 19**).

This is also something that may have been of concern seeing as the system we are working with is not necessarily optimised for protein expression/and or membrane expression. As is shown in the research, we can see that *E. coli* has extensive work done creating strains that are appropriate for such experiments, namely the walker strains BL21 DE3/DE5 both of which have undergone several genomic alterations in order to maximise the capacity of the membrane for heterologous membrane proteins.

2.7. Activity in from cells expressing only cytosolic Tfu0937

Having carried out multiple iterations of the beta glucosidase assay, a common inconsistency became abundantly clear. The amount of activity being seen in the pBBR1c-Tfu0937 cells was not consistent. It appeared that in some assays the activity would be much higher than normal, and other times it would be as low as the cells with no plasmid. It was believed that this was because the cells were lysing during the assay. This was suspected because the assay incubates the cells at 50 °C at a pH of 4.8 These conditions are not ideal conditions for maintaining cell integrity.

2.7.1. Assessing pH and Temperature

To investigate the effect of the assay conditions on the cells, an experiment was conducted in which all strains were induced for 24 hours (excluding the pBBR1c-InpN-Tfu0937). The cells were then harvested, pelleted, and resuspended in fresh media.

The cells were then "pre-incubated" at 30 °C or 50 °C, and at either pH 4.8 or pH 7.0. The media was then collected, and the cells removed, and the beta glucosidase assay carried out on the media. If any lysis had occurred, free Tfu0937 would be present in this media (see **Figure 20**).

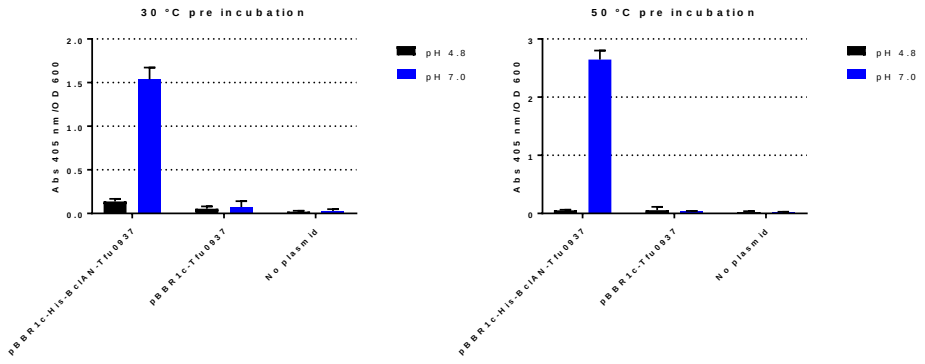

Figure 20 *Pre incubation of induced cells to investigate the effects of temperature and pH on cellular lysis.*

The samples treated at pH 7.0 show exacerbated activity in both samples. The results indicate that there is activity in the supernatant after incubation at pH 7.0 and at 30 °C. However, this is unlikely due to

lysis as this is the condition used to culture the bacteria. There is a small but notable increase in activity in the at pH 4.8. This is also seen in the pBBR1c-Tfu0937 strain, but to a lesser degree. There may have been very low levels of cell lysis here, but not enough to dramatically impact the outcome of the experiments (see **Figure 20**).

The results show only elevated levels of activity in the cells incubated at pH 7.0. It has been documented that the pH 7.0 is the optimal temperature for activity of Tfu0937 (Spiridonov and Wilson, 2001). With that in mind, it is possible that the elevated activities observed are not due to increased quantity of enzyme, but due to more efficient activity.

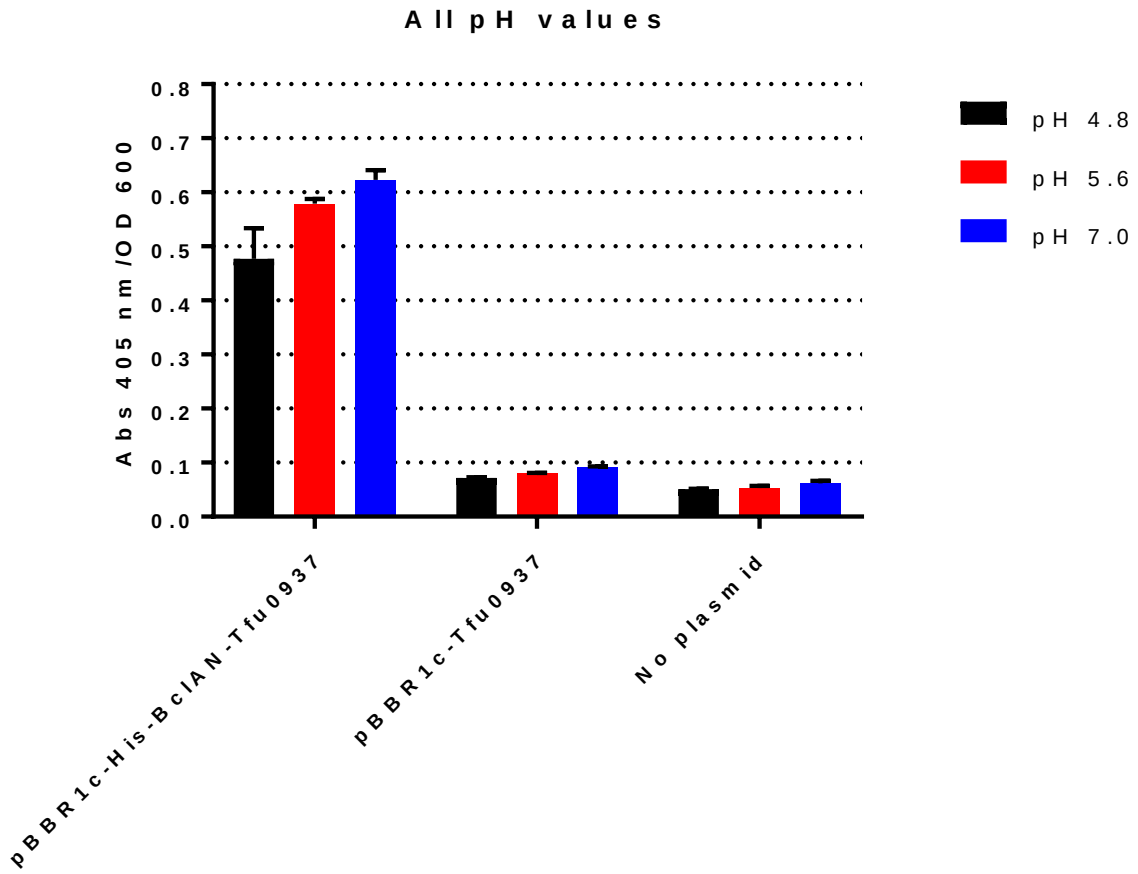

Figure 21 *Relative activities of cells when incubated with pNPG at different pH values of 4.8, 5.6, and 7.0*

The effect of pH on the activity of the cells can be seen in above in **Figure 21**. While there is an increase in activity when comparing pH 4.8 to pH 7.0, the difference in activity is only about 0.5x fold. The

difference in activity observed in the lysis test showed a difference well over a 3-fold difference in activity. This suggests there is another factor at play increasing the measured activity. One possible theory is that the change of environment from culture to buffer caused the destabilization of the enzyme on the surface, causing large amounts of enzyme to be liberated into the buffer during the incubation period.

Another key experiment that was carried out was that which looked specifically at the pH of the experimental system as samples were taken at different stages in the cultivation. It is well documented that liquid cultures of bacteria begin to become acidic as the culture ages. This is due to the accumulation of carbonic ions that lower the pH over time. Tfu0937 is a very pH sensitive enzyme as discussed earlier. As such, it was important to ensure that the buffering strength of the sodium acetate used in the experiment was sufficient to maintain the correct pH during the beta glucosidase assay.

2.7.2. Enzyme kinetics

The aim of the experiments here was to identify the optimum concentration of *p*NPG to use when assaying whole cells for beta glucosidase activity (see **Figure 22**).

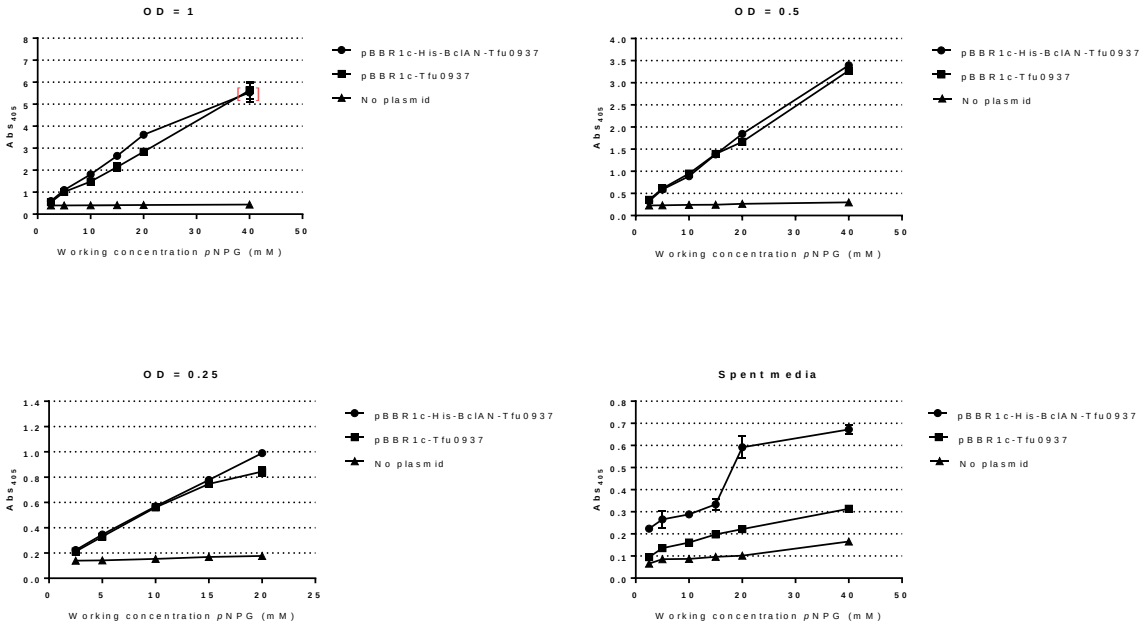

Figure 22 *Different enzyme kinetics profile using pBBR1c-His-BclAN, and pBBR1c-Tfu0937 on pNPG. Different concentrations of cells ranging for and OD_{600} of 1 to 0.25. The spent media was also assessed.*

The point around the red brackets were above the threshold for accurate reading of the spectrophotometer. There is a consistent increase in activity of the enzyme as the working concentration of *p*NPG is increased. At concentrations of 40 mM *p*NPG, it was expected that the substrate concentration would no longer cause an increase in activity of the whole cells.

The activity profile of the spent media from ReH16 pBBR1c-His-BclAN-Tfu0937 does not follow an asymptotic curve typical of those seen in any Michaelis Menten plot, as would have been expected given these experimental parameters. Following this, it made sense to observe the activity of free Tfu0937 at varying concentrations of *p*NPG substrate. If the free enzyme displays different kinetics compared to its membrane bound variant, then we can stipulate that the difference in kinetics is due to the presence of the cells, or the fact that the enzyme is bound to the membrane.

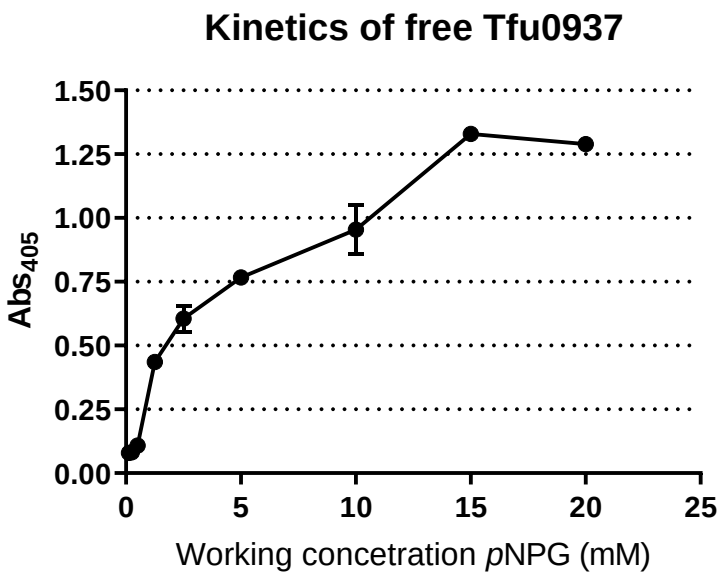

Figure 23 *Kinetic profile of Tfu0937 taken from whole cell lysate of pBBR1c-Tfu0937 to simulate free Tfu0937. (Error bars for 0 mM, 2.5 mM, 7.5 mM and 15mM are extremely small and cannot be seen on this graph)*

The graph showed that at concentrations of 15-20 mM *p*NPG, the V_{max} is reached. However, when this same concentration of *p*NPG is used with the membrane bound Tfu0937, the activity appears to continue to be increasing. This confirms the idea that the membrane bound nature of the Tfu0937 affects the activity (see **Figure 23**). Later work was carried out to further investigate the kinetic relationship between the concentration of cells and concentration of pNPG.

The data from this graph showed that the optimal concentration for the assay is at a significantly higher concentration of pNPG than was being used. Here we can see that at ~25 mg/mL offers a significantly higher activity, but more importantly, it is outside the region in which changing the concentration of the cells, changes the activity as well as the concentration of pNPG. By running the experiment at these suboptimal concentrations of pNPG, an extra variable is inadvertently introduced the experiment, and may well could have been the primary cause of inconsistent results (see **Figure 24**).

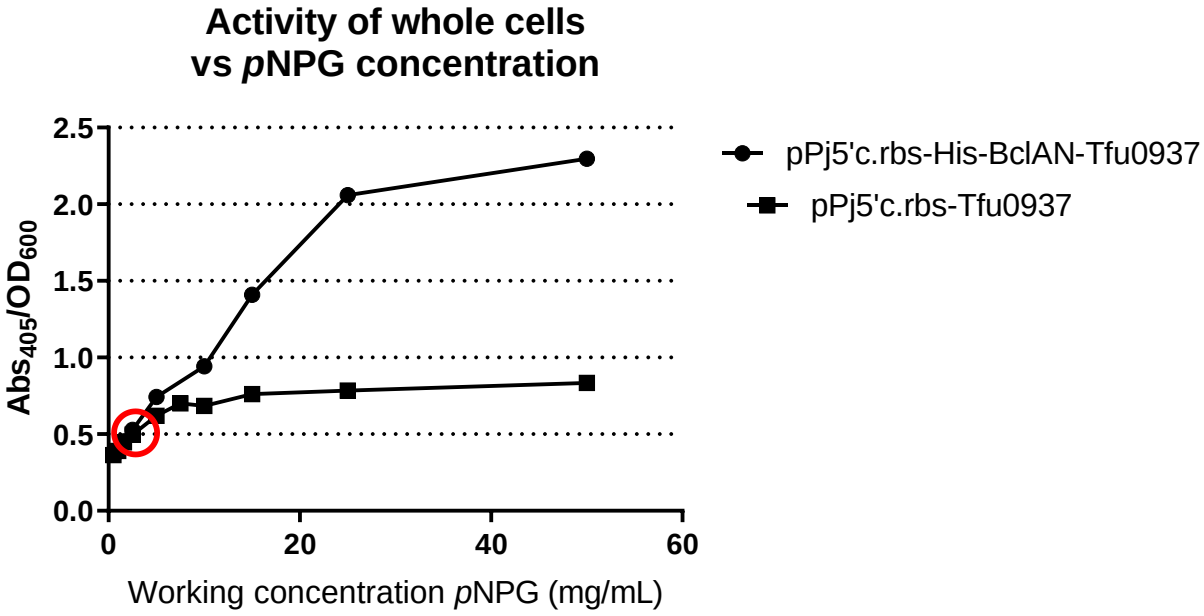

Figure 24 *Kinetic profile of whole cells* $P_{j5[A1A3C2]}$ *expressing His-BclAN-Tfu0937 and Tfu0937.*

At concentrations of >35 mg/mL, the pNPG is tends to crystallise as we approach the saturation point of the buffer. It is also interesting to note that the optimal concentration for pj5-BclAN strain is 2.5x higher than that of the Tfu0937 strain. This clear distinction in activity between the two strains at higher pNPG concentrations, suggests that there is a different system at work when it comes to how activity is being conveyed in the pJ5-BclAN strain is displaying Tfu0937.

More time was committed to try and investigate why the activity between experiments can fluctuate. After some time, an unusual experimental result was found to be the case, and it was found that the relationship between the activity and cell concentration are not linear.

Doubling the concentration of cells from 0.3 to 0.6 did not lead to double the activity, and doubling it from 0.6 to 1.2, led to a disproportionately high increase in activity.

When assessing older data sets in which the activity is particularly high, it was observed that the carried out this experiment using cells at an OD600 of 0.5.

I believe that the reason the activity values are so different is because the activity I report is shown in Abs405/OD600. If the culture is yielding similar activities at different OD values, then the sample which is calculated with a lower OD is going to give a much higher Abs_{405}/OD_{600}.

2.7.3. Checking for leaky expression

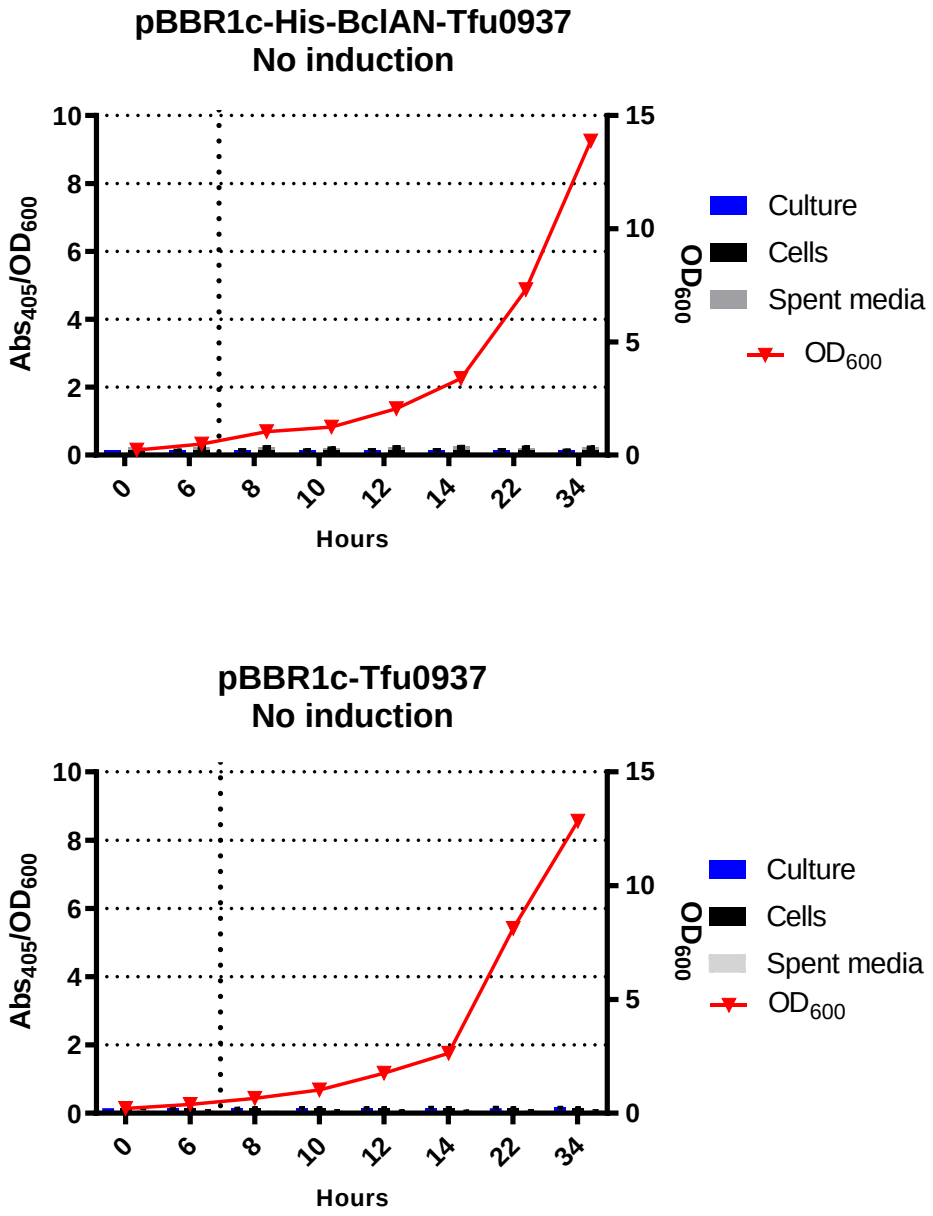

Figure 25 *Activity profile of pBBR1c strains with no arabinose added.*

Here some basic experiments were carried purely to ensure that there was no leaky expression from the pBBR1c system (see **Figure 25**). This could have had some explanation as to why there were issues with the consistency of the expression of the cells. In addition to this, this is generally an important control to have to ensure no activity is attributed to background expression.

2.8. Constitutive expression using $P_{j5[A1A3C2]}$

There was increasing difficulty to generate consistent activity profiles of the Tfu0937 products expressed using the pbbr1c plasmid. One feasible way of alleviating this issue was to move to a constitutive promoter and evaluate the stability and consistency of the new expression system. Using the constitutive promoter $P_{j5[A1A3C2]}$, the activity profile and growth profile were measured over the course of 41 hours as shown in **Figure 26**.

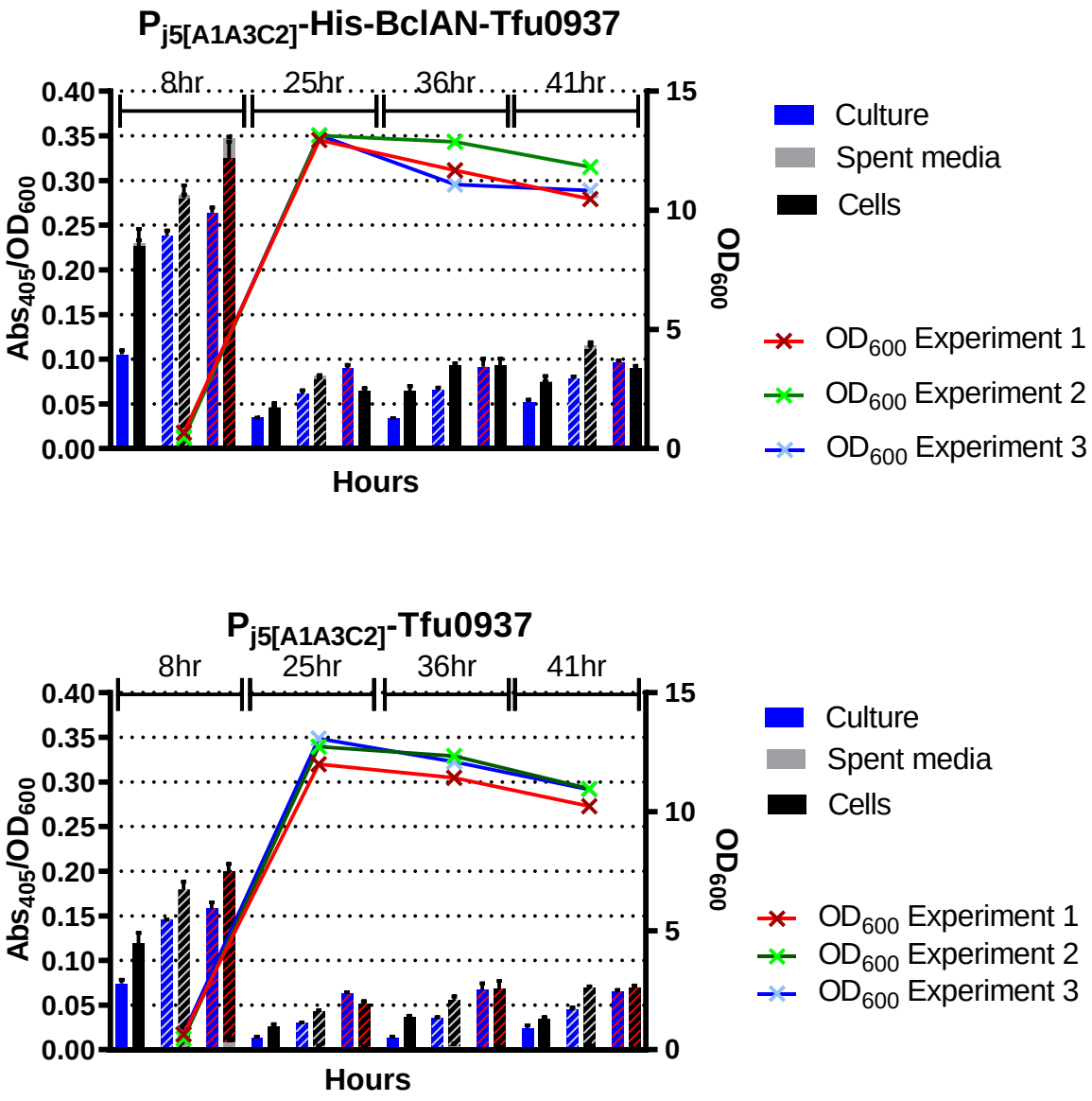

Figure 26 *Detailed and consolidated set of experiments looking at the expression of* $P_{j5[A1A3C2]}$ *system for both His-BclAN-Tfu0937 and Tfu0937. Unhatched bars correspond to experiment 1, white hatched bars correspond to experiment 2, red hatched bars correspond to experiment 3.*

The main aim of this change was to reduce the variance between the experiments, and to some degree this was achieved. Using the constitutive system appeared to give more consistent results than the inducible counterpart. However, there was still some discernible difference in activity when looking specifically at the first reading taken after 8 hours.

The most variance between experiments is observed in the samples taken from the 25 hour and 36-hour samples. However, the activity values observed at this point are so low that experimental error is likely to be more pronounced.

It may also be a good idea to look at the activity in earlier phases of growth between 8 and 25 hours. The data suggests that the display seems to be more effective in the earlier stages of growth as opposed to the later stages of growth.

One thing that was unusual about this system however was the fact that one data set showed unusually low readings for the activity of the culture sample. This was consistent throughout the entirety of the that set of experiments. However, this issue appears to be alleviated in the next set of experiments. It is also obvious that the experiments tend to show similar results and trends but with their own individual skewedness (a particular fraction showing low activity, general activity across all the samples). For example, experiment 2 did not never had the culture show total activity that was higher than that of the summation. However, when we look at the data specifically for experiment 3 (blue lines **Figure 26**), the summation is almost always the same as the culture. This suggests that the system was prone to some other systematic error.

2.9. Modifying the protocol to remove cell interference

Another problem that was later discovered in the protocol that was having a negative effect on the readings was the absorbance that was coming from the cells was the fact that the cells present in the samples were affecting the absorbance. This was further being compounded by the fact that the cells at different stages in the growth curve will have accumulated different amounts of PHA. This becomes problematic as this PHA absorbance will affect the OD readings of the cells. These readings were used to standardise the assay, and as such this discovery alerted us to the fact that the activity readings may not be accurate. To work around this problem, an extra step was introduced to the protocol that removed the cells by centrifugation before reading the absorbance. This way the cells absorbance no longer affected the cells.

The second issue that was discovered was the fact that the activity of the cells is not linear. A sample of cells was taken, and the activity measured alongside a sample with exactly half as many cells. It was astonishing to find that the activity of the cells did not halve as you would expect. This meant that it was not possible to standardise the data from different experiments given the OD_{600} of the cells was not very similar. This was an unexpected result and weakened the comparability of the results provided. This was a serious issue that made comparison between some older experiments less reliable. To circumvent this specific issue all experiments had to be carried out using identical OD_{600} values when samples were being assayed. This differed in comparison to other experiments where this value would often be changed in order to obtain higher activity readings as to not have the generated values be so close to 0.

Here a final comprehensive data set was acquired showing the most accurate representation of activity over the course of a cultivation. Many of the aforementioned issues had now been resolved and we are able to obtain a much more accurate depiction of what is going on (see **Figure 27** and **Figure 28**).

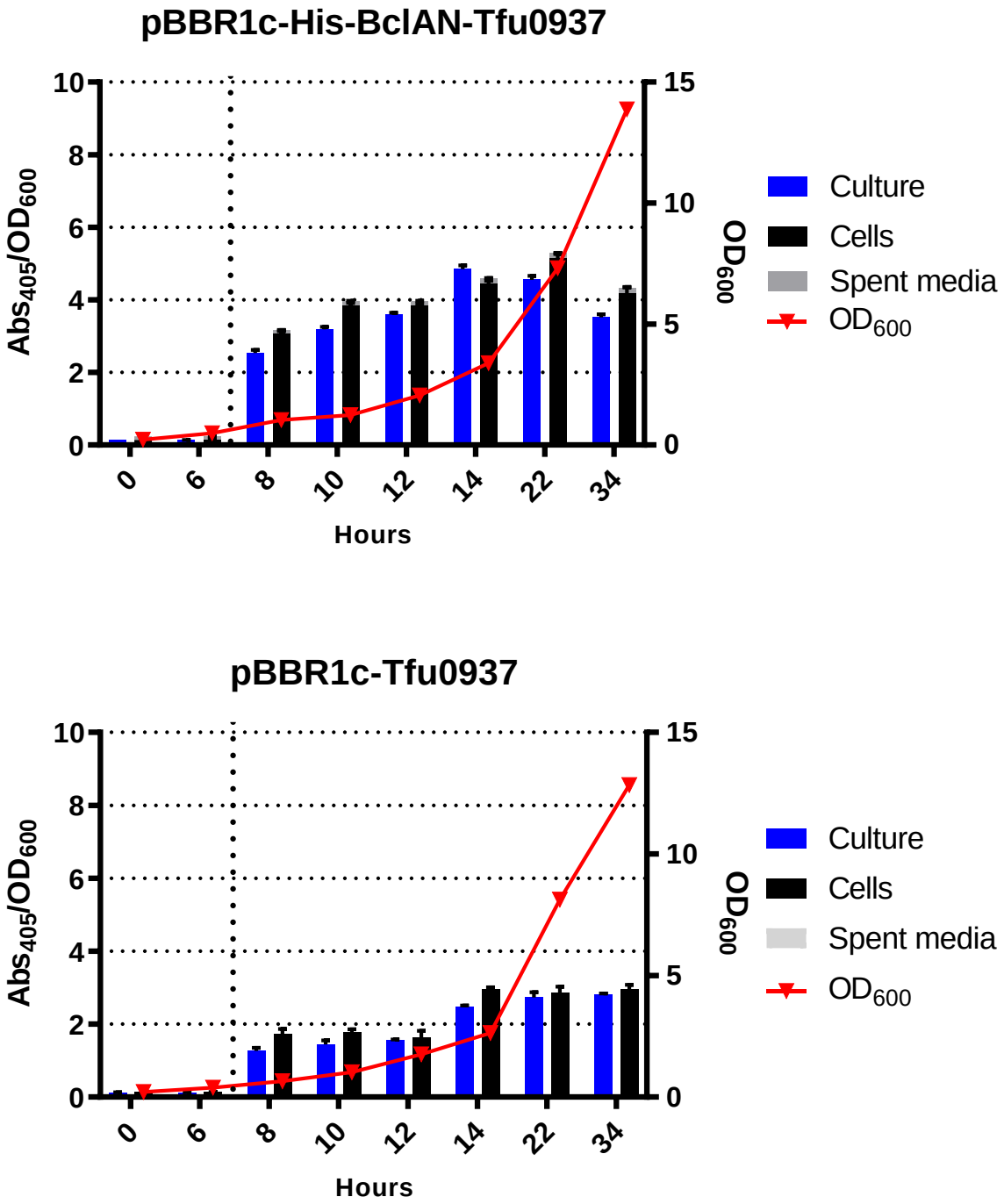

Figure 27 *Final activity profile showcasing the most accurate version of the whole cell beta glucosidase assay. The dotted line indicates where the cells were induced with 0.005% arabinose and measured over the course of ~24 hours of induction.*

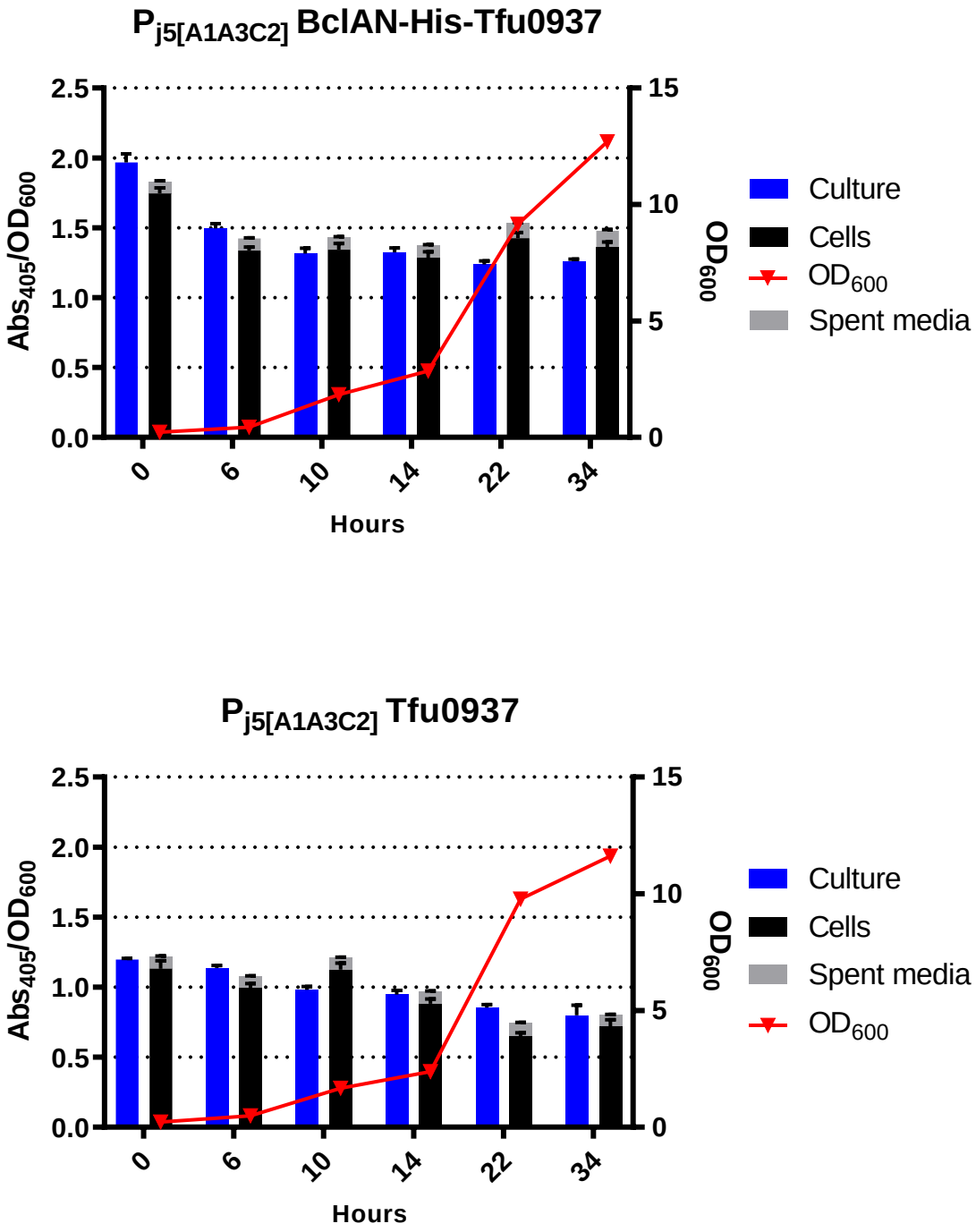

Figure 28 *Final activity profile showcasing the most accurate version of the whole cell beta glucosidase assay when using the constitutive expression system. The dotted line indicates where the cells were induced with 0.005% arabinose and measured over the course of ~24 hours of induction.*

Looking first at the inducible system, it was evident that using these new conditions for cultivation, many of the trends in activity and growth are similar to what had been observed in previous experiments. There was an increase in activity over time in both inducible systems, suggesting an accumulation of the Tfu0937.

The key difference lies in the total amount of activity seen between the pBBR1c-BclaN system and the pBBR1c-Tfu0937 only system the new cultivation and assay methodology illustrated that there is a significant difference between the amount of Tfu0937 interacting with the extracellular space. At the maximum recorded activity for both systems, we can see there was a 2.2-fold difference in activity between the pBBR1c-BclAN system and the pBBR1c-Tfu0937 system. In addition to this, the

When looking specifically at the pj5 activity, we can see that the activity remained relatively stable throughout the course of the cultivation, but there is still a significant difference in activity between the pJ5-BclAN system and the pJ5-Tfu0937 system.

The general findings here were relatively intuitive with the differences in activity being explained by the differences in the strength of the induction. The only questions that still remain pertain to the activity of the pBBR1c-Tfu0937 system which has already been discussed in detail.

2.10. Conclusion

The development of a functioning and accurate whole cell beta glucosidase assay is necessary for being assessment of the functionality of the anchoring motifs we wish to use in *C. necator* H16. The ability for us to measure the activity in this way has not only allowed us to decipher whether the BclAN anchor is working, but also to create activity profiles to measure changes in extracellular activity relative to the different growth stages of the organism, allowing us to understand the sensitivities of the system even more than we had originally anticipated.

The activity from these different expression systems illustrates that the BclAN anchor is likely to be functioning as an anchoring motif that localises Tfu0937 to the outer membrane. This methodology of proving that a display system has been used in the past primarily as the final way of illustrating extracellular display and continues to do so in this work. Here we get conclusive evidence that the BclAN system is capable of showing significantly more extracellular activity than its non-display counterpart, heavily suggesting that the BclAN is displaying the Tfu0937 successfully.

In addition to this, we learn that the InpN system is also capable of display in *C. necator* H16 but is not stable for long periods of time (over 24 hours of continuous expression). This has serious implications for using a InpN as a means of supporting Tfu0937 as an enzyme used to support growth, but does mean that InpN could potentially find some use as a reporter protein for other functional protein screening in *C. necator* H16

In summary, the assay that has been developed is sufficient for showing that BclAN is a method for display of Tfu0937 in *C. necator* H16.

3. Confirming Membrane Localisation of Displayed Tfu0937

3.1. Introduction

Many publications in this field of work employ multiple methods to prove that the location of a proposedly displayed protein has in fact made its way to the surface of the cell. This avoids the potential problem of false negatives and increased the reliability of the data. In such work, the typical workflow will first look at the localisation of a simple reporter protein such as GFP or another fluorescent biomarker that can be easily screened for using either immunological or fluorescent techniques. After this, the GFP is often replaced with a functional enzyme to illustrate the ability of the novel anchor to display and support extracellular catalysis of a given substrate. In the case of this work, the primary method of illustrating cell surface display is the enzymatic display of Tfu0937. Here, different techniques are explored to give further confirmation that the display systems are in fact working as intended. Below are some of the many methodologies used to confirm the location of artificially displayed proteins (see **Table 10**).

Table 10 *Summary of the different methods employed in the literature to illustrate membrane localisation of heterologous proteins*

Method	**Paper**
Protease accessibility **Outer membrane fractionation with western blot.**	Functional Display of Foreign Protein on Surface of *Escherichia coli* Using N-Terminal Domain of Ice Nucleation Protein (Li, Gyun Kang and Joon Cha, 2004)
Congo red zone of inhibition on stained media	Expression of Carboxymethylcellulase on the Surface of *Escherichia Coli* Using *Pseudomonas Syringae* Ice Nucleation Protein (Jung *et al.*, 1998)

Fluorescence activated cell sorting (FACS) using fluorescent antibodies **Outer membrane fractionation with western blot.** **Whole cell activity**	Improved phosphate biosorption by bacterial surface display of phosphate-binding protein utilizing ice nucleation protein (Li *et al.*, 2009)
Outer membrane fractionation with western blot. **Immunofluorescence microscopy (FITC)** **Whole cell activity**	Cell surface display of Chi92 on *Escherichia coli* using ice nucleation protein for improved catalytic and antifungal activity (Wu, Tsai and Chen, 2006)
Immunofluorescence microscopy **FACS** **Protease accessibility assay (proteinase K)** **Whole cell activity**	Cell Surface Display of Carbonic Anhydrase on *Escherichia coli* Using Ice Nucleation Protein for CO2 Sequestration (Fan *et al.*, 2011)
Outer membrane fractionation with western blot. **FACS** **Whole cell activity**	Surface display of *Zymomonas mobilis* levansucrase by using the ice-nucleation protein of *Pseudomonas syringae* (Jung, Lebeault and Pan, 1998)
Outer membrane fractionation with western blot. **FACS**	Surface-displayed viral antigens on *Salmonella* carrier vaccine (Lee *et al.*, 2000)
Outer membrane fractionation with western blot. **ELISA**	Surface Display of GFP by *Pseudomonas syringae* Truncated Ice Nucleation Protein in Attenuated *Vibrio anguillarum* Strain (Xu *et al.*, 2008)

Outer membrane fractionation with western blot. **Immunofluorescence microscopy**	Simultaneous Degradation of Organophosphorus Pesticides and p-Nitrophenol by a Genetically Engineered Moraxella sp. with Surface-Expressed Organophosphorus Hydrolase (Mark Shimazu, Mulchandani and Chen, 2001)
Fluorimetry using outer membrane fraction **Western blot (Whole cell extract was used).** **Protease accessibility assay**	Translocation of Green Fluorescent Protein to Cyanobacterial Periplasm Using Ice Nucleation Protein (Chungjatupornchai and Fa-aroonsawat, 2009)
Outer membrane fractionation with western blot. **FACS** **Immunofluorescence microscopy** **Protease accessibility assay**	Surface Immobilization of Human Arginase-1 with an Engineered Ice Nucleation Protein Display System in *E. coli* (Zhang *et al.*, 2016)

3.1.1. Protease accessibility assays

The protease accessibility assay works by subjecting whole cells to non-specific proteolytic enzymes. These proteases hydrolyse proteins that are located on the extracellular surface of the cells. By degrading Tfu0937 that is on the surface the cells, the cells treated by with the protease should lose their activity. Proteases that have been used for this purpose are listed below. A protocol for this method is detailed in this methods paper (Besingi and Clark, 2015).

- Trypsin
- Pronase (protease cocktail from *Streptomyces griseus*)
- Proteinase K

3.1.2. Isolation and assessment of the outer membrane

Cell fractionation can be used to separate the different components of a cell. In this instance, the outer membrane can be separated from the whole cell, leaving behind a spheroplast. There are numerous ways in which this can be achieved as detailed in the work done by Hobb and Fields (Hobb *et al.*, 2009). The focus will be on these two methodologies: isolation of membrane using lysozyme and isolation using N-lauroylsarcosine.

Lysozyme can degrade the peptidoglycan layer that stabilises the outer membrane. This allows the outer membrane to separate from the inner membrane, allowing separation of the freshly formed spheroplasts. The cells are treated with these reagents and then centrifuged. The spheroplasts pellet during the centrifugation, and the supernatant contains harbours the membrane fraction which can then be analysed further. While this procedure has been reported to work in *E. coli*, it has been reported that other gram-negative organisms such as *Salmonella sp.* can be resistant to this methodology of outer membrane isolation. In the paper, *C. jejuni* was the organism that was used for the assays (Hobb *et al.*, 2009).

Using N-laurylsarcosine is slightly more complicated procedure. The “sarkosyl” technique utilises this detergent to dissolve the inner membrane of the bacteria. This leaves an insoluble outer membrane that is separated from the rest of the reaction contents via centrifugation.

Once the outer membrane has been separated by either of the methods outlined above, the membrane and its proteinaceous content can be assayed easily by using it in place of cells in the whole cell catalysis Tfu0937 assay. The membrane fraction can then be used to comparatively analyse the localisation of its components.

3.1.3. Immunological identification

A common way of confirming the surface localisation of the enzyme is using antibody binding assays. In most cases it is used in tandem with membrane isolation. The isolated outer membrane is used in a western blotting procedure. The cells can also be assayed using an ELISA procedure. However, there are some other methods that use antibodies such as using antibodies with fluorescent probes. These are

used to bind to the target membrane protein, and then can be visualised using fluorescence microscopy, fluorimetry, or fluorescence activated cell sorting.

It was decided that the simplest assay that can be conducted is the isolation of the outer membrane using lysozyme, and then assaying the outer membrane fraction, followed by the protease accessibility assay. The method chosen was dependent on the availability of the reagents.

3.2. Materials and methods

3.2.1. Proteinase K assay

In 5 mL of MSM supplemented with 1% sodium gluconate, grow pre-cultures of *C. necator* H16 cells transformed with: pPJ5'c.rbs-His-BclAN-Tfu0937/pBBR1c-His-BclAN-Tfu0937pPJ5'c.rbs-Tfu0937/pBBR1c-Tfu0937/pBBR1c-InpN-Tfu0937, or no plasmid. Ensure all cultures are supplemented with gentamicin (10 µg/mL working concentration), and cultures containing pPJ5'c.rbs-His-BclAN-Tfu0937/ pBBR1c-His-BclAN-Tfu0937 and pPJ5'c.rbs-Tfu0937/ pBBR1c-Tfu0937 are supplemented with chloramphenicol (25 µg/mL working concentration). Cultivate the pre-cultures for 24 hours. Sub-culture the precultures into 5 mL of MSM supplemented with 1% gluconate, in a 50 mL falcon tube to an OD_{600} of 0.2. For tubes inoculated with pBBR1c strains, cells are cultivated to an OD_{600} of 0.4-0.6 before the addition of 25 µL of 20% arabinose, this induces the cells at a working concentration of 0.1% arabinose. Cultivate over the course of 24 hours. Harvest the cells by centrifugation at 10000g at room temperature. Remove and discard the supernatant. Resuspend the cells in proteinase K buffer to an OD of 1.45 and transfer 1 mL to a 1.5 mL Eppendorf tube to each tube, add 7.5 µL of stock proteinase K (Qiagen, Germany) (20 mg/mL). This will create a working concentration of 150 µg/mL. Incubate the cells for 1 hour at 50 °C, 700 rpm. After 1 hour, take a sample of 150 µL and assay for whole cell enzymatic activity.

3.2.2. Trypsinisation of C. necator H16

Prepare the cells for protein expression and treatment in an identical fashion to the proteinase K assay, but instead resuspend the cells in Trypsin buffer to an OD of 1.45 and transfer 1 mL to a 1.5 mL

Eppendorf tube to each tube, add of stock trypsin (Qiagen, Germany) to a working concentration of 500 µg/mL. Incubate the cells for 1 hour at 50 °C, 700 rpm. After 1 hour, take a sample of 150 µL and assay for whole cell enzymatic activity.

3.2.3. Lysozyme protocol with osmotic shock treatment

Reagents

- Buffer 1 – 100 mM Tris acetate pH 8.2, 500 mM sucrose, 5mM EDTA
- Buffer 2 – 50 mM Tris acetate pH 8.2, 250 mM sucrose, 10 mM $MgSO_4$
- 1 M $MgSO_4$
- 1 mg/mL lysozyme
- ddH_2O

All reagents must be cooled on ice before use.

Protocol

For each culture, prepare 1 mL of cells at an OD_{600} of 10 in a 1.5 mL tube.

Centrifuge the cells for 1 minute, 10000 g, at 4 C.

Aspirate and discard the supernatant (spent media).

Resuspend the cells in 1 mL of cold buffer 1.

Add 500 µL cold ddH_2O.

Add 40 µL of stock lysozyme (1 mg/mL).

Incubate on ice for exactly 5 minutes.

Add 20 µL of cold 1 M $MgSO_4$.

Centrifuge the cells 14000 g at 4 C, for 2 minutes.

Aspirate the supernatant and keep separately. This will contain the periplasmic fraction and outer membrane.

Sonicate the spheroplasts at an amplitude of 40% for 10 cycles. (1 cycle = 15 s, on 45 s off).

Centrifuge the lysate from the sonication at 14000g for 2 minutes to remove any whole cells and cell debris.

Aspirate the supernatant containing the cytosolic fraction, insoluble protein, and membrane fractions.

Centrifuge at 14,000g for 30 minutes at 4 C.

Aspirate the supernatant.

Resuspend the pellet in 200 µL of 10 mM Na_2HPO_4.

3.2.4. SDS gel preparation and analysis

Samples were prepared and processed in an identical fashion as to what is described in Chapter 2

3.2.5. Whole cell beta glucosidase assay

Whole cell beta glucosidase assay (modified for purified membrane samples)

Reagents

Reaction buffer: 0.2 M sodium acetate, pH 4.8. 100 mL of reaction buffer is prepared by mixing 59 mL 0.2 M sodium acetate, and 41 mL 0.2 M acetic acid.

NaOH glycine buffer pH 10.8: 15 g of glycine dissolved in 300 mL of milliQ water. Adjust to pH 10.8 with NaOH pellets. Bring volume to 500 mL with milliQ water.

*p*NPG solution: Dissolve 80 mg of *p*NPG in 50 mL of reaction buffer

Preparatory steps

Pre-heat *p*NPG solution to 50 °C (10-15 minutes). Pre-heat the plate shaker to 50 °C.

Protocol

To a well, add 50 µL of the purified membrane sample. Add 50 µL of pre-warmed *p*NPG solution to the each well containing membrane sample. Incubate at 50 °C for 15 minutes with shaking at 750 rpm. After the incubation is complete add 100 µL of sodium hydroxide-glycine buffer to each well.

Shake samples for 5 seconds in the plate reader before measuring the absorbance of the samples at 405 nm.

3.2.6. Sarkosyl outer membrane extraction

Prepare: Tris-EDTA pH 8.0 and 10 mM Na_2HPO4 pH 7.2 (cold)

Prepare the cells for protein expression and treatment in an identical fashion to the proteinase K assay, but instead resuspend the cells in 10 mL of cold 10 mM Na_2HPO_4. Sonicate 45 seconds off, 15 seconds on, 10 cycles, amplitude 40%. Keep on ice during sonication. Centrifuge sonicated samples 3500g, at 4 C, for 5 minutes to remove whole cells. Aspirate the supernatant containing the membranes and cytosol then discard the pellet. Centrifuge the supernatant at 12000 g, 4 C, for 30 minutes. Aspirate the supernatant and keep separately. This should contain the cytosolic protein fraction. Resuspend the pellets in 800 µL of 10 mM Na_2HPO_4 and add L-sarcosine sodium salt to a working concentration of 0.5% to all samples. Incubate all samples at 37 C, for 30 minutes with shaking (700 rpm). Centrifuge the samples to pellet the insoluble outer membrane fraction. Resuspend the pellets in 80 µL of TE buffer.

3.3. Proteinase K

Translocation of protein to the extracellular surface can be demonstrated in a multitude of different ways. Most of these methods utilize 2 main approaches. The first is the whole cell assay, as we have used for all the experiments prior, and the second revolves around isolation of the membranous fraction of the bacterial cell. Another common method used is using a proteinase to degrade the protein on the extracellular surface on the cell. In this work, it was important that more than one method was used for confirmation of translocation in order to have a robust set of evidence.

Here, two methods were investigated as means of confirming that BclAN-Tfu0937 was present in the membrane/on the extracellular surface. The first of these methods was using proteinase K to degrade extracellular protein. By incubating whole cells displaying the Tfu0937, the cells should lose activity after the protein has been degraded (see **Figure 29**).

3.3.1. Preliminary experiments using proteinase K

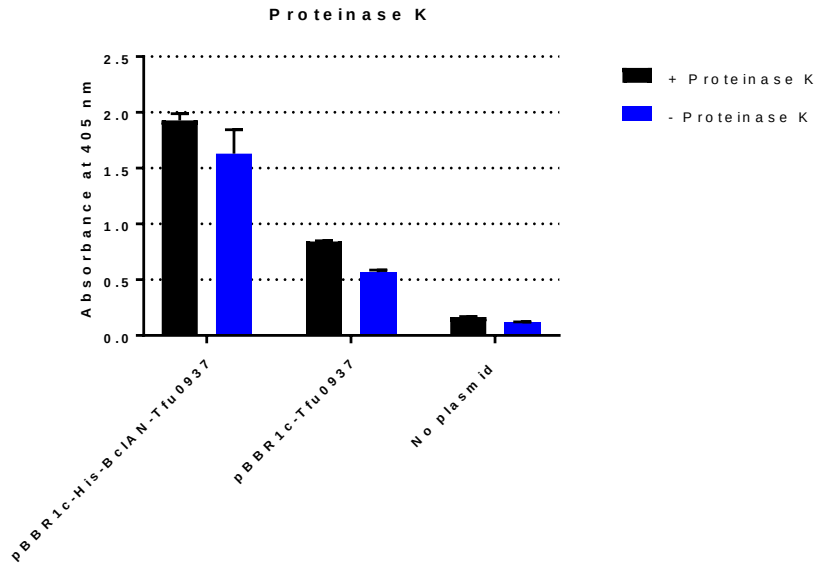

Figure 29 *Effect of proteinase K on strains pBBR1c-His-BclAN-Tdu0937, and pBBR1c- Tfu0937. 50 µg/mL was the working concentration of proteinase K and cells were incubated at 37 °C for 30 minutes.*

The pBBR1c-His-BclAN-Tfu0937 and pBBR1c-Tfu0937 strains were investigated to observe the effect of proteinase K on the Tfu0937 activity of the cells. The activity of cells displaying the BclAN-Tfu0937 was not affected dramatically upon incubation with proteinase K. It was suspected that this was because proteinase K may not be able to degrade Tfu0937 efficiently.

C. necator expressing pBBR1c-Tfu0937 was sonicated and prepped to isolate free Tfu0937. The free Tfu0937 was then used to assess whether proteinase K was able to degrade it. A series of different concentrations of proteinase K were used for this (see **Figure 30**). Another change to the protocol that was implemented was the incubation temperature for optimal activity of proteinase K. The temperature of the incubation was increased to 50 °C (see **Figure 31**). This was informed by an assessment of the literature, which states that the optimum temperature of proteinase K activity is 57 °C (Ebeling *et al.*, 1974).

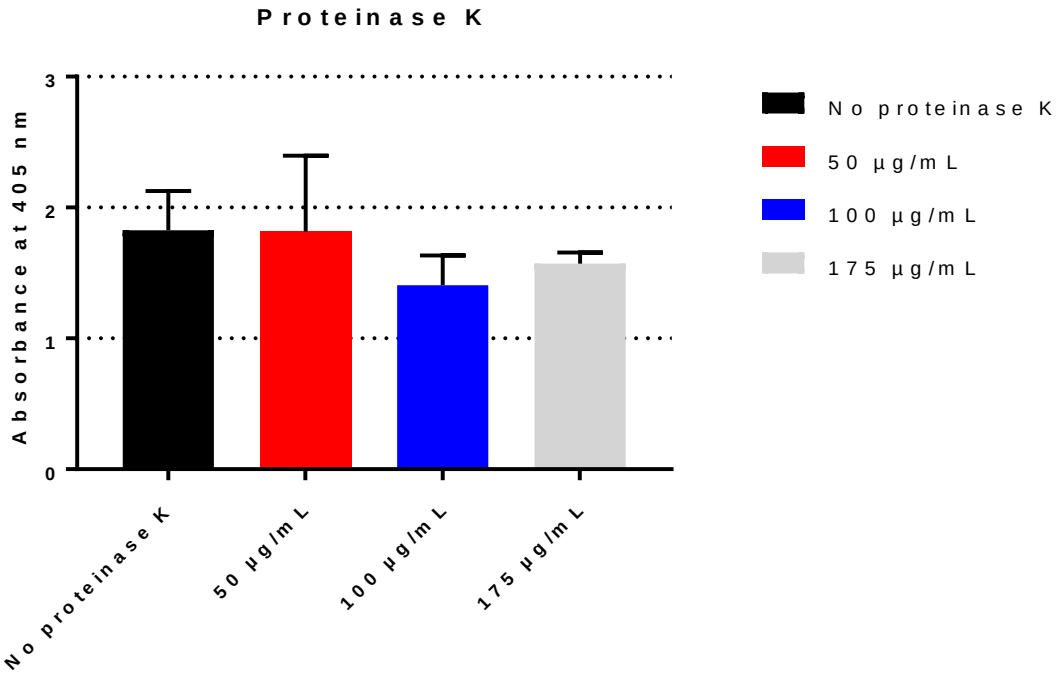

Figure 30 *Effect of increasing the working concentration of proteinase K but keeping incubation temperature and duration the same as the previous experiment. Cells not used in this experiment but instead, free Tfu0937 (prepped from sonicated cells expressing pBBR1c-Tfu0937)*

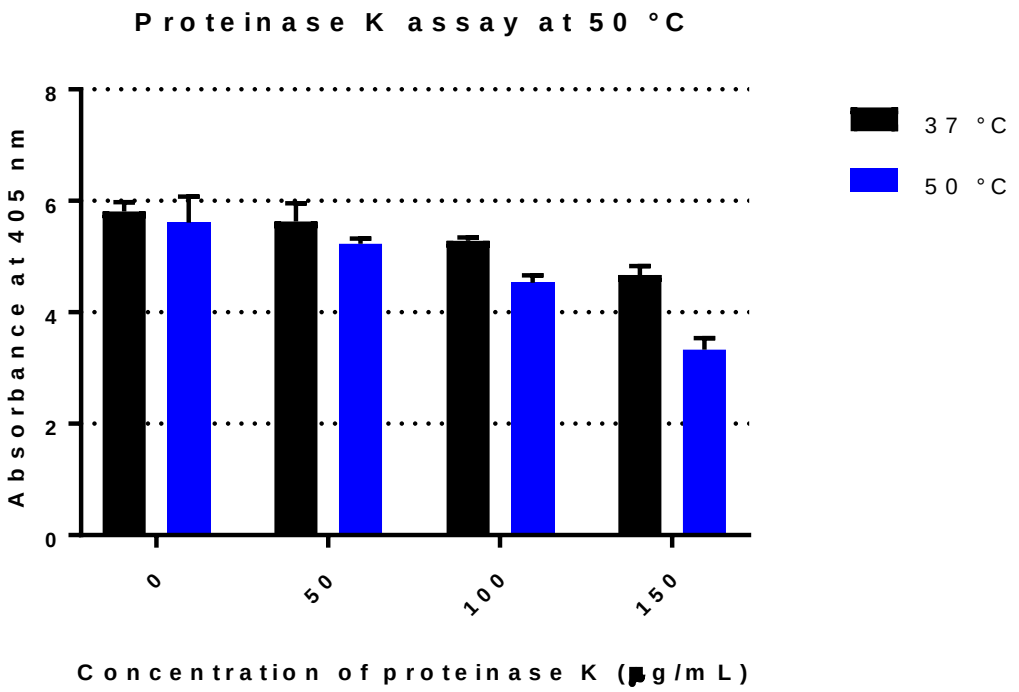

Figure 31 *Effect of increasing the temperature of the incubation of proteinase K and Free Tfu0937 (prepped from sonicated cells expressing pBBR1c-Tfu0937)*

There appeared to be minimal abrogation of activity even after increasing the concentration of the proteinase by over 3 times. There was speculation that the buffer being used may be causing a problem, or there is a problem with the processing in the practical aspect of the experiment. A peptide analysis was also done believe this is the case because 245 cleavage sites were identified in Tfu0937, using the ExPASy peptide cutter.

However, across all the different concentrations used, there was a consistent reduction in activity when the temperature was increased to 50 °C. The next step was to increase the incubation time. The first iteration of the protocol instructed that the cells be incubated with the proteinase K for 30 minutes. In some other studies, the digestion was done for as long as 16 hours. As such, the incubation time was increased to 16 hours, and was tested at both temperatures of 37 °C and 50 °C to observe any differences in proteolytic activity as shown in **Figure 32**.

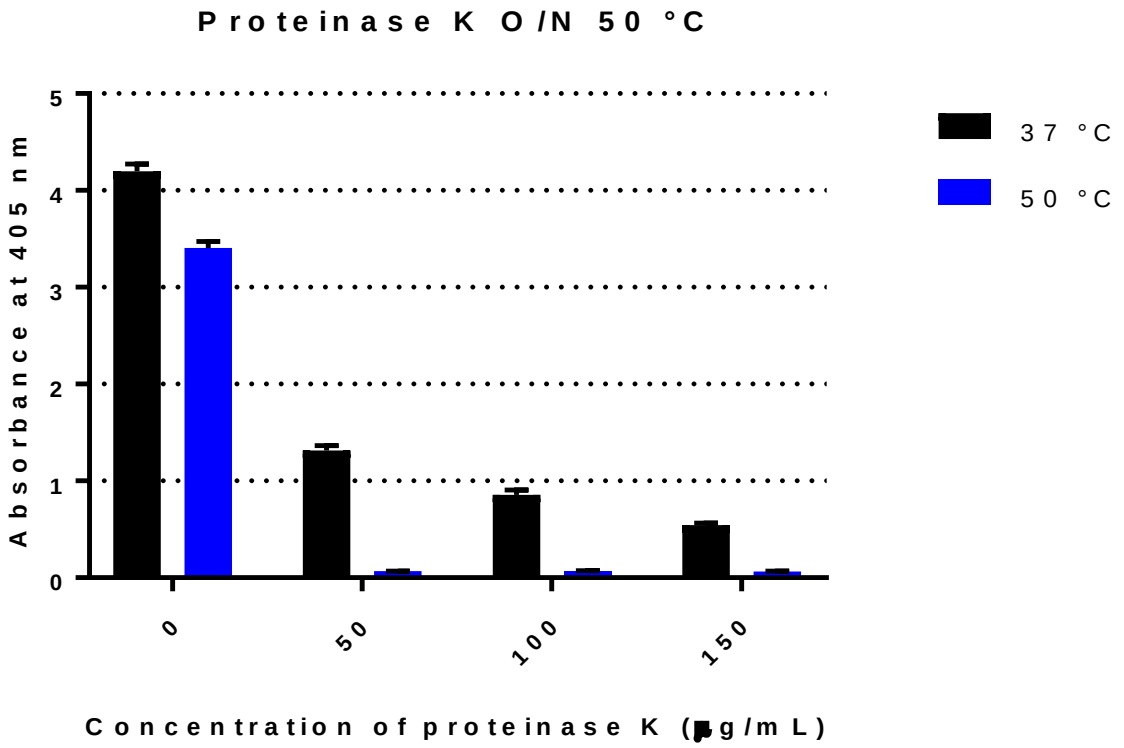

Figure 32 *Effect of increasing the duration of the incubation from 30 minutes to O/N (overnight, or 16 hours).*

The changes to the incubation time were very positive. There was complete abrogation of activity when the Tfu0937 was incubated at 50 °C overnight with proteinase K. This result was achieved at all concentrations of proteinase K used.

3.3.2. Utilising Trypsin for proteolysis of BclAN-Tfu0937

Due to the difficulties that arose using proteinase K, trypsin was used to see if the proteolysis could be better achieved through this protease. To see if trypsin could degrade Tfu0937, it was used to degrade free Tfu0937 that had been prepped in the same way as was done for proteinase K. The free Tfu0937 and was incubated at 37 °C for 2 hours, and another sample was incubated over overnight (see **Figure 33**).

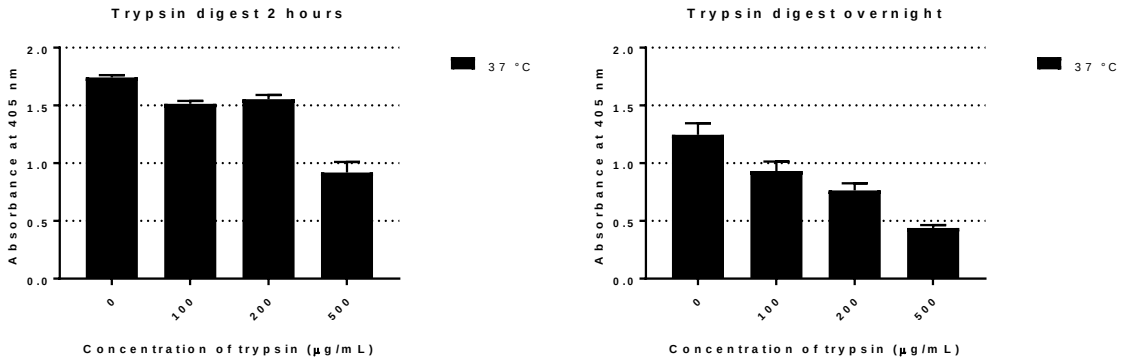

Figure 33 *Effect of utilising trypsin instead of Proteinase K for the degradation of free Tfu0937 prepped from sonicated cells expressing pBBR1c-Tfu0937.*

The overnight digest was more effective than the shorter 2-hour digest. There is a loss of activity in the control (no trypsin) over night. It is not clear if this is related to how the samples were stored prior to the assay being run, or if there is a loss of stability when kept at 37 °C for 12 hours.

3.3.3. Proteinase K digest of cells after 2-hour digest

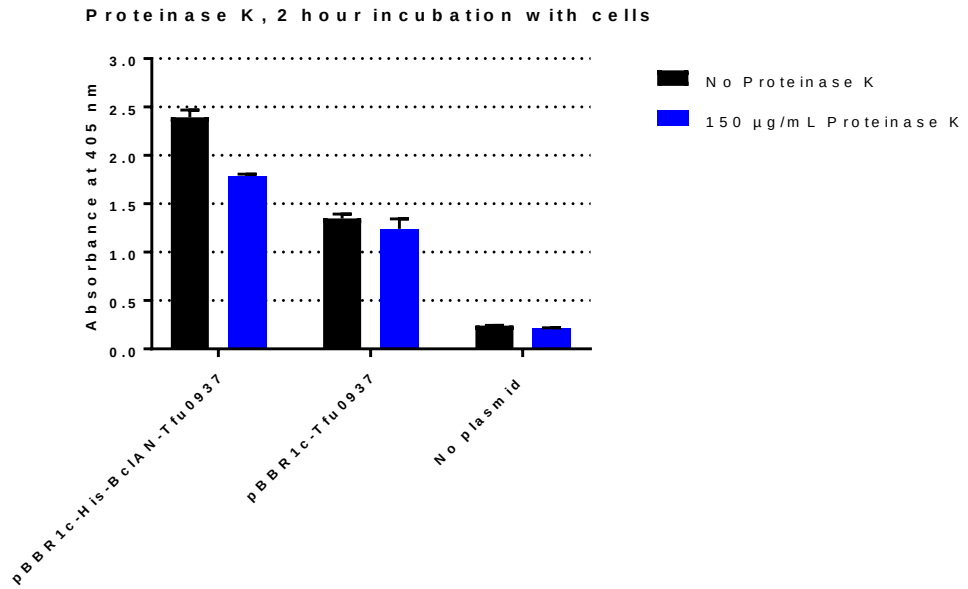

Figure 34 *Effect of using the new optimised parameters to degrade Tfu0937 on the extracellular surface of pBBR1c-His-BclAN-Tfu0937.*

In the pBBR1c-His-BclAN-Tfu0937 strain, the amount of activity lost due to degradation of the Tfu0937 is not as high as seen in the digest of the free Tfu0937 as shown in **Figure 34**. When degrading

free Tfu0937, activity is reduced to barely detectable levels. However, when the cells displaying Tfu0937 are subject to the same conditions, the efficiency of the proteinase is reduced. This is likely to be caused by stearic hinderance imposed by the presence of the cell. This may prevent effective binding of the proteinase K to the Tfu0937.

Following the previous experiments, it was clear that further optimisation was required before the proteinase K could be used to fully degrade the Tfu0937. When optimising a protocol, there are often many different parameters that need to be looked at and individually assessed to find out the best combination that yield the best results. To apply this approach to this work, the following parameters of the proteinase incubation were assessed as detailed in the table below (see **Table 11**).

Table 11 *Different parameters that can affect the efficacy of proteinase K*

Temperature	This can change the activity of the enzyme but will also affect the stability of the cells.
Duration of the incubation	How long the cells are incubated with the proteinase K can lead to increased degradation of the Tfu0937.
Duration of induction	By reducing the expression time, the surface will be less decorated with protein. This may allow better access of the proteinase K to the Tfu0937, increasing the amount of proteinase K.
The OD_{600} of cells used in the experiment	By decreasing the number of cells present, there is less protein that needs to be degraded, and will hopefully allow for the proteinase K to be less inundated with protein to degrade. This system is not specific for Tfu0937, so introducing more cells introduces a lot more excess protein that will occupy the proteinase K

Table 12 *Different parameters measured to investigate whether they would increase the ability of proteinase K to degrade the protein on the extracellular surface. Reduction in activity was measured by assessing the amount of activity on the surface of the cells after the cells were treated with 150 µg/mL of proteinase K.*

Temperature (°C)	Duration of incubation (hrs)	Induction (hrs)	OD_{600}	Reaction solution	Reduction in activity after treatment	
					BclAN	Tfu0937
50	2	24	2	PKB	23%	0%
37	2	24	2	PKB	8%	0%
50	4	24	2	PKB	4%	1%
50	24	24	2	PKB	0%	0%
50	2	2	2	PKB	4%	2%
50	2	4	2	PKB	20%	2%
50	2	24	1	PKB	11%	0%
50	2	24	0.5	PKB	5%	0%
On ice	2	2	2	PKB	6%	0%
On ice	2	2	2	MSM	2%	0%

Assessment of all the different variations on the experiment, none of the proposed alterations were able to yield higher levels of degradation of extracellular Tfu0937. While it was evident that these was not the right direction for increasing the efficacy of degradation via proteinase K, the consistent degradation seen on the pBBR1c-BclAN strain, heavily suggests there is difference in sensitivity to the assay when treating the cells with an extracellular protease. Despite not seeing high levels of abrogated activity,

this finding allows for the postulation that the only reason there is any loss of activity is precisely due to the fact that the degraded Tfu0937 can only be accessed because it is on the surface of the cells.

There are some theories that could explain why the efficacy of the degradation is so low when using this system. It is possible that the conjugation of the Tfu0937 to the cell surface, inhibited the activity of the proteinase K, or the proteinase K was unable to properly access the protein due to the presence of other membrane bound proteins or other outer membrane moieties. These issues have been reported in other studies that utilise this methodology for proving cell surface display (Fedeson and Ducat, 2017).

In order to increase the efficacy of degradation, and replicate the levels seen in other publications, a different method was devised. It was hypothesised that the proteinase K may be either getting inundated, inactivated or destroyed over the long duration of some of these experiments. We tested the addition of extra proteinase K during an extended digestion would lead to more degradation of extracellular Tfu0937 (see **Figure 35**).

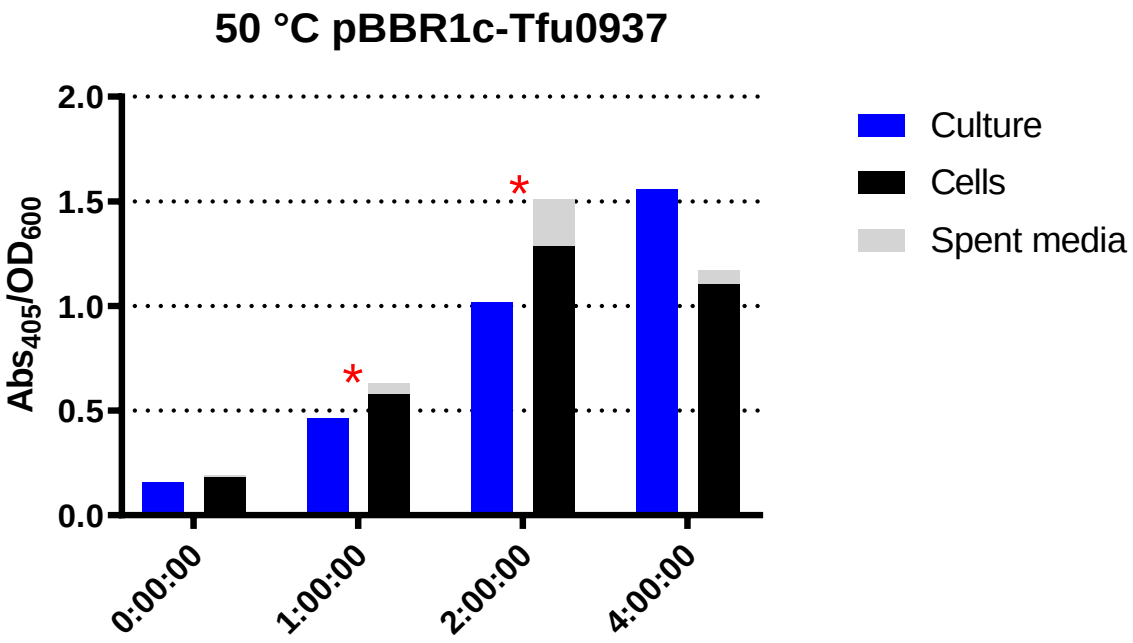
50 °C pBBR1c-Tfu0937
Abs405/OD600
2.0
1.5
1.0
0.5
0.0
*
*
0:00:00
1:00:00
2:00:00
4:00:00
Culture
Cells
Spent media

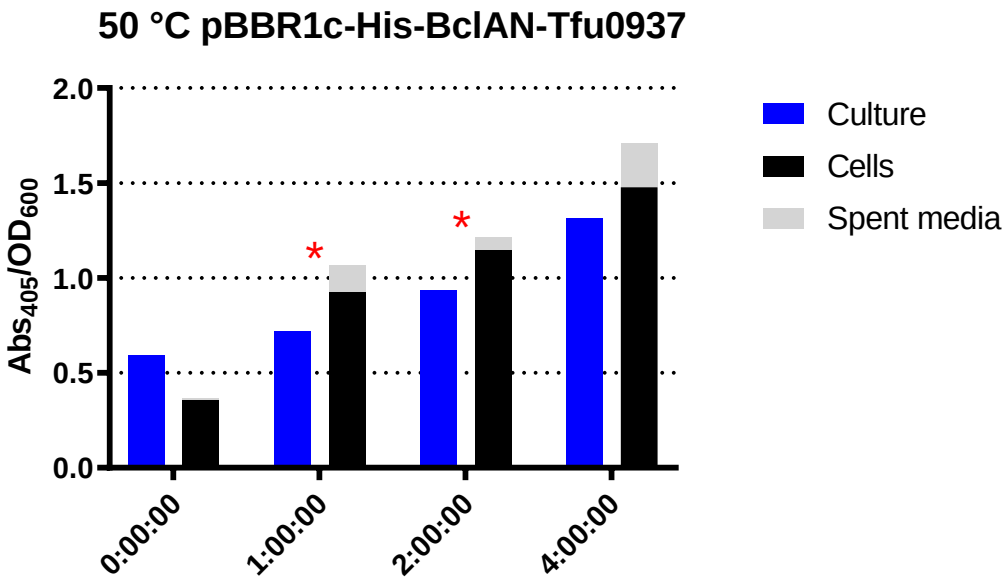
50 °C pBBR1c-His-BclAN-Tfu0937
Abs405/OD600
2.0
1.5
1.0
0.5
0.0
*
*
0:00:00
1:00:00
2:00:00
4:00:00
Culture
Cells
Spent media

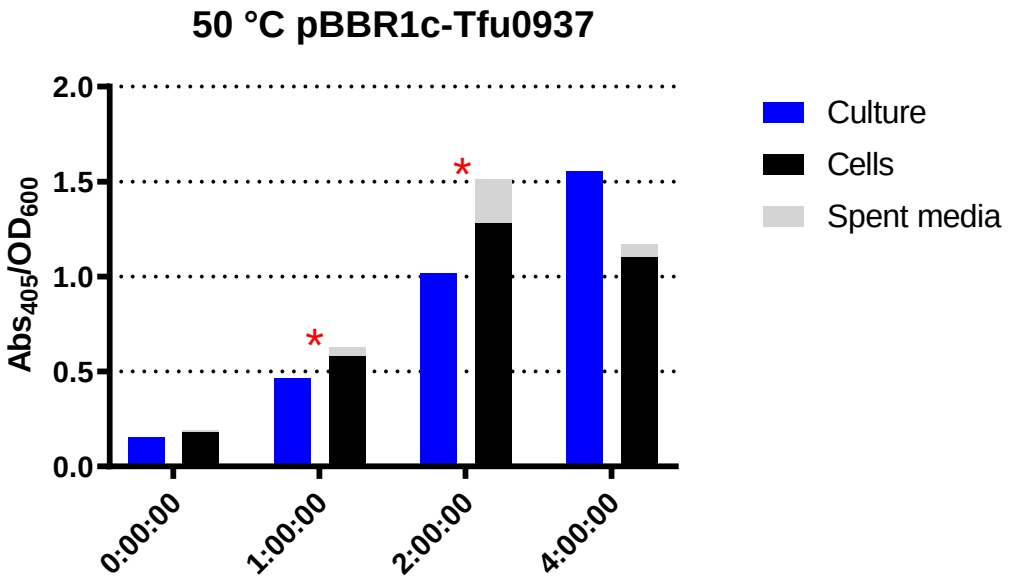

Figure 35 *Proteinase K assay measuring the activity over time, while adding more proteinase K after 1 hour of treatment, and a second addition after 2 hours. Red asterisks indicate the addition of extra proteinase K.*

Activity in the spent media directly after harvesting is close to 0 in both cases, however, after 1 hour of induction, there appears to be evident activity in the supernatant. This may be a consequence of the extended incubation at 50 °C. It has been stated in literature that the permeability of the membrane and general robustness of the bacterial cells like *E. coli* are susceptible to changes in physiology when subject to temperatures above 45 °C (Souzu, 1982). Another consequence that was likely caused by the conditions of incubation was the formation of a precipitate in the reaction mixture observed after 2 hours of incubation. It was suspected that the shaking provided in an Eppendorf tube would not give the same efficacy of mixing compared to that of a plate shaker. The assay was re-done in the plate shaker, but the viscous membrane was then centrifuged to remove as much background as possible.

The primary aim of this experiment was to demonstrate that the BclAN-Tfu0937 was located in the cell membrane after induction. The consensus of this data does show selective localisation of the protein in the membrane when using the protease accessibility assay as a means of illustrating its localisation to the outer membrane. In addition to this, cells expressing intracellular Tfu0937 show no sensitivity to the assay, allowing the clear distinction in activity between the two systems.

3.4. Lysozyme extractions

Previous assessment of the literature illustrated that there are several ways to localise the outer membrane protein to the membrane of a bacterial cell. As one of the more accessible methods available to us, we decided on the use of an extraction that would utilise lysozyme to purify the membrane fraction of gram-negative cells. The principle of the method lies in the fact that the lysozyme enzyme is able to degrade the peptidoglycan layer underneath the outer membrane layer, destabilising the outer membrane and allowing it to slough off the cells. To give the lysozyme access to the peptidoglycan, the cells undergo osmotic shock making the membrane permeable to the protein.

The lysozyme's activity is controlled by incubating at cold temperatures, preventing the lysozyme from rapidly destroying the cells. The data shown below looks at the measured Tfu0937 activity of the outer membrane fraction, against the spheroplasts.

3.4.1. Preliminary experiments using lysozyme membrane extraction

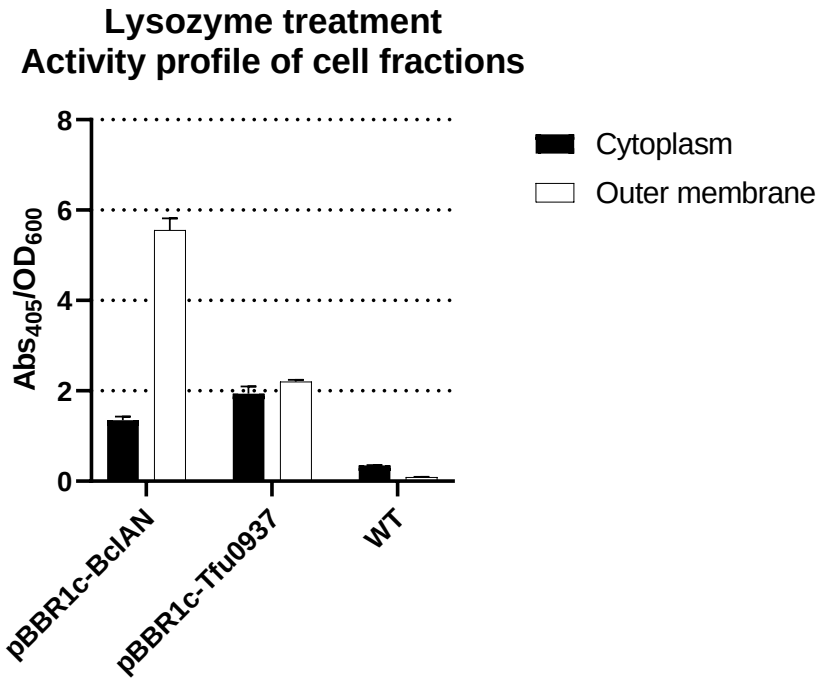

Figure 36 *Activity profile of different fractions purified from whole cell lysate of pBBR1c-BclAN-Tfu0937, pBBR1c-Tfu0937, and C. necator H16 with no plasmid. Here, the periplasmic fraction and periplasmic fraction were collected.*

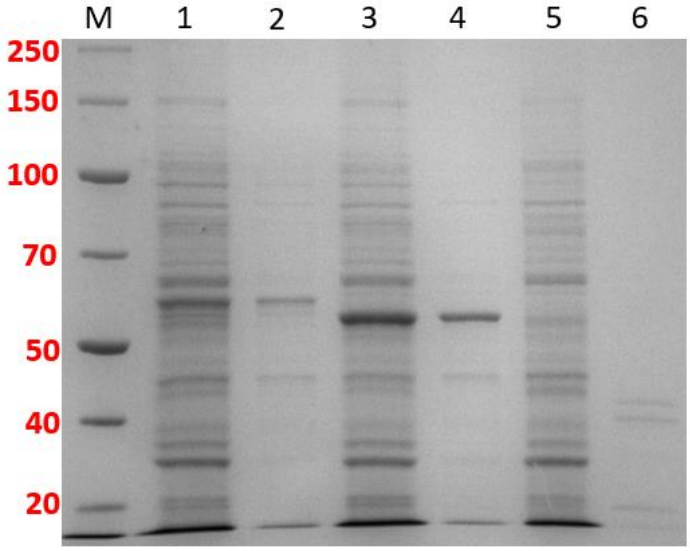

Figure 37 *SDS gel of spheroplasts and purified outer membrane fraction. Lane 1: pBBR1c-His His-BclAN-Tfu0937 spheroplast fraction, Lane 2: pBBR1c-His-BclAN-Tfu0937 outer membrane fraction, Lane 3: pBBR1c-Tfu0937 spheroplasts fraction, Lane 4: pBBR1c-Tfu0937 outer membrane fraction, Lane 5 C. necator H16 WT no plasmid spheroplasts, Lane 6: C. necator H16 WT no plasmid outer membrane fraction. MW of His-BclAN-Tfu0937: 56.7 kDa, MW of Tfu0937: 53.4 kDa.*

The data showed a clear enrichment of activity in the membrane fraction of the pBBR1c-BclAN cells and there is still substantial activity in the spheroplasts of BclAN. However, there was also notable activity in both the membrane and spheroplast of the pBBR1c-Tfu0937 cells, however, these values are likely coming from spheroplasts lysed through shearing forces during the processing. As was expected the cells with no plasmid showed nearly no activity, and what little was observed was due to the turbidity of the purified membranes/spheroplasts present in the reaction mixture (see **Figure 36** and **Figure 37**).

It was also noted that the spheroplast activity for both the pBBR1c-BclAN-Tfu0937 and pBBR1c-Tfu0937 cells was quite similar. However, this observed activity was likely attributed to Tfu0937 leaked from the spheroplasts. I am very confident that the activity seen in these samples, is largely going to be coming from cytosolic Tfu0937. To continue to assess the location of the Tfu0937 in these specific locations, an SDS gel was run using these samples.

The analysis of the gel showed us that there was banding at the corresponding MW for both His-BclAN-Tfu0937 and Tfu0937 in their respective spheroplast and outer membrane fractions. This data suggests that the system had successfully isolated the correct fraction, and that we had obtained conclusive evidence of the subcellular location of the Tfu0937 in the membrane. However, there were two problems with what was observed in this data set. Firstly, the protein profile of the membrane looked too similar to that of the spheroplast. This suggested that what we were observing might not necessarily have been the profile of the outer membrane, but cytosolic protein that ended up in the wrong fraction due to the nature of the protocol. This is further verified by the fact that the outer membrane fraction should be enriched in other outer membrane proteins, which were not visible in this fraction. This came down to understanding the exact mechanism of the of the protocol and identifying that there was a possibility that the controlled degradation of the peptidoglycan could also potentially destabilise the inner membrane and cause some intracellular contents to leak into the extracellular milieu.

As a result of these findings, other measures were taken to verify the results. The first of these methods was attempting to see if the same results would be obtained using when repeating the experiments when taking exceptional care to prevent the potential leaking from happening. It was also noted that it would be important to also have a control looking at the cell associated activity before treatment as a comparison to help elucidate the validity of the results.

3.4.2. Optimization of lysozyme protocol

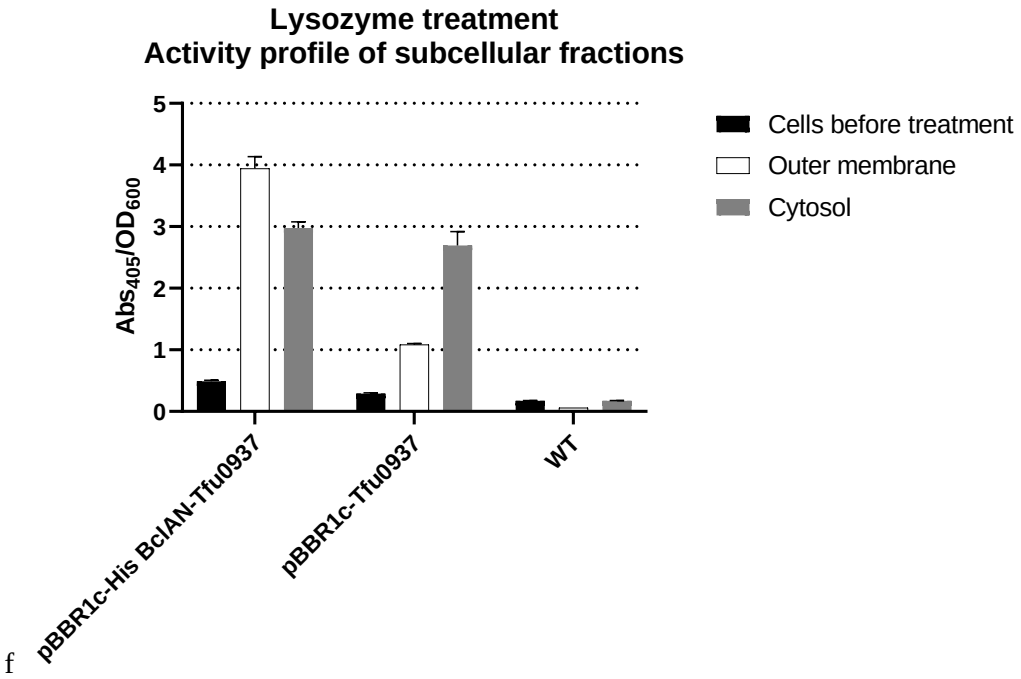

f

Figure 38 *Activity profile of the cells before treatment (Cells that had been washed with media and subsequently assayed) vs the spheroplast and membrane fraction activity.*

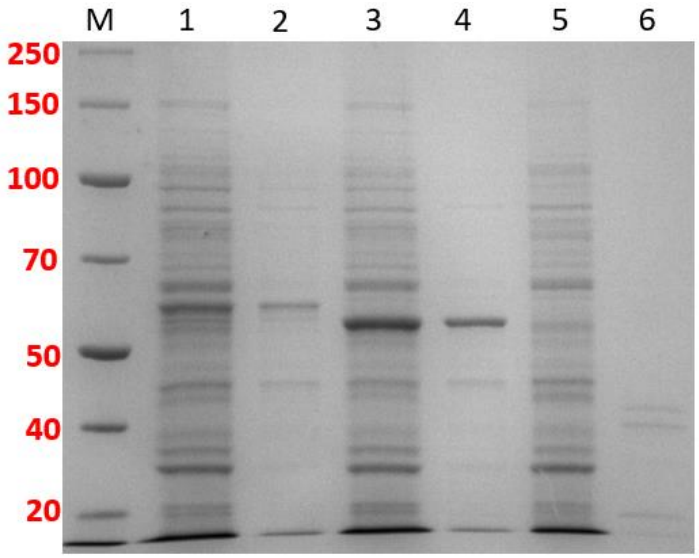

Figure 39 *SDS gel of spheroplasts and purified outer membrane fraction. Lane 1: pBBR1c-His His-BclAN-Tfu0937 spheroplast fraction, Lane 2: pBBR1c-Tfu0937 spheroplasts fraction Lane 3: pBBR1c-His-BclAN-Tfu0937 outer membrane fraction, Lane 4: pBBR1c-Tfu0937 outer membrane fraction, Lane 5 C. necator H16 WT no plasmid spheroplasts, Lane 6: C. necator H16 WT no plasmid outer membrane fraction. MW of His-BclAN-Tfu0937: 56.7 kDa, MW of Tfu0937: 53.4 kDa.*

The activity profile of this biological repeat with the added measurement of the cells before treatment highlighted some irregularities in the data that only further increased the concern that there was

significant cell lysis during the lysozyme treatment. The measured activity of the spheroplasts subsequent to the lysozyme treatment increased the visible activity by a factor of 6. This was likely due to the fact that the spheroplasts are significantly less stable after the outer membrane has been shed, and the only membrane holding the contents of the spheroplast would have been the encapsulating the inner membrane. This would have likely resulted in the liberation of the cytosolic Tfu0937 once they enter the beta glucosidase assay (see **Figure 38** and **Figure 39**).

This notion is further supported by the fact that the cytosolic fraction collected here gave lower values than that of the outer membrane fraction, even in the cells that were expressing Tfu0937 without any anchoring motif. This strongly suggested that the protocol was allowing cytosolic protein to enter the membrane fraction (see **Figure 38**).

The final key issue that was identified with this preparation was the fact that there was no way to distinguish between the outer membrane fraction and the periplasmic contents of the cell using this current protocol. As a result, the protocol needed to be further modified in order for to obtain a set of data that would be robust enough to confidently show that Tfu0937 was present in the outer membrane fraction.

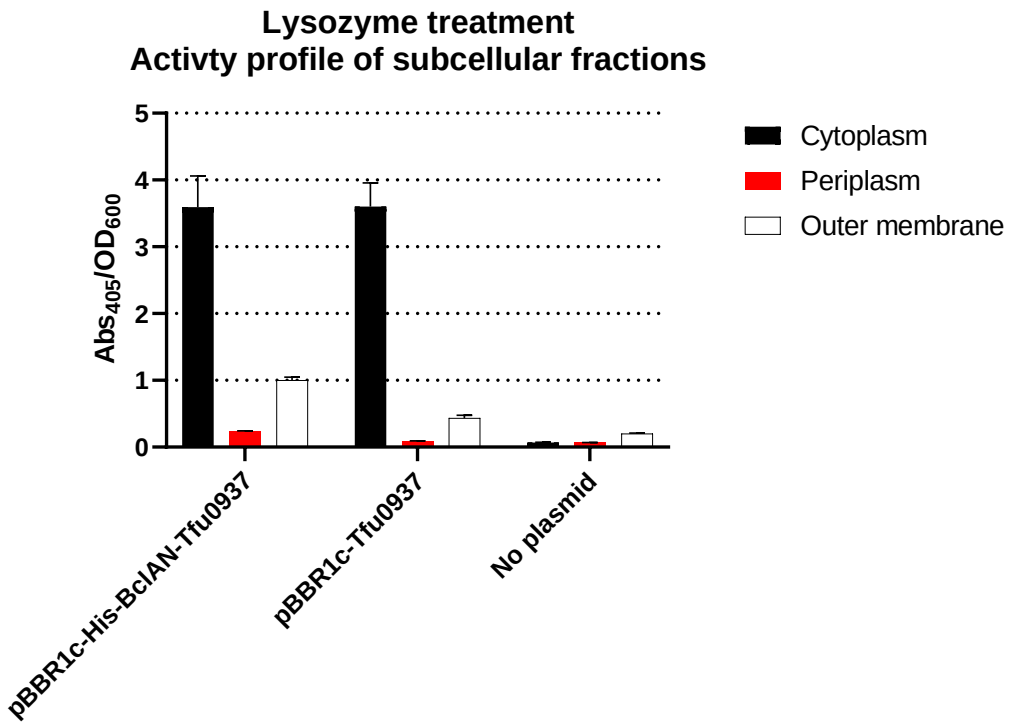

Figure 40 *Activity profile of pJ5 strains that have been fractionated using the lysozyme treatment. Steps were taken to separate the periplasmic fraction from the outer membrane fraction to identify the presence of any periplasmic protein*

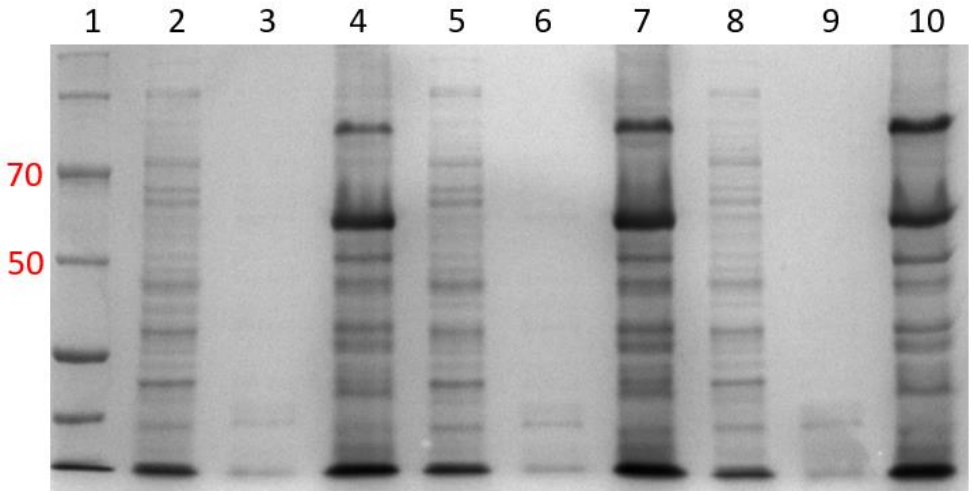

Figure 41 *SDS gel analysis pBBR1c system, cytosolic, periplasmic and membrane fractions. Lane 1: Marker, Lane 2: pBBR1c -His-BclAN-Tfu0937 – membrane fraction, Lane 3: pBBR1c -His-BclAN-Tfu0937 – periplasmic fraction, Lane 4: pBBR1c -His-BclAN-Tfu0937- Cytosol, Lane 5: pBBR1c -Tfu0937 – membrane fraction, Lane 6: pBBR1c -Tfu0937 – periplasmic fraction, Lane 7: pBBR1c -Tfu0937 – cytosol, Lane 8: No plasmid C. necator H16 – membrane fraction, Lane 9 – periplasmic fraction, Lane 10: No plasmid C. necator H16 – cytosol.*

At the time of carrying out this experiment, a temporary decision had been made to use the pJ5 system as the main strain for carrying out any analysis on Tfu0937 expressing strains. It had been concluded

that it was a more stable and reliable method for producing the same activity profiles between experiments, as the true issues with the beta glucosidase assay had not yet been ascertained. Despite this, these data still illustrate the way we had chosen to optimise the lysozyme system to give a better depiction of what was happening with the lysozyme protocol (see **Figure 40** and **Figure 41**).

The cells that were fractionated using the lysozyme protocol allowed us to see an accumulation of activity in the periplasm and the outer membrane fraction. However, when we look at the data specifically for this system, we can see that we could resolve better resolution in the SDS gel analysis of the outer membrane fraction. The membrane fraction appears to have resolved some bands that are not identical to those seen in the cytosolic fraction. This increases the likelihood that the fractionation was successful in separating the membrane fraction from the periplasm and cytosol (see **Figure 40** and **Figure 41**).

The main issue highlighted in this experiment is the fact that the cells outer membrane fractions for both the pBBR1c-His-BclAN-Tfu0937 strain and pBBR1c-Tfu0937 strain give a clear reading in the activity profile, however, their visibility in the SDS gel is negligible. This effectively meant that the SDS gel did not have the sensitivity needed to visualise the target protein in membrane fraction. This is something that could have been resolved by using a different method of staining the proteins such as silver staining or some form of immunoblotting, but these optimisations were not something we were able to pursue with the available time and resources (see **Figure 40** and **Figure 41**).

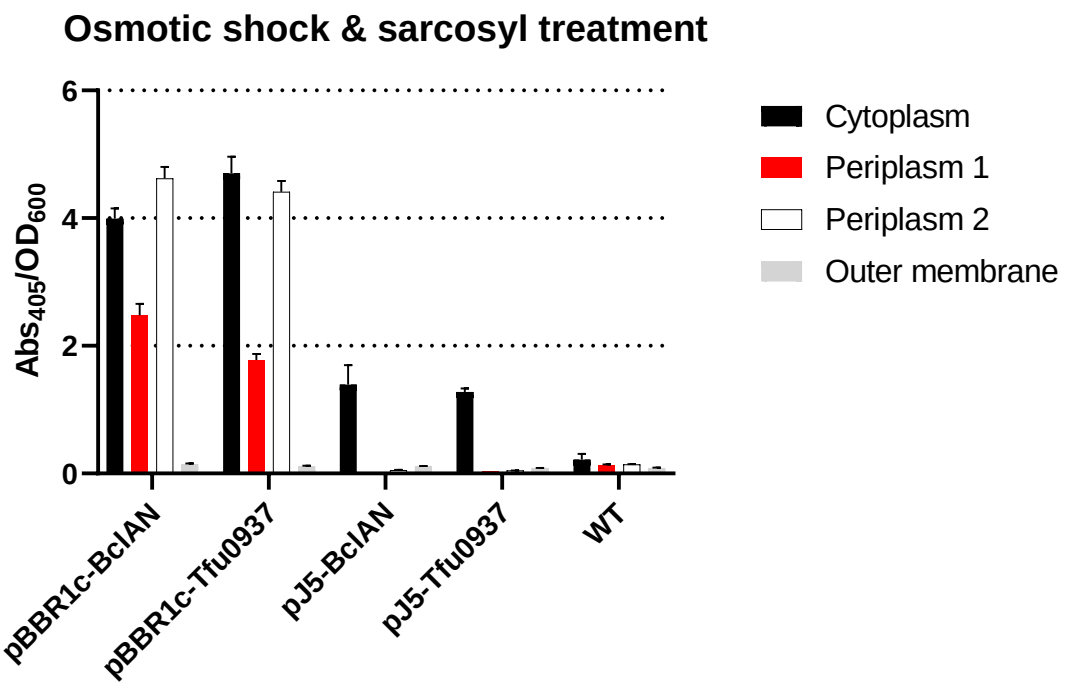

Figure 42 *Activity profile of pBBR1c strains that have been fractionated using the lysozyme treatment. With the distinction that these activity values have been calculated using the optimized protocols that give the most accurate representation of activity and two periplasmic fractions have been obtained.*

The final iteration of this experiment that was going to be carried out would be there to verify the results but also run the experiment using the optimised beta glucosidase assay. Many of the experiment that had been carried out at this time had actually been carried out using older versions of the assay as we had not yet identified certain issues that were causing some of the data to not be more accurate. However, this is not as detrimental to the data gathered prior as we were still able to learn a substantial amount of information pertaining to the way the characterisation should be done, and the sensitivity of the SDS gel. In addition to this, it is clear that even though the data is marginally different to previously gathered activity profiles, the actual trends, and activity ratios remain almost identical (see **Figure 42**).

The final conclusions of the lysozyme treatment however show us that there is a significant difference in activity measured in the outer membrane fraction especially between the BclAN anchored system and the non-anchored system. However, we are not able to consolidate these findings by providing supporting evidence that Tfu0937 is localised in the outer membrane fraction

3.5. Sarkosyl extraction

3.5.1. Initial investigation into sarkosyl membrane extraction

The second method of purifying an outer membrane fraction from the bacteria was to use a detergent to solubilise it. The method used here allows the selective solubilisation of the inner membrane, allowing the cells to be separated into a cytoplasmic/soluble fraction and an insoluble fraction containing the elements of the outer membrane. Inside these fractions, we are able to use SDS gels analysis to search for the target bands of the BclAN-Tfu0937.

The advantage of using a membrane isolation technique lies in the robust nature of the isolation technique, as well as having other methods that can be used to help confirm that the method used to isolate the membrane fraction was successful.

Using this technique in conjunction with the other data we have collected so far may allow us to consolidate the findings from the different data sets and give a more robust set of evidence to prove that BclAN localises Tfu0937 to the outer membrane of the *C. necator* H16.

To begin these experiments, the assay was carried out in similar fashion to that of the lysozyme membrane purifications.

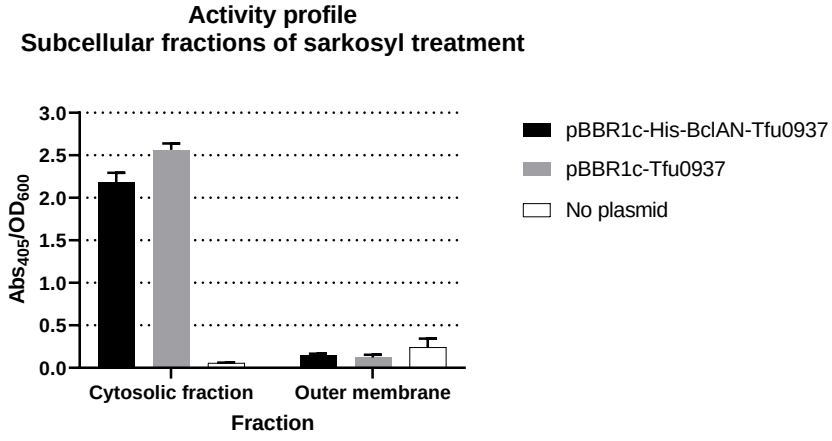

Figure 43 *Activity profile of the subcellular fractions purified using the sarkosyl method.*

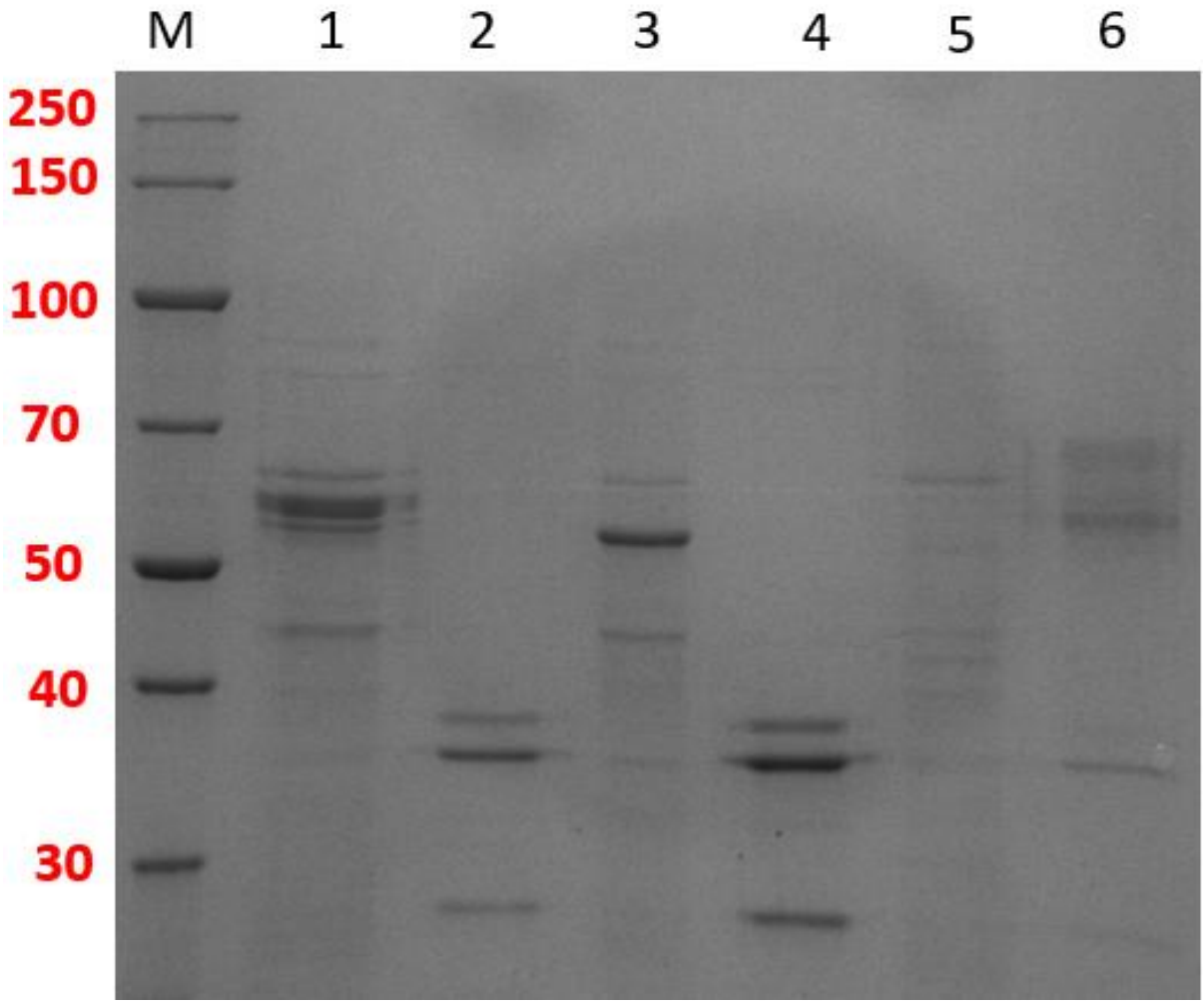

Figure 44 *SDS gel analysis of the subcellular fractions purified from the sarkosyl membrane purification Lane 1: pBBR1c-BclAN-Tfu0937 cytosolic fraction, Lane 2: pBBR1c-BclAN-Tfu0937 outer membrane fraction, Lane 3 pBBR1c-Tfu cytosolic fraction, Lane 4 p pBBR1c-Tfu0937 outer membrane fraction. Lane 5 WT C. necator H16 soluble fraction, Lane 6: WT C. necator H16 outer membrane fraction. MW of Tfu0937: 53.4 kDa, MW of His-BclAN-Tfu0937: 56.7 kDa. Cytosolic fraction contains both the cytosolic and inner membrane fraction that has been treated with sarkosyl detergent.*

The fractions from pBBR1c-BclAN-Tfu0937 show an unusual banding pattern around the 55 kDa mark. There is a thin band at 53 kDa and then above it is a more diffuse set of bands that are 3-4 kDa heavier. This is around the molecular weight of fusion protein His-BclAN-Tfu0937. While this may be a sign of fusion stability after the processing it has undergone (sarkosyl treatment, heat denaturation, multiple freeze thaw cycles), it is also possible that the gel had some aberrations in this area that caused us to lose resolution. This possible degradation theory is also made significantly less likely as there is no reason why sarkosyl should illicit such a response in a protein, and this is the first and only time we

have observed instability in the His-BclAN-Tfu0937 fusion protein. The Tfu0937 in the pBBR1c-Tfu0937 cytosolic fraction, shows no signs of aberration.

The protein profiles of the purified membrane fractions show prominent banding at ~48 kDa, 46 kDa, and ~28 kDa in both the pBBR1c-BclAN-Tfu0937 strain and the pBBR1c-Tfu0937 strain but does not appear to be as evident in the wild type with no plasmid. There are still visible bands at 46 kDa and 28 kDa. There is also diffuse banding in the ~50 kDa area in the WT. This difference between the WT and other pBBR1c strains, can really only be attributed to the presence of different proteins present during the expression Tfu0937. However, why protein expression would affect the proteome of the outer membrane is not clear. The amount of expression seen in the outer membrane fraction was so low that it was clear that there was no banding at the correct molecular weight. This correlates with the amount of Tfu0937 visualized in the outer membrane fraction of the SDS gel. At the time this experiment was conducted, we had not yet learnt that the SDS gel was not sensitive enough to show the presence of Tfu0937, but there was still a chance it could show up as the amount of protein that is isolated using this methodology was of a higher concentration of that in the lysozyme. To try and make an iterative improvement on what we see in this experimental data, the volume of the cells used in the preparation to potentially allow us to see the Tfu0937 in the outer membrane fraction

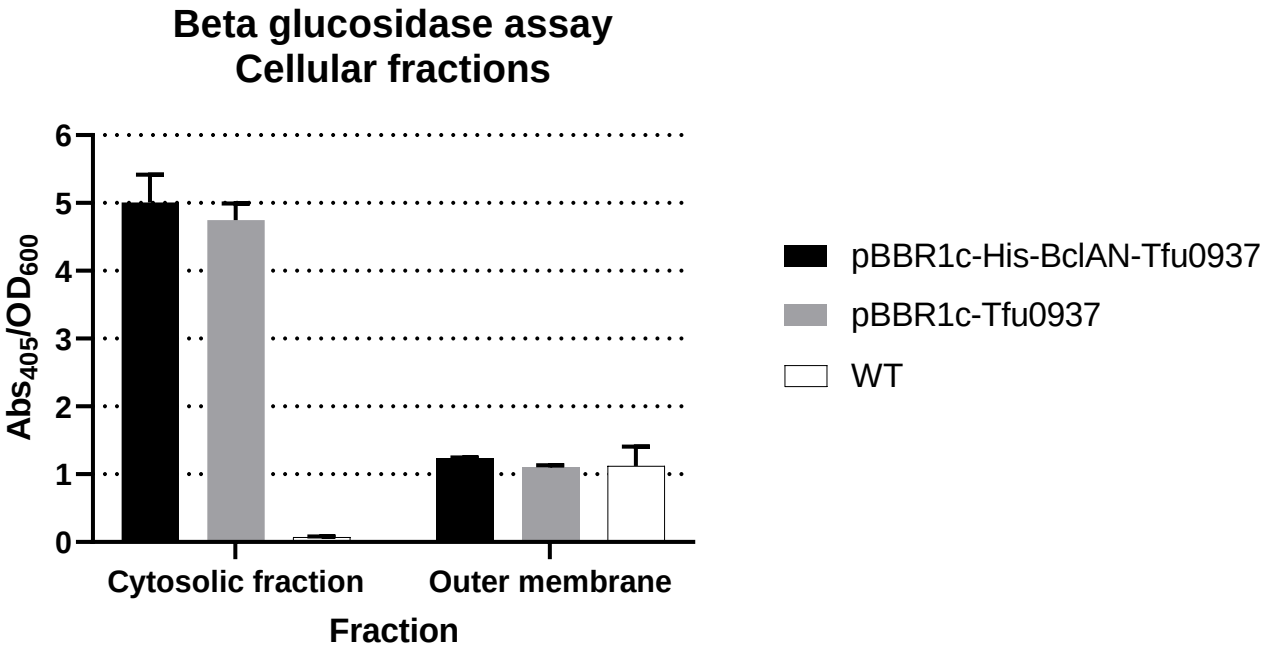

Figure 45 *Activity profile of the sarkosyl treatment after increasing the volume of cell from 5mL to 20 mL of culture.*

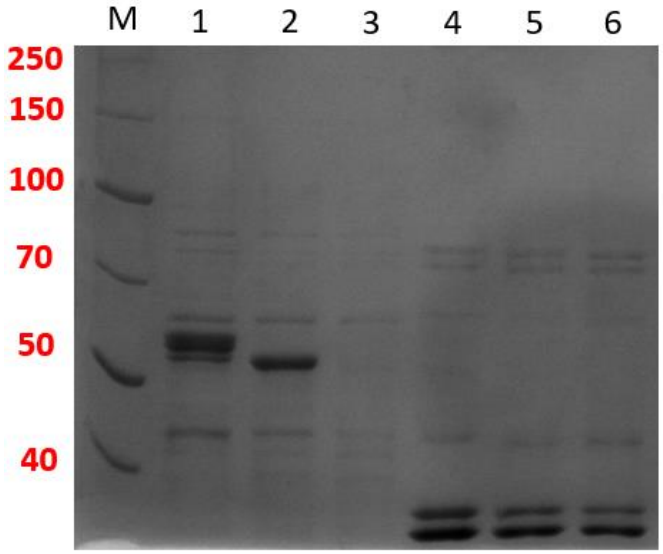

Figure 46 *SDS Gel analysis of sarkosyl membrane isolation. Lane 1: pBBR1c-His-BclAN-Tfu0937 - cytosolic fraction, Lane 2: pBBR1c-Tfu0937 – cytosolic fraction, Lane 3: C. necator H16 no plasmid – cytosolic fraction. Lane 4: pBBR1c-His-BclAN-Tfu0937 – outer membrane fraction, Lane 5: pBBR1c-Tfu0937 – outer membrane fraction, C. necator H16 no plasmid – outer membrane fraction. MW of Tfu0937: 53.4 kDa, MW of His-BclAN-Tfu0937: 56.7 kDa*

In this iteration of the experiment, I opted to increase the number of cells used for the purification of the membrane. When this experiment was first carried out, only 5 mL of culture was used instead of the 20 mL shown here. This was done to increase the amount of Tfu0937 purified in the membrane fraction, so that enough yellow colour would be produced for it to overcome the very cloudy lipid fraction. The high reading of the WT outer membrane fraction is attributed purely to how cloudy the purified membrane fraction is.

The SDS gel profile shows an increase in the accumulation of Tfu0937 specifically in the cytosolic fraction for the pBBR1c-His-BclAN-Tfu0937, and the pBBR1c-Tfu0937 system, but we also see a clear accumulation of banding in the 20-30 kDa region of the outer membrane fraction. This banding is a great marker to show that the membrane isolation is likely to have been successful. Unlike in the lysozyme purification, these bands are likely to be known outer membrane proteins. OmpA and OmpC. Similar bands are present in the purification done in the original publication that utilises the BclAN anchoring motif (Park *et al.*, 2013).

The problem with this data is that despite all these outer membrane protein markers being present, and the increase in protein concentration because of the modification to the protocol, there is still no Tfu0937 present in the outer membrane fraction of the pBBR1c-BclAN-Tfu0937 strain. At this point, there was concern that the Tfu0937 was not actually present in the within the outer membrane fraction.

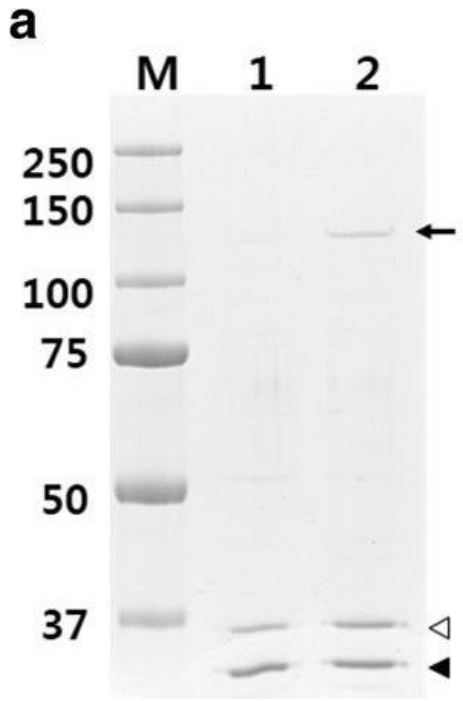

Figure 47 *Outer membrane purification using the sarkosyl method from a publication. Lane 1 is the outer membrane fraction of the control cells (E. coli with no plasmid), Lane 2 shows the outer membrane fraction of the cells expressing their 150 kDa target protein endoxylanase. Bottom two bands OmpA and OmpC (Figure taken from Park et al., 2013). The cells used for this paper were E. coli BL21 cells.*

3.5.2. Comparing *E. coli* DH5α to *C. necator* H16

As a result of this concern, it was decided that we should carry out membrane extraction in *E. coli* DH5α to see if it was possible to replicate the data in the paper where BclAN is used as an anchoring motif. The aim of this comparative experiment was to get some insight into whether the usage of *C. necator* H16 was potentially having a detrimental effect on the efficacy of the extraction protocol, but also to see if we were able to replicate the results that were reported in the original publication.

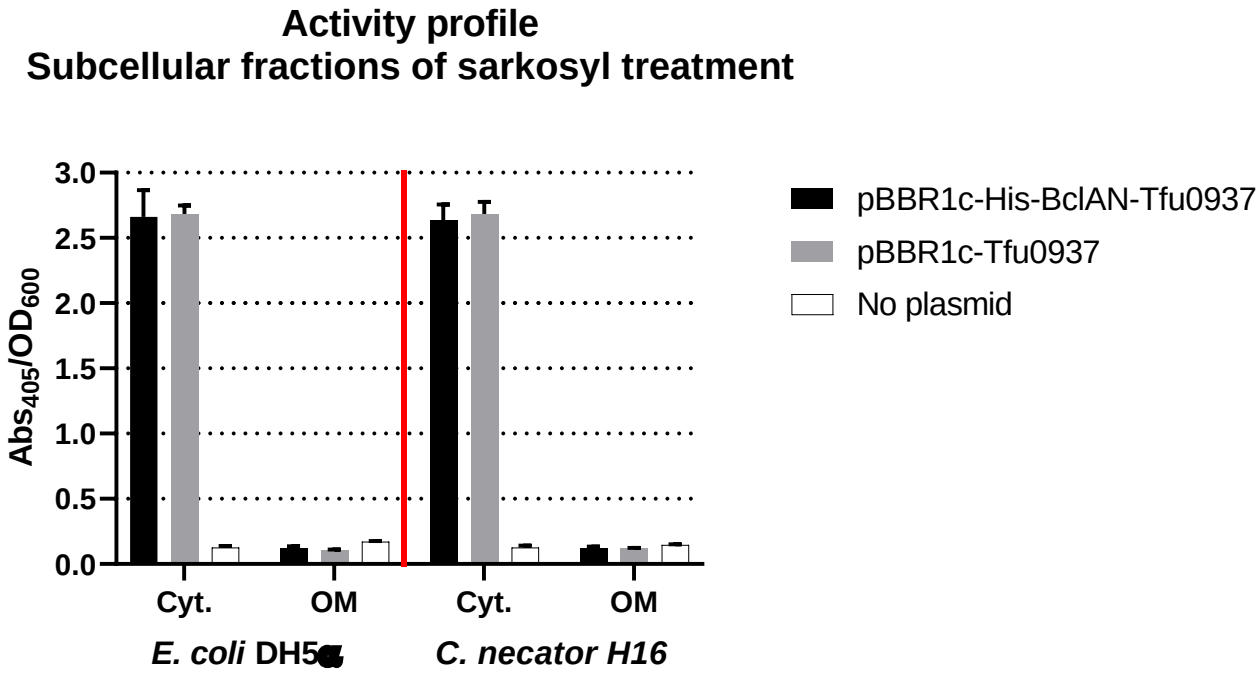

Figure 48 *Activity profile of sarkosyl membrane isolation from Tfu0937 from pBBR1c-His-BclAN-Tfu0937, pBBR1c-Tfu0937 in both E. coli DH5α and C. necator H16*

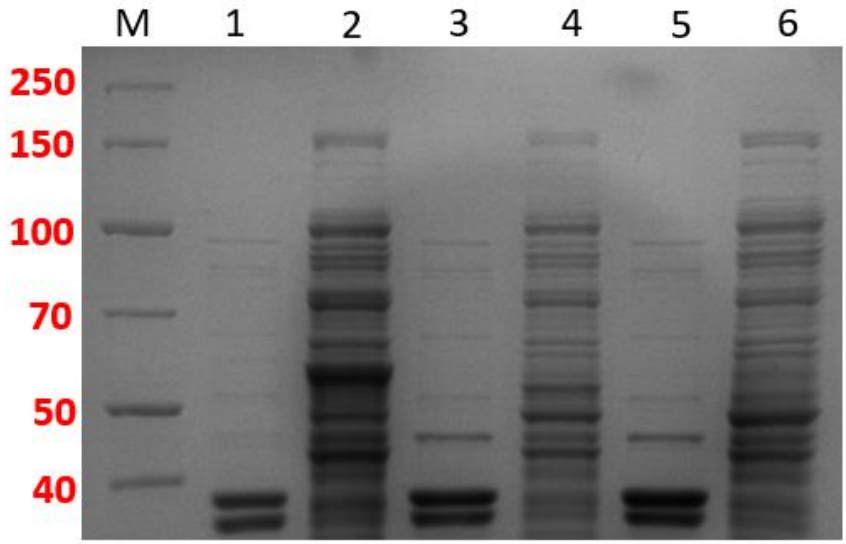

Figure 49 *SDS gel analysis of the cells with the outer membrane purified using the sarkosyl method. Lane M: Marker, Lane 1: pBBR1c-His-BclAN-Tfu0937 – outer membrane, Lane 2 pBBR1c-His-BclAN-Tfu0937 – cytosolic fraction, Lane 3 pBBR1c-Tfu0937 – outer membrane fraction, Lane 4: pBBR1c-Tfu0937 – cytosolic fraction, Lane 5: E. coli DH5α no plasmid – outer membrane fraction, Lane 6: E. coli DH5α– cytosolic fraction. MW of Tfu0937: 53.4 kDa MW of His-BclAN-Tfu0937: 56.7 kDa. Some of the E. coli DH5α pBBR1c-Tfu0937 strain sample was lost during sonication, and I was only able to recover 60% of the sample, which is the reason for the lowered intensity of the bands in that specific lane.*

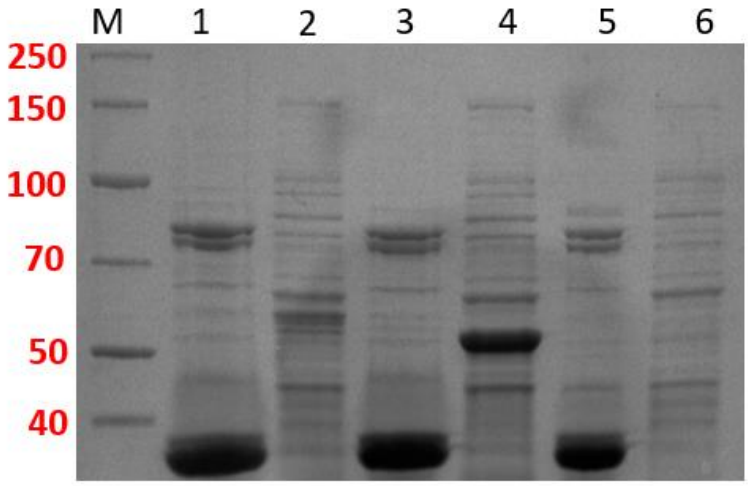

Figure 50 *SDS gel analysis of the cells with the outer membrane purified using the sarkosyl method. Lane M: Marker, Lane 1: pBBR1c-His-BclAN-Tfu0937 – outer membrane, Lane 2 pBBR1c-His-BclAN-Tfu0937 – cytosolic fraction, Lane 3 pBBR1c-Tfu0937 – outer membrane fraction, Lane 4: pBBR1c-Tfu0937 – cytosolic fraction, Lane 5: C. necator H16 no plasmid – outer membrane fraction, Lane 6 C. necator H16 no plasmid – cytosolic fraction. MW of Tfu0937: 53.4 kDa MW of His-BclAN-Tfu0937: 56.7 kDa*

We were able to see that even in the *E. coli* DH5α, we were not able to identify the Tfu0937 in the outer membrane fraction. This led us to believe that there may be an issue with the way the Tfu0937 may be getting translocated to the membrane. In the publication by Park et. Al where this exact anchoring motif was used to display endoxylanase, we can see that there even in their work, the amount of their passenger protein, endoxylanase, was very low in concentration in the outer membrane fraction. The fact that we are not able to resolve the Tfu0937 despite getting such clear accumulation of the outer membrane protein homologues, suggests that perhaps BclAN-Tfu0937 protein may not be being translocated to the membrane in high enough concentrations that allow us to see it.

There may also be issues with the optimisation of the preparation that allow us to see more of the other membrane proteins. Often times protocols that have been optimised for use in *E. coli* do not necessarily work with the same efficacy when changing the organism despite the existing similarities between them. In our case, it is possible that the incubation time, sarkosyl concentration, or even the displayed protein may need to have been changed in order to allow for visualisation on an SDS gel.

Previous membrane extraction using sarkosyl method showed the possibility of some localisation of Tfu0937 within the membrane fraction. The experiments were repeated to verify this finding alongside modifications to the protocol to reduce the amount of background absorption produced from the lipids in the membrane sample. This was done because the high concentration of lipids in the outer membrane was causing the sample to be too turbid. This made it impossible to tell whether there was a significant amount of 4-nitrophenol being generated by any potential Tfu0937.

3.5.3. Checking sensitivity of Tfu0937 to sarkosyl

At this time, it was postulated that the sarkosyl, being a detergent has a negative effect on the structure of Tfu0937. Sarkosyl was added to free Tfu0937 to the same working concentration used in the membrane isolation

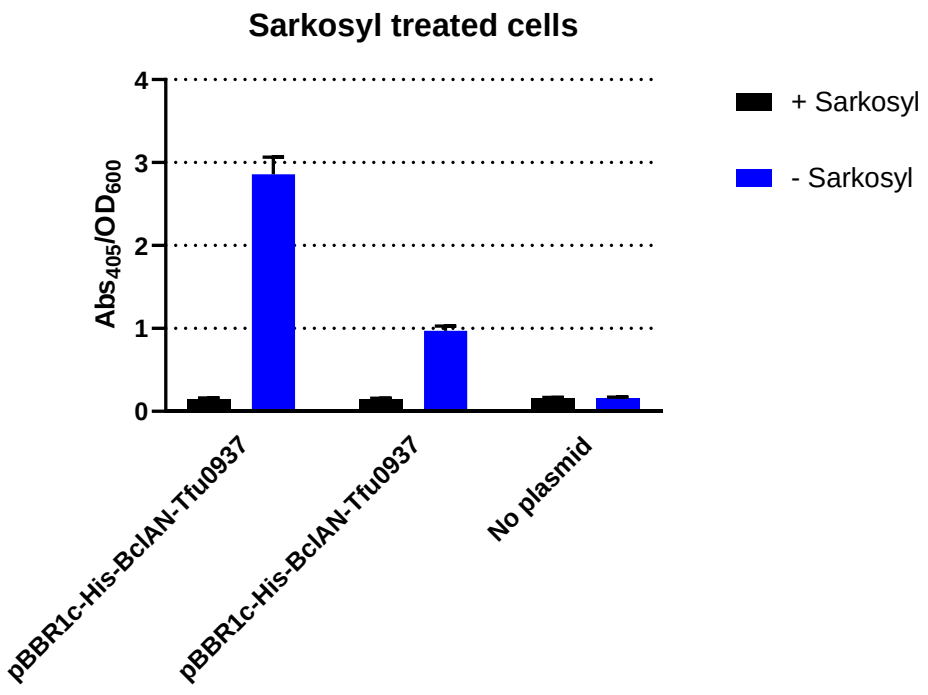

Figure 51 *Testing the ability of sarkosyl to denature Tfu0937.*

Addition of Sarkosyl leads to total abrogation of activity. The data collected from previous experiment suggesting there might be activity within the purified fraction is anomalous. Given that the SDS gel is not clear about whether or not the band is present, this method of membrane purification will need to be reconsidered in order see what can be done to ascertain some meaningful data.

3.6. Conclusions

The work done here was aimed at orthogonally confirming whether or not BclAN is functioning as an anchoring motif for *C. necator* H16. This data is meant to work in conjunction with the data that had been collected in the previous chapter. What we were able to do is show that using proteinase K, we can illustrate that the BclAN-Tfu0937 strains are more sensitive to the extracellular proteases when compared to the cytosolic version. But more importantly, the Tfu0937 strain does not show significant sensitivity to the assay. This is important because it highlights a key difference in illustrating the localisation of activity in a relatively binary fashion. To that end, it provides a robust piece of evidence that supports the idea the subcellular location of some of the BclAN-Tfu0937 is in the membrane. However, it was important to note that the combination of the enzyme Tfu0937 and the fact that the protocol was not really optimized for use in *C. necator* H16 meant that we failed to see the extreme levels of protein abrogation that are often reported when this method is used in other cells.

The outer membrane isolation techniques also suffered from this issue, while also being significantly more difficult to get meaningful data from. The combination of sarkosyl denaturing the Tfu0937 and the fact that the SDS gel was not able to resolve the bands well unless a high concentration of Tfu0937 was present has meant that the overall value of these experiments is low.

However, the lysozyme osmotic shock treatment did show us that there is significant amount of Tfu0937 present in the periplasm of strains of both the pBBR1c-Tfu0937 strain and the pBBR1c-His-BclaN-Tfu0937 strain. This gives some potential insight into the high incidence of background activity observed by the pBBR1c-Tfu0937 strain.

The lysozyme treatments were also challenging to analyse as they did consistently show that there was an accumulation of Tfu0937 in the membrane fractions of these purifications, but there were too many shortcomings in the protocol that made us lose confidence in the accuracy of the results. This included membrane localisation of Tfu0937 in pBBR1c-Tfu0937, when there is no reason, this should be possible.

4. Chapter 4: Cellobiose cultivation

4.1. Introduction

One of the key goals of this project is to demonstrate the ability of displayed enzymes to augment the metabolic capabilities of an organism. This section looks at how the display of tfu0937 facilitates this in C. necator H16.

Extracellular display has been shown to function in this manner even when implemented in the most rudimentary fashion (Tanaka *et al.*, 2011). The elements used for the degradation of cellulose have been displayed on the cell surface of *E. coli*. Combined with integration of the genetic elements required for ethanol metabolism, it is possible to produce a strain of *E*. coli that was now able to use cellulosic carbon as a means of producing biofuels (Tanaka *et al.*, 2011).

However, it is important to note that creating a system of this nature is not without its own shortfalls. The extracellular metabolism of the target metabolite means that if this system were to become modular, the organism still needs to be able to transport the product into the cell. Without the necessary means to do this, further systems would need to be introduced to the organism to facilitate that process. There can also be issues with accumulation of the certain metabolites, such as carbon dioxide in the extracellular space creating an environment that is not fit for growth. This calls into question the certain issues that might come with flux between the production of the target metabolite, its transport, and metabolism into other products. These issues could be expedited by the fact that the transporters may be introduced into the other heterologous proteins, however as we increase the burden of resource allocation towards these different systems, it becomes increasingly more important to integrate regulatory processes to ensure that the cells are capable of delivering on all fronts without compromising on cell growth and health.

C. necator, while capable of utilising many carbon sources, is not readily able to metabolise specific carbohydrates whose main constituents are glucose. This is due to the fact that the organism does not possess the right enzymatic toolkit for the breakdown of the polymers such as starch and cellulose.

These are of particular interest because they are the primary monomers found in lignocellulosic biomass. The primary aims of using *C. necator* H16 as a microbial biorefinery, requires that the feedstock be a readily available carbon source.

4.2. Materials and Methods

4.2.1. Cultivation of C. necator H16

4.2.1.1. Cultivation of C. necator H16

Unless stated otherwise, *C. necator* H16 was cultivated at 30 °C, 250 rpm, in MSM media supplemented with 1% gluconate ,0.5% cellobiose or NB media. For some experiments MSM was supplement with both 0.5% gluconate and 0.5% cellobiose. Ensure all cultures are supplemented with gentamicin (10 µg/mL working concentration), and cultures containing pPJ5'c.rbs-His-BclAN-Tfu0937/ pBBR1c-His-BclAN-Tfu0937 and pPJ5'c.rbs-Tfu0937/ pBBR1c-Tfu0937 are supplemented with chloramphenicol (25 µg/mL working concentration)

4.2.2. Whole cell beta glucosidase assay

Whole cell beta glucosidase assay for characterisation of whole cell activity was identical to that which was used in Chapter 2 with no modifications.

4.3. Results and discussion

4.3.1. Characterisation of glucose utilizing mutant

The first thing that needed to be done in creating such as system was first circumventing the problem of metabolism, and transport. In the work done by (Sichwart *et al.*, 2011) a strain of *C. necator H16* ΔnagRnagE (*C. necator* G+) mutant was that was capable of metabolising glucose. This work was done because, despite not having the native ability to grow using glucose as a primary carbon source, they observed that the genes for the gluconeogenesis were present in the genome of the organism.

Characterising the growth of the strain in glucose was the first step. This information would serve as a baseline for understanding the exact growth rate and characteristics. These rates could then be compared to those of the strain in MSM supplemented with gluconate.

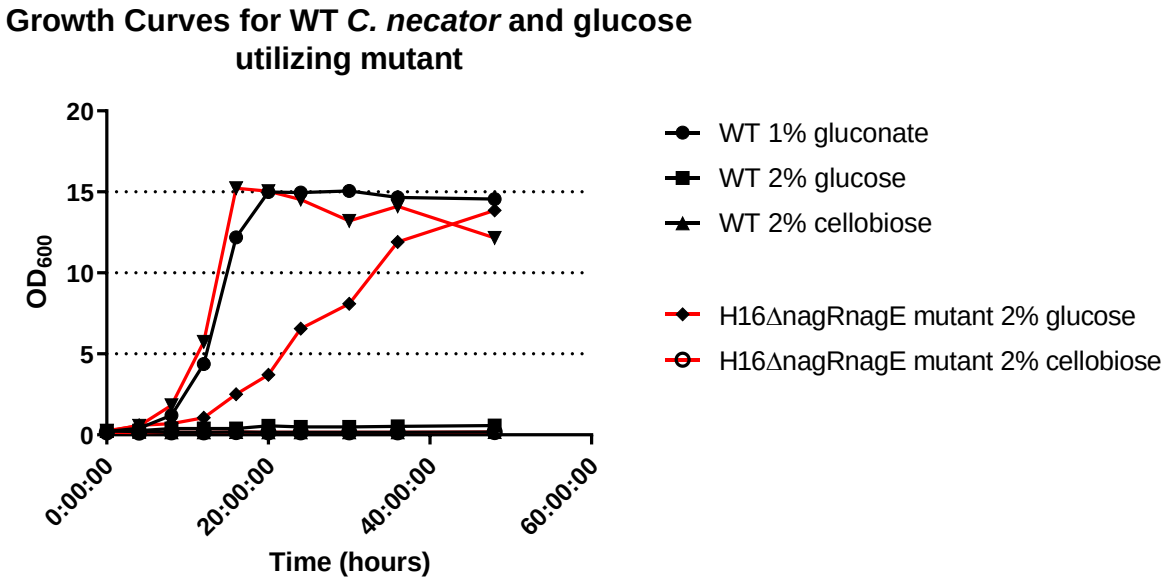

Figure 52 *Growth curves of glucose utilising C. necator H16 mutant in different carbon sources (glucose, gluconate, and cellobiose)*

The growth rates of the mutant were comparable to that of the WT *C. necator*. This was a suspected result as the specific parts of the organism that are mutated in the glucose utilising variant, should not affect its ability to metabolised gluconate.

Here we also confirm that the wild type of strain is incapable of growing in glucose or cellobiose. We also demonstrate that there is no growth in cellobiose for the glucose utilising strain.

The growth of the glucose utilising strain is notably slower than the growth in gluconate, however we can see that the maximum OD reached of ~13 is reached after roughly 2 days of cultivation. This discrepancy in growth rate is likely due to the limiting factor of the rate of glucose uptake in the G+ strain. However, the growth is still relatively fast and would allow for clear growth analysis in later experiments.

Now that the baseline growth rates had been established, the next step was to tentatively attempt to assemble the system in order to allow the Tfu0937 containing strains to be cultivated in the cellobiose media. From here, we could then look at different optimisations that could be introduced in order to make the process work better.

At this stage of the experimental design, it became clear that there were some considerations that needed to be made that we had not yet experienced in our other experiments. Namely, at which point should the cells be induced. One protocol that could grow the cells first in MSM media supplemented with glucose until an induction OD of about 0.4, at which point the cells were to be induced and then transferred to cellobiose containing media. However, another idea was to continue the cultivations in gluconate media for 8 more hours to fully allow the system to start displaying before moving it to the cellobiose media. The idea here was to mitigate some of the metabolic shock of moving the cells to a media with no immediate available carbon source. To identify which method would be more suitable, both were tested. Here we identified that the pBBR1c-BclAN-Tfu0937 was capable of growing in the 2% cellobiose regardless of when the cells were transferred to the cellobiose medium and induced. However, we did notice that the pBBR1c strain was not able to grow in cellobiose medium when transferred to the new medium and subsequently induced.

This was not concomitant with other data we had previously collected regarding the ability of the pBBR1c-Tfu0937 cells extracellular Tfu0937 activity. To that end, all the experiments were repeated and triplicate values for all growth curves was obtained.

4.3.2. Optimising cultivation temperature, and induction timing

There was also the concern about the temperature at which the cultivation should be carried out at a temperature that favoured native metabolic processes, or at one that favoured the efficiency of the Tfu0937.

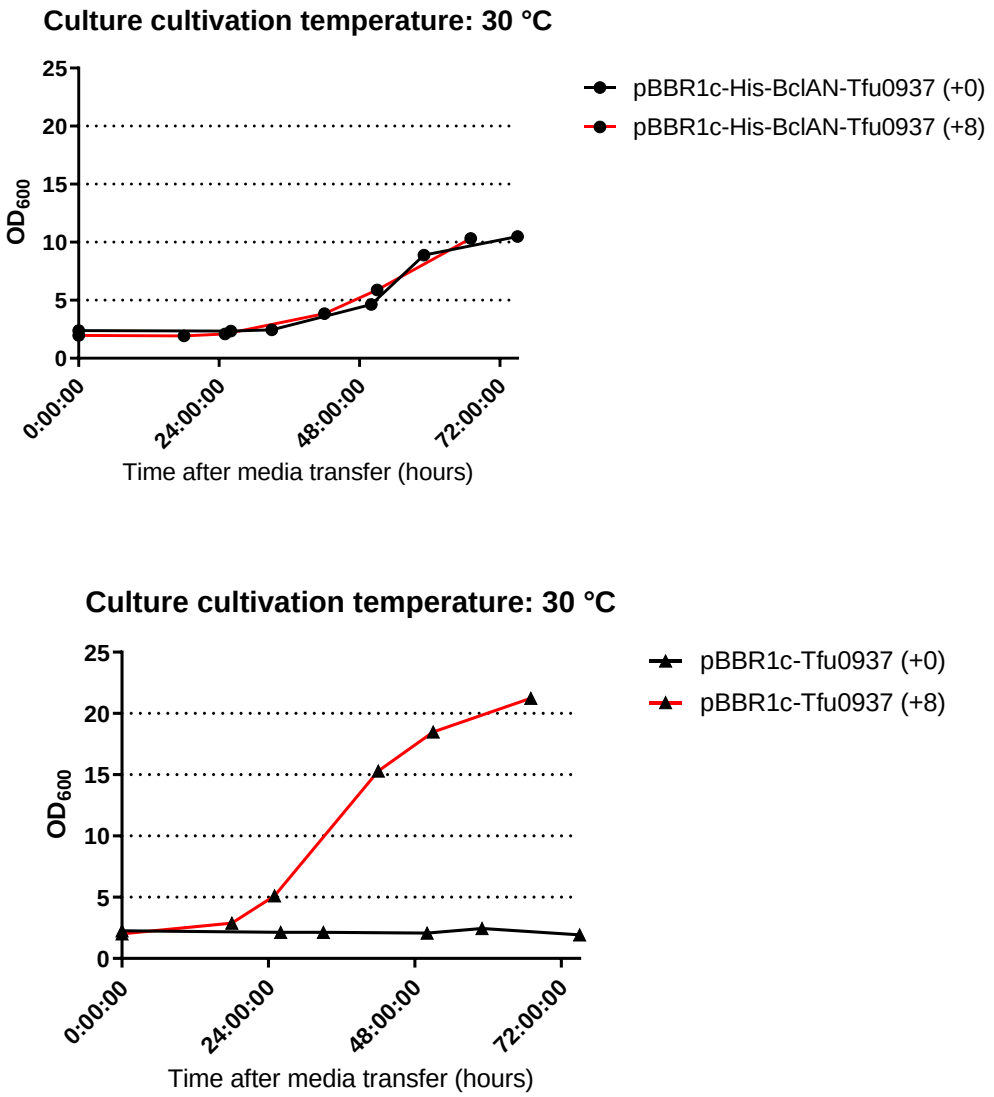

Figure 53 *Cultivations of C. necator H16 expressing pBBR1c-His-BclAN-Tfu0937 and pBBR1c-Tfu0937. +0 indicates that the cells were transferred from gluconate media to cellobiose media and then induced immediately, +8 denotes that the cells were induced for 8 hours first before transferring the cells to cellobiose media containing the same 0.1% arabinose. These cultures were cultivated at 30 °C*

Here we see that cultivation at 30 °C was successful. The pBBR1c-BclAN cultivation shows us that it the display system is allowing growth on cellobiose. It is unusual that at this cultivation allows us to grow the cells to only a maximum OD_{600} of roughly 10. This appears to be the case regardless of when the cells are moved into the media before or after induction. This would suggest that the cells are capable of using carbon stores to express and display the Tfu0937. However, when we look at the data from the cultivation of pBBR1c-Tfu0937, there was clear difference in the growth characteristics.

Here, we see a failure of the cells to grow when they were transferred to the new media after being induced for 8 hours. This was an interesting development as this result does not necessarily reflect passed data, we have regarding the extracellular activity of Tfu0937. Previous data showed us that there has consistently been extracellular activity shown by this system, and as such we expected to see some level of growth. This was made more unusual by the fact that the cells appeared to manage to grow when the induction is carried out after the transfer to cellobiose media. This suggested that there had been an erroneous error in the cultivation of this culture.

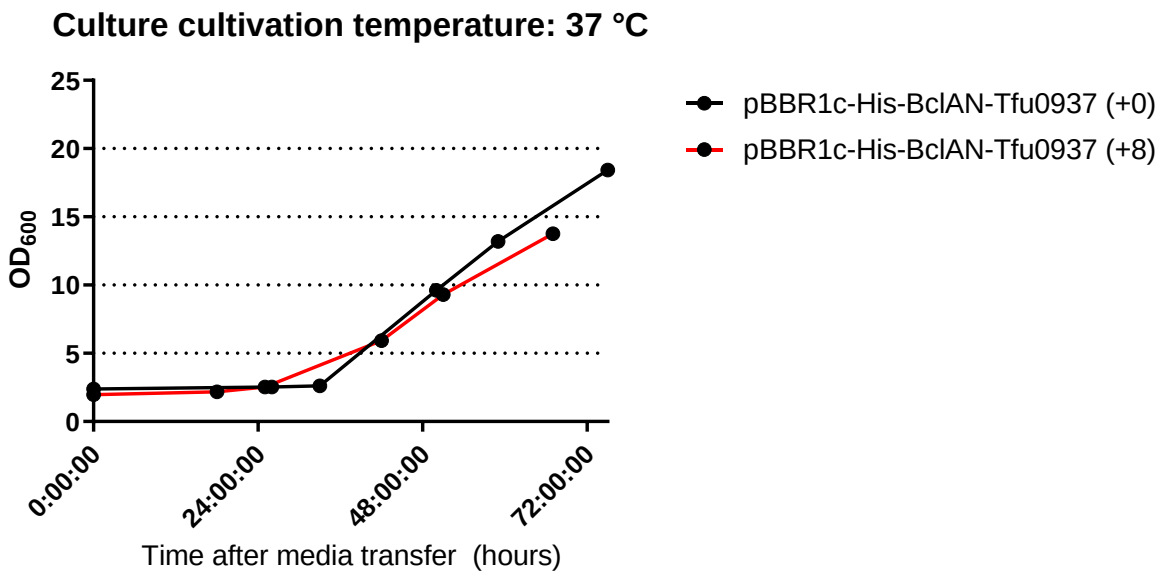

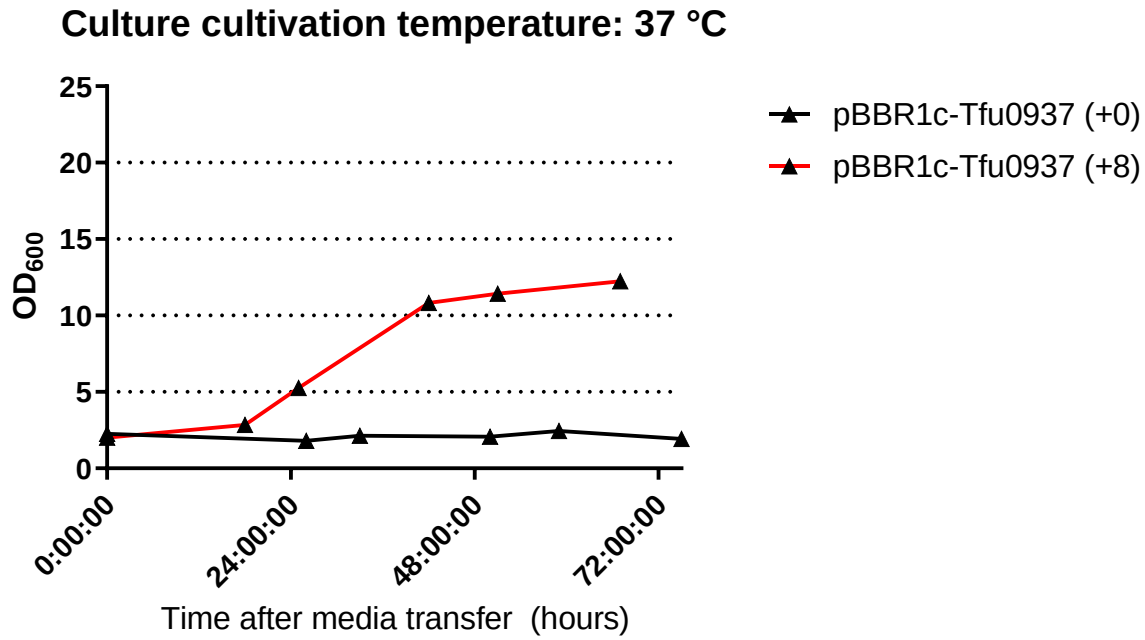

Figure 54 *Cultivations of C. necator H16 expressing pBBR1c-His-BclAN-Tfu0937 and pBBR1c-Tfu0937. +0 indicates that the cells were transferred from gluconate media to cellobiose media and then induced immediately, +8 denotes that the cells were induced for 8 hours first before transferring the cells to cellobiose media containing the same 0.1% arabinose. These cultures were cultivated at 37 C*

Cultivation at a higher temperature gave us insight into the growth characteristics of the cells under different metabolic stress. The growth rate of the cells was shown to be significantly higher in the pBBR1c-BclAN strain when compared to the cultivation at 30 °C. we also see that a higher maximal OD_{600} than when cultivated at 37 °C. This would suggest that that despite the cells not being able to grow well at 37 °C, the higher availability of carbon is permitting the cells to grow faster.

This theory does not correlate with the growth seen in the pBBR1c-Tfu0937 strain when grown at 37 °C. It was also noted that the culture that did grow in pBBR1c-Tfu0937 was the one that was not first induced and then transferred, suggesting that the growth was possible for this strain. The data here shows us that the growth was not as fast as the growth at a temperature of 30 °C. This also does not fall in line with the previous postulations about the implications of growing at different temperatures. These seemingly contradictory results led us to run these experiments again to see if similar growth would be observed. These repeats were carried out for all the different cultivations under different

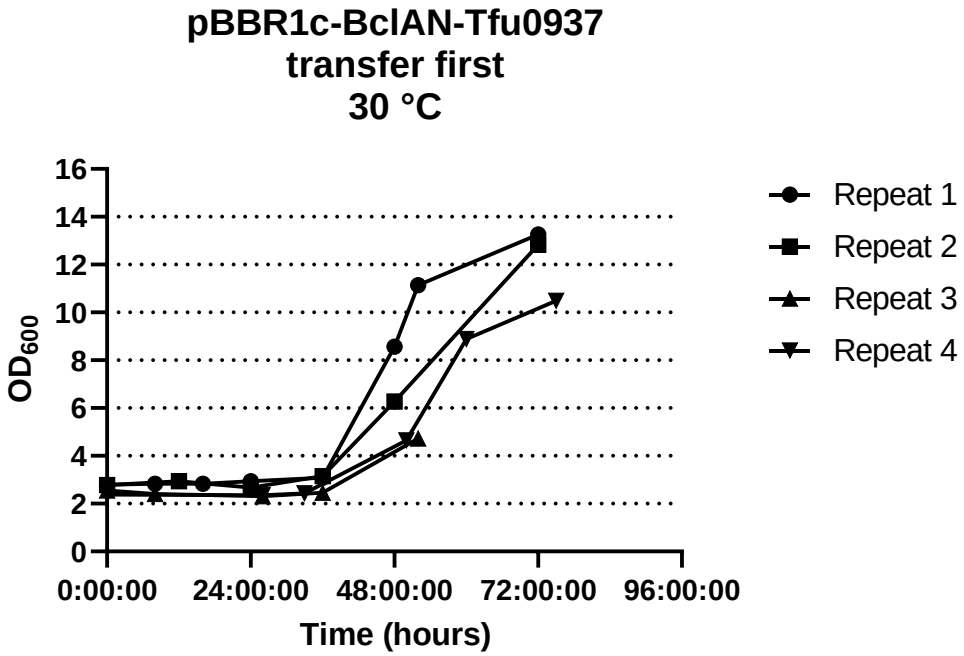

Figure 55 *Series of biological repeats looking specifically at pBBR1c-His-BclAN-Tfu0937 using the +0 as a system to test for the stability, and reliability of the cultivation method.*

For the pBBR1c-BclAN-Tfu0937 cultures grown at 30 degrees, with the transfer to cellobiose media happening before induction, we can see that there is always consistent growth in the media. The specific growth rate however is shown to vary between cultivations. It is possible that these differences are arising primarily from the natural variance that we would ordinarily see between the cultivations. The cultures also seem to consistently enter the exponential growth phase between 36 and 48 hours after the transfer into cellobiose media. This does support the notion that the variance is not due to experimental error.

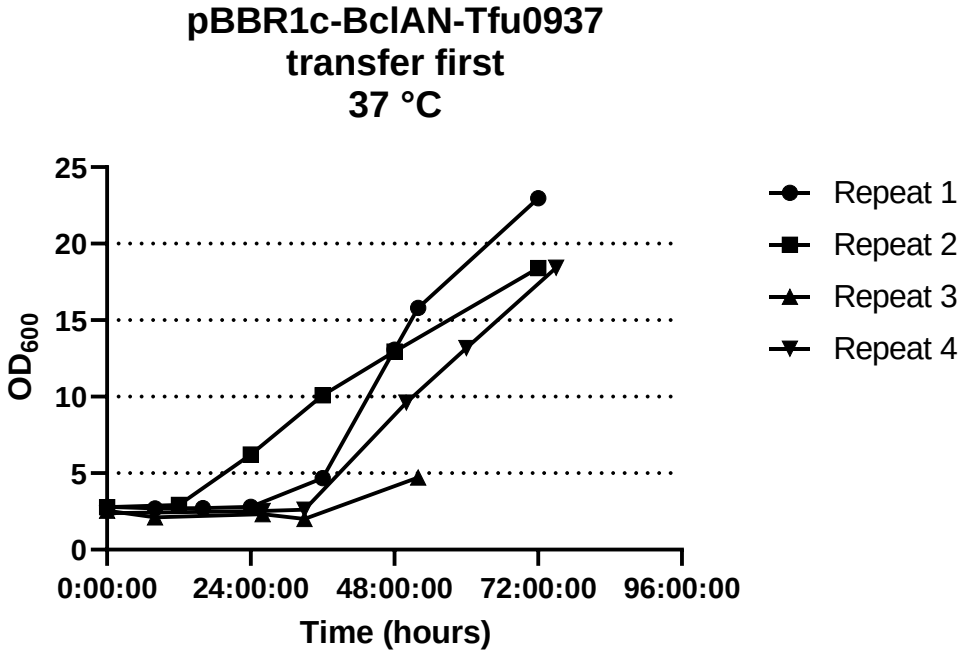

Figure 56 *Series of biological repeats looking specifically at pBBR1c-His-BclAN-Tfu0937 using the +0 as a system to test for the stability, and reliability of the cultivation method, but increasing the temperature of cultivation.*

Now when we look at the same system but grown at 37 C, we see that there is significantly more variance in the growth of the cultures, with some repeats entering the exponential phase as early as 12 hours into the cultivation, and others lagging as late as 40 hours into the cultivation. The other thing that was unusual about this, was the fact that the cells would grow at different rates once they enter exponential phase. The reasoning for this should be to do with the fact that the increased temperature is having an effect on the cell's metabolism. However, the reason as to why this effect is erratic and unpredictable is not clear. One possible reason for this is the fact that the different temperatures are causing the production and display of the recombinant protein and display to be at a large imbalance, changing the availability of glucose for growth. However, this is not something that we can easily measure unless we were to look specifically at the amount of glucose and cellobiose at different stages of the cultivation. These temperature changes could also exacerbate the already existing variance in the cultivation being cause by the growth conditions, but this is not a particularly strong argument for the variance in the growth rates. To further our understanding of these growth characteristics, consolidating our understanding with data from the pBBR1c-Tfu0937 system is necessary.

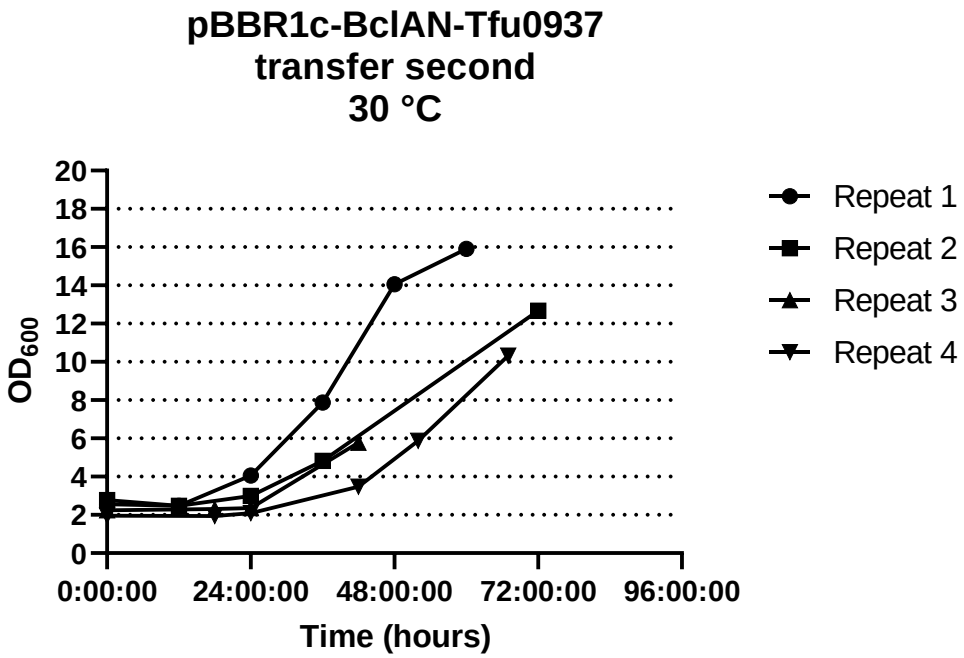

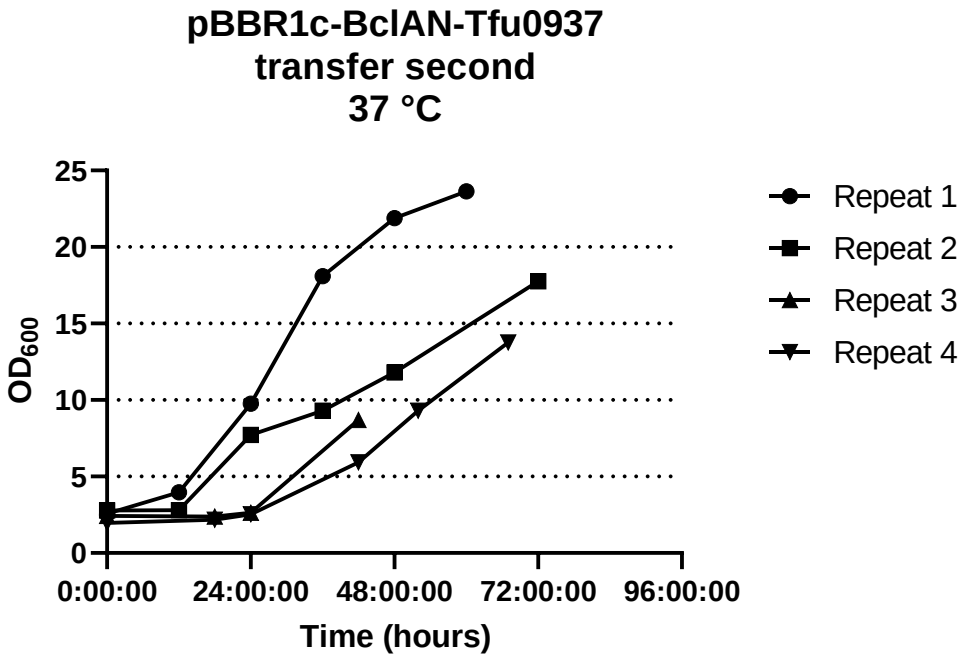

Figure 57 *Graphs of pBBR1c-His-BclAN-Tfu0937 system comparing the +8 system at both temperature across a series of 5 biological repeats.*

When we look at the performance of the pBBR1c-BclAN-Tfu0937 cells grown when the transfer was done after 8 hours of induction, we observe a few similarities for the cultures grown at 30 °C. The first of these is the fact that the cells growth rate appears to fluctuate between experiments. This is reminiscent of what we see when the cells were grown at 37 C, with no pre-induction. However, we do see that the cells still enter the exponential phase at around the same time around 12 hours. This is in line with the idea that the catalysis of cellobiose to cellulose faster when the cells enter the media already displaying the protein.

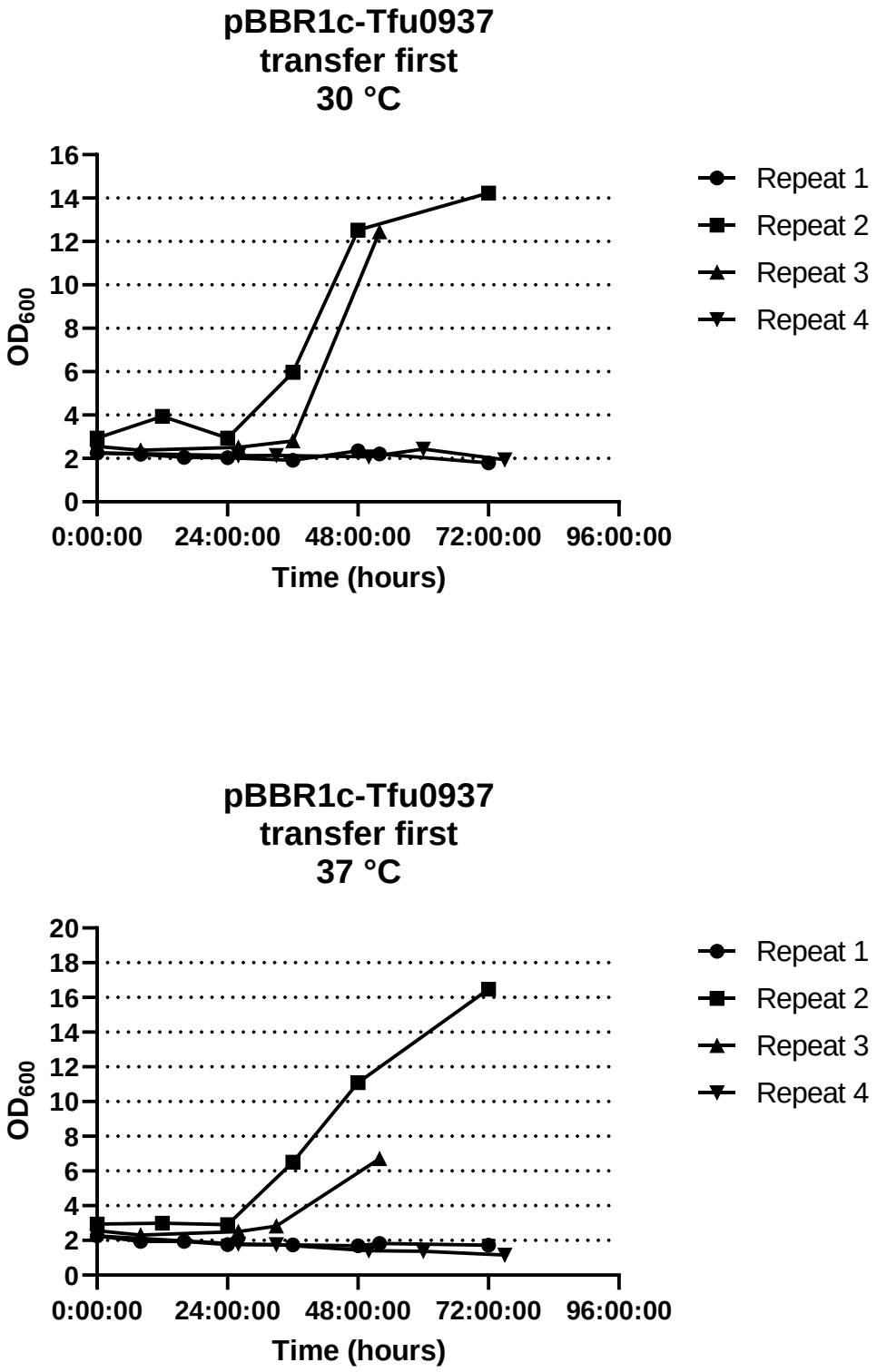

Figure 58 *Graphs of pBBR1c-Tfu0937 system comparing the +0 system at both temperature across a series of 5 biological repeats.*

As we have seen before, the ability of the cells to grow in a predictable fashion is influenced by the accessibility of the Tfu0937 to the Cellobiose. The way in which this occurs appears to be different for

the pBBR1c-Tfu0937 and the pBBR1c-BclAN-Tfu0937 systems, and this is reflected in the large inconsistencies in the way the cultures behave across repeats. For the pBBR1c-Tfu0937 system we can see that regardless of the conditions, there is variance in the cells growth. We see the cultures struggle to consistently enter the exponential phase at a steady time.

This is something that could be caused by the fact that extracellular Tfu0937 is being introduced to the media in an erratic fashion. First, through the natural mechanism we observe in the standard activity assay, but also through cell lysis. It is very feasible that as the cells enter the new media, some do not survive, and these cells burst releasing their proteinaceous content into the media. In the case of the pre induced cells this would be a problem that would lead to high amounts of extracellular activity.

The other notable difference that we see here is actually the fact that in 2 of the cultivations, the cells did not grow at all. This was an unusual observation as the activity of the cells was present, but the cells were never able to recover from the transfer. The reasoning for this result was not clear from the experimental data gathered so far.

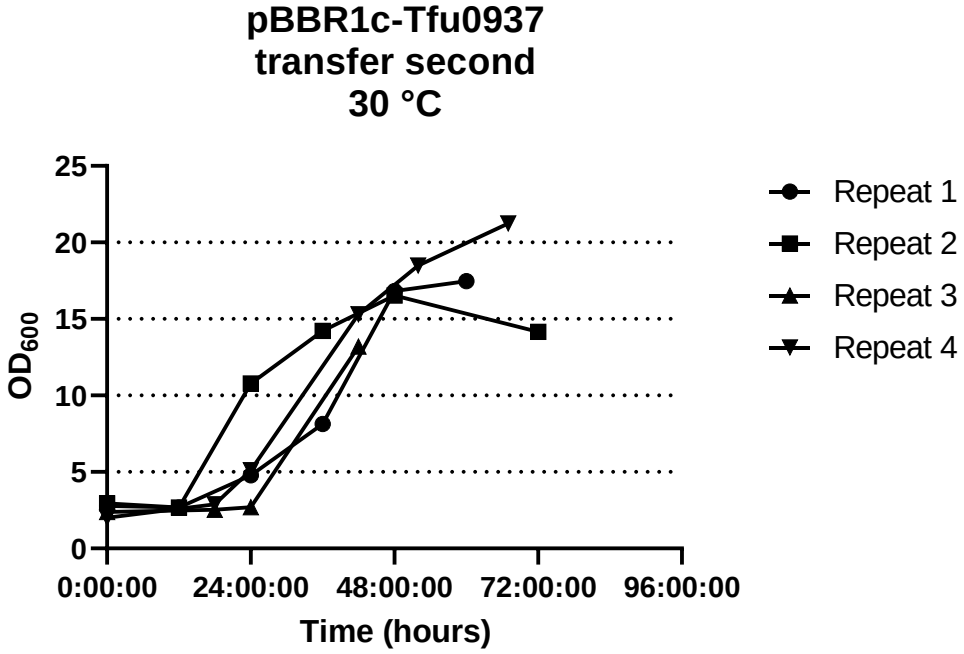

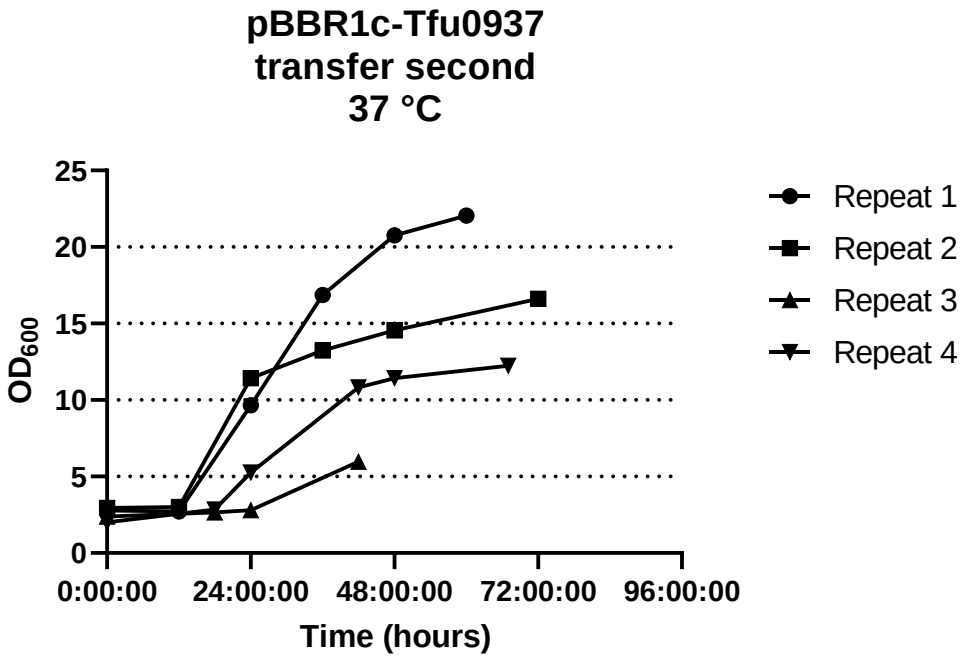

Figure 59 *Graphs of pBBR1c-Tfu0937 system comparing the +8 system at both temperature across a series of 5 biological repeats.*

The cultivations from the next set of experiments only further emphasised the findings seen earlier. Cultivation at 37 °C still produces more erratic growth patterns. But we also see that this cultivation method always leads to growth in the Tfu0937 system. The only way the Tfu0937 is interfacing with the cellobiose in the media must be through extracellular leaking. This methodology of cultivating the cells appears to yield a system in which the cells have an increased incidence of extracellular/periplasmic activity. This is not necessarily conducive with what we are trying to achieve with this experiment.

4.3.3. Comparison of activity profiles during cellobiose cultivation

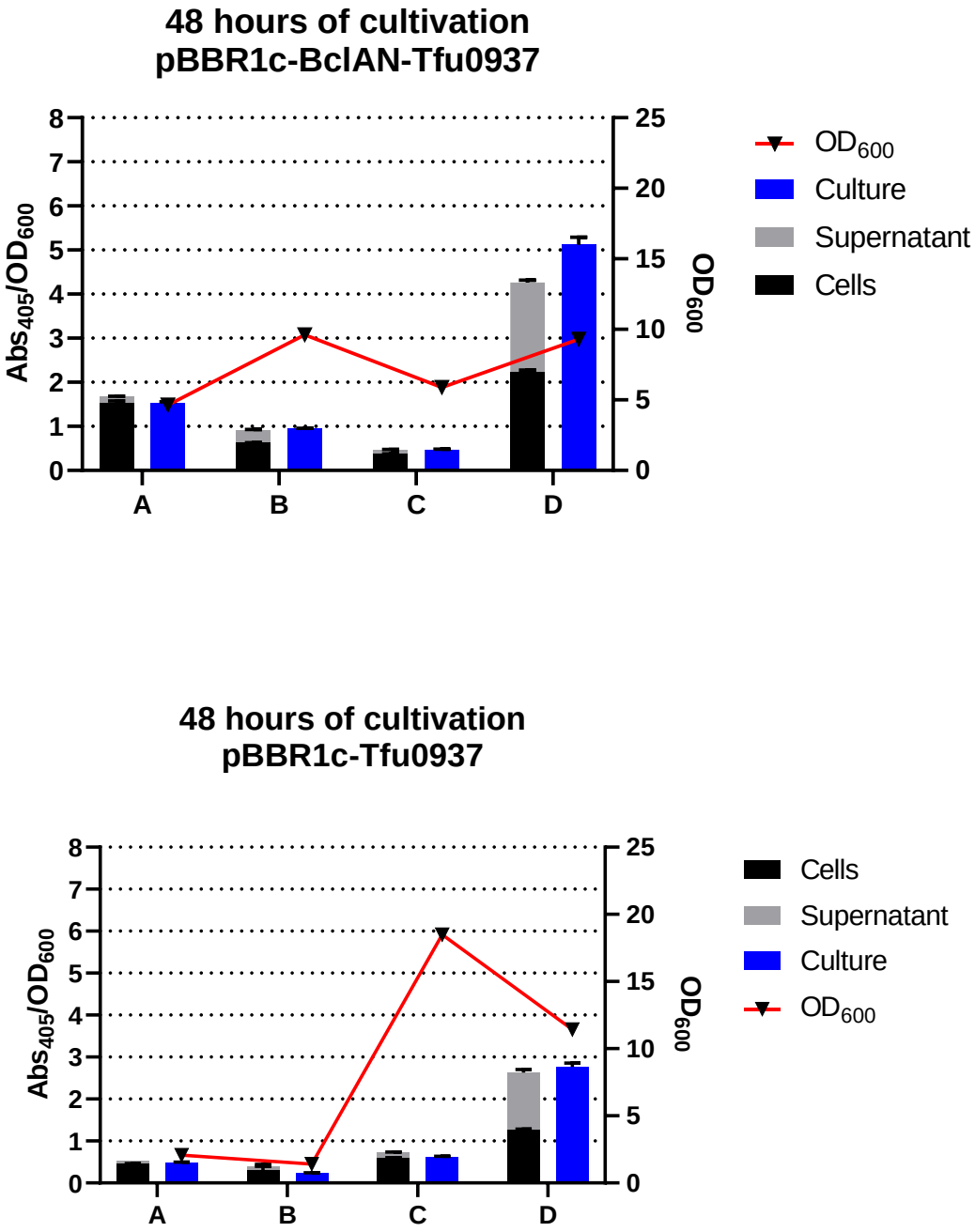

Figure 60 *Comparison of difference in activity profiles after 48 hours of cultivation. A: +0, cultivation temp. of 30 °C. B +0, cultivation temperature of 37 C. C+8, cultivation temperature of 37 C, D, +8, cultivation temperature of 37.*

The other key contributor to the growth of the cells is going to be the subcellular location and efficacy of Tfu0937. The activity for the cultures was taken 48 hours of cultivation. The first key observation was that the culture grown at 37 °C with a pre induction (D) has the highest incidence of extracellular activity. This could be for a number of reasons, such as cells lysing after the or loss of stability. The most likely culprit is however the leaking of Tfu0937 into the media after the transfer. It is very likely that many of the cells do not survive the initial transfer, and this liberates a large amount of Tfu0937 into the media. This is probably made worse by the fact that the cultivation temperature increases by 7 C, further causing excessive cell lysis. The extra activity is also seen clearly in both the cell associated activity and the supernatant. The supernatant activity can be accounted for by the aforementioned hypothesis, but it is still not clear as to why the cells display more activity when we look at the cultivation of cells at 37 C, with a pre induction.

Looking specifically at cultures (A) and (B), that there is a significant difference in the amount of activity. The culture grown at 30 °C shows more activity overall, and less activity in the supernatant fraction when compared to the cells that were grown at 37 C. The higher temperature seems to have a negative effect on the activity when the cultures are induced before transfer.

In its totality, the data gathered here gives an unclear picture that does not make it easy to make any postulations about the relationship between the availability and localisation of Tfu0937 with ability of the cells to grow in the cellobiose media. The data is challenging to evaluate here because of the unclear outcomes due to the combination of variables. Cultivation at 37 °C clearly has a detrimental effect on growth across all systems. We can see that whenever the culture is cultivated at 37 C, the OD is always lower when compared to its 30 °C counterpart when looking specifically at the Tfu0937 system. However, when we look at the BclAN system, it is interesting to note that the opposite is true. This suggests a biological difference in the two systems sensitivities to temperature and how this affects growth.

This data was used to inform the decision that refraining from utilisation of a delayed transfer to the new media was likely going to have an unpredictable and detrimental effect to the reliability of the experiment. Cultivation at 30 °C also appeared to introduce another variable in a system that was already

proving to be challenging to replicate experimentally. Moving forward, the decision was made to use an induction system that was as unimposing on the cells as possible, in this case, induction at transfer and cultivation at 30 °C. Both the 37 °C cultivation and the later induction were potentially having adverse effects on the growth of the cells or the amount of extracellular activity. Negating both of these effects by moving away from both systems seemed to be the safest protocol to allow us to generate reliable data.

To verify the notion that this was the best way to carry out the cultivation, the experiments were then run again in triplicate. Again, the growth was monitored, and the activity was checked at regular intervals to observe the amount of Tfu0937 being displayed. The cellobiose concentration used prior to this was 2% cellobiose. This was reduced to 0.5% which is more in line with the carbon concentration in the MSM cultivations that were being carried out. This allowed us to have more insight regarding the growth

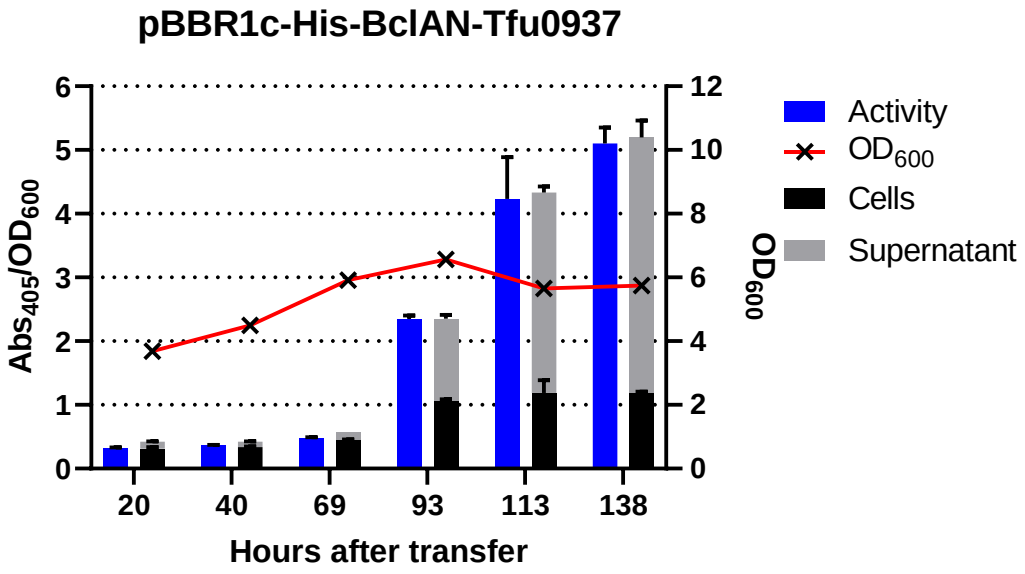
pBBR1c-His-BclAN-Tfu0937
Abs405/OD600
OD600
Hours after transfer
20
40
69
93
113
138
Activity
OD600
Cells
Supernatant

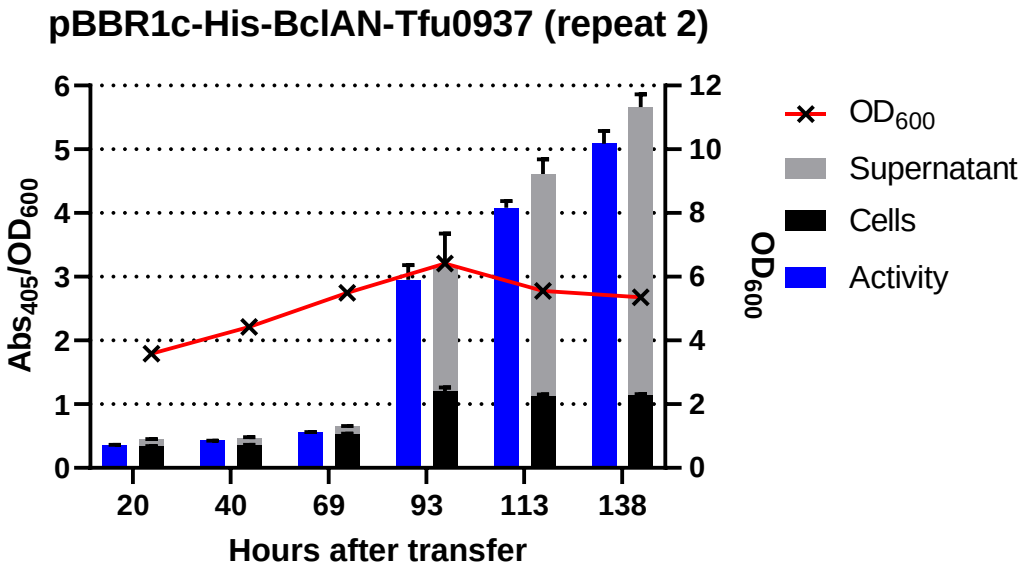
pBBR1c-His-BclAN-Tfu0937 (repeat 2)
Abs405/OD600
OD600
Hours after transfer
20
40
69
93
113
138
OD600
Supernatant
Cells
Activity

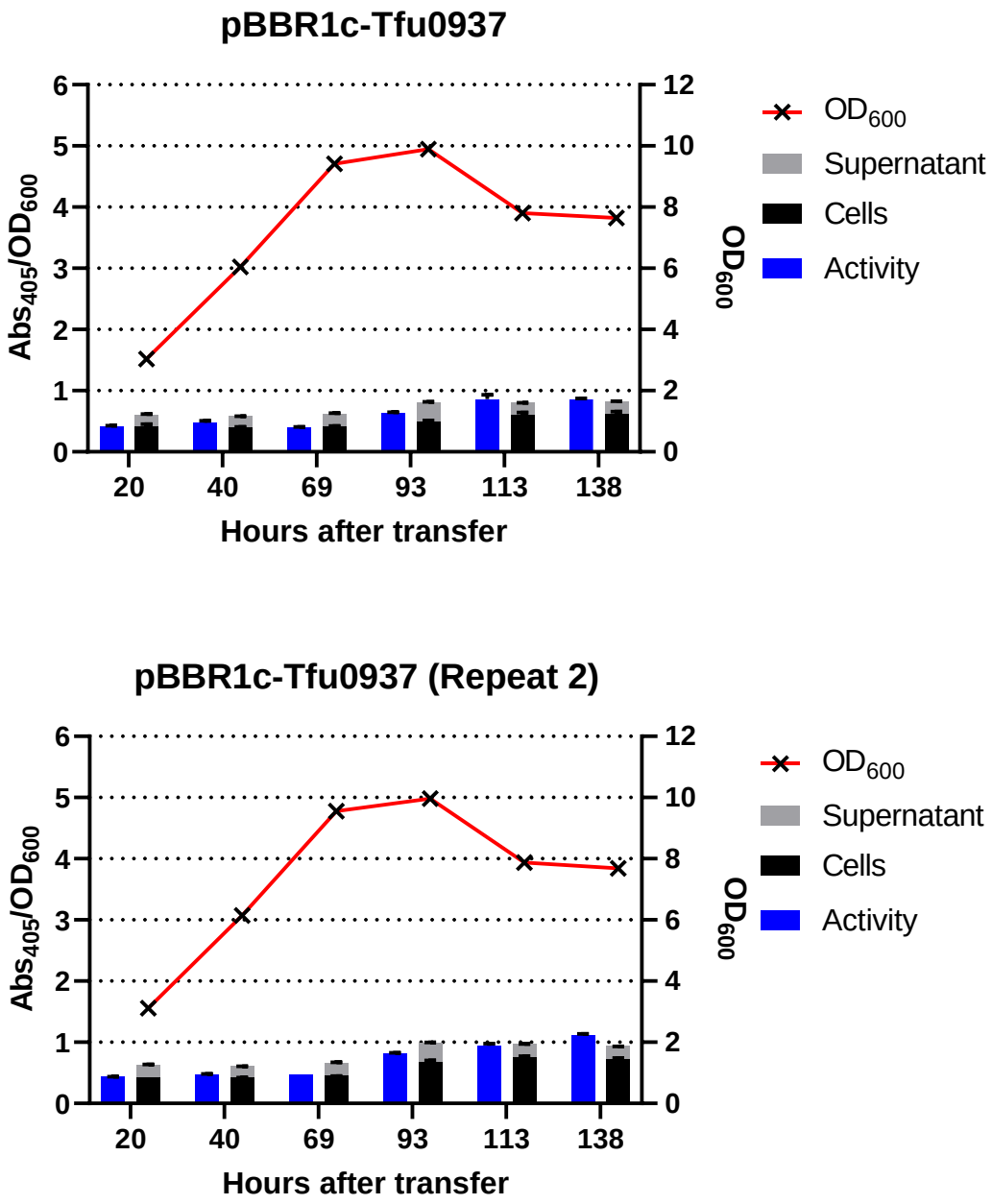

Figure 61 *Biological repeats following the cultivation of the cells over the course of 138 hours. Using the +0 30C degree system.*

The growth characteristics of these cultures appears to be quite stable, however, not only did the pBBR1c-Tfu0937 culture grow to a higher maximum OD, but it also had a much faster entry into the exponential phase.

The ability of the cells to grow does not seem to have a clear relationship between the measured activity and the growth rate. In both the pBBR1c-BclAN strain and the pBBR1c-Tfu0937 the cells are entering the exponential phase of growth while there appeared to be no fluctuations in activity. Not only were

there no changes in activity, but the activity seen in the cells appeared to be capable of supporting different rates of growth. This was an unusual phenomenon as it demonstrates issues regarding the effect of the background activity of the pBBR1c-Tfu0937. The growth of the system is hypothesised to be predicated on the cells ability to breakdown cellobiose. However, what is observed does not clearly illustrate that relationship. The primary issue here is that the amount of activity present in the media or cells cannot be quantified in such a way that allows us to know how much is necessary to support growth under these specific conditions. Due to this, small amounts of anomalous or "misplaced" Tfu0937 may be able to facilitate growth.

Despite this, it was clear that the interface of the Tfu0937 and the cellobiose was not the same for these two systems, as the total amount of activity in the culture would be the same yet the growth would be different. This could be due to the aforementioned glucose availability but may also be to do with the efficiency of expression of the different proteins and the metabolic strain this has on the cells. There is also the idea that the viability of the cells may be compromised by the display of the protein, potentially giving some explanation as to why the cells appear to be unable to grow well in the pBBR1c-His-BclAN strain vs the pBBR1c-Tfu0937 strain. However, many of these metrics were not able to be measured and can only be theorised as to how they may have led to some of these readings. Another interesting concept seen in the data is how the accumulation of extracellular Tfu0937 appeared to have little to no effect on the growth rate of the cells. This could have happened for a number of reasons, but the first is that the cells had reached a point of saturation and had already used the majority of available carbon in the system. However, this doesn't appear to be the case as the carbon availability is the same as that present in a 1% gluconate system. 1% gluconate as previously shown is capable of supporting the growth of cells of up to an OD of 14. However, it is important to note that the production of PHB does play a role in altering the optical density of the culture. As a result of this, what we may have observed here was not necessarily a lower cell density but in fact a lowered amount of accumulated PHB attributed to lower carbon availability throughout out the extended growth period. This is possible because it has been documented that the accumulation of PHB in the cells is induced by limitation of nitrogen in the media and more importantly the availability of a carbon source. From what is observed

in these activity graphs, we can theorise that overall lower PHB may be a result of a bottleneck in the production of glucose.

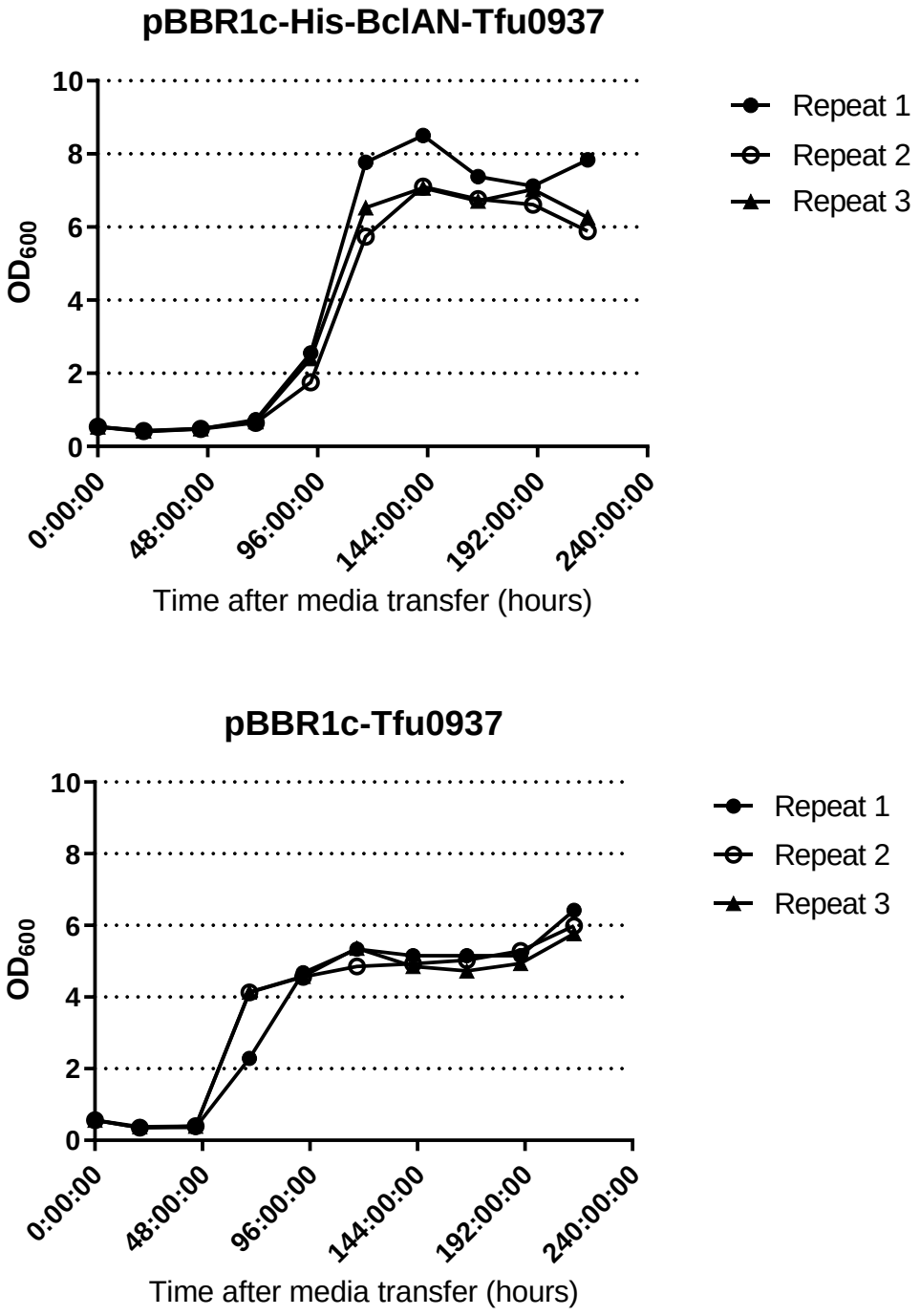

Figure 62 *Cultivation when using a significantly lower starting OD_{600} of 0.5 as opposed to ~2*

The previous data led us to believe that reducing the starting OD of the cultures may allow us to make more apt comparison between other cultivations and the new cellobiose system. We also wanted to

reduce the induction It was thought that this may help in lowering the background effect of the Tfu0937 strain (control) and allow it to have a less pronounced effect on growth.

By lowering the starting OD, we understood that it would likely have a negative effect on growth rate, and this is the first observation made from the growth curves. Here we can see there was an extended lag phase which extended well over 48 hours for the pBBR1c-BclaN strain. The maximum OD reached by the cells here is the same as prior data showed, but it was inverted for the different systems, i.e., the pBBR1c-BclAN system was able to support an OD of ~8, whereas the pBBR1c-Tfu0937 system only grew up to an OD of 6. When we look at this data in tandem with the activity data from the biological repeats, we can see that in this instance there appeared to be a higher activity in the pBBR1c-BclAN system in the earlier stages of the cultivation. However, this clearly was not enough to support an increased growth rate in this specific system. When looking at the growth curves, the pBBR1c-Tfu0937 system showed that there was a faster entry into the exponential phase when compared to the pBBR1c-BclAN system.

Many of the observations that we saw here were not in line with the previously postulated ideas. To recap, all of the alterations to the system were being made in order to give repeatable results that we could use to characterise the relationship between activity and growth of these strains in cellobiose media, however, as optimisations were being made to the system, the profiles of both the growth and the activity in the cells and media, were fluctuating.

The growth curves we had observed here were significantly more in line with what we were expecting to see, and as such continued to try and replicate and improve on this. We would be able to try and optimize the growth as this is the more important metric, regardless of whether the activity profile is logically representative of what we expect. When we do look at the activity profile of the cells after these changes, we can see that activity does not at all appear to be correlated to the growth. Now this is not to say that they aren't related as they completely must be, but the rate at which the glucose is being produced is important. On the one hand, the necessary production of glucose to sustain growth can be easily supported a very small amount of Tfu0937 activity. This would mean that the reason for the difference in growth is not actually down to the amount of displayed activity but a different variable

such as the metabolic stress imparted by protein expression. It is possible that the cells expressing the Tfu0937 on its own, are under less metabolic stress which leads to more consistent growth in the earlier stages of the cultivation.

The other possibility that could be affecting cell growth is the cells' ability to grow using the Tfu0937. One of the main issues that we see in these systems is that the pBBR1c-Tfu0937 is showing the ability to grow, when there is no clear reason why this should be the case. As previously stated, there is evidence to suggest that the Tfu0937 is part of the natural secretome of its native organism *T. fusca* YX, and as such there may be some secretory mechanism that is responsible for some amount of extracellular Tfu0937. This alone may be able to account for the viability of the cells in cellobiose media, but it is unlikely that this alone is not only responsible for the growth, but that this mechanism is also superior to the display system.

However, what this definitely does suggest, is that the mechanism in which the protein is able to interface with the cellobiose, is different for the two systems, otherwise it would likely have yielded different results.

We also need to take into consideration the fact that the two different systems may also not have the same level of activity. No quantitative analysis was carried out to look at the difference in activity between displayed Tfu0937 and free tfu0937. The presence of the fusion protein BclAN may well have had a negative effect on the ability of the protein to carry out its job. If this were the case, we would be observing a skewed growth profile.

Another unusual observation was the extracellular activity in the pBBR1c-Tfu0937 repeats. While the amount of activity associated with the cells appeared to stay consistent across the different experiments, the accumulated Tfu0937 appeared to fluctuate heavily. Despite this, it seems that there was no real effect on the growth of the strain, again suggesting that the correlation between observed activity and growth is not as clear as we had thought.

4.3.4. Using a dual media system to stabilise expression and growth

These experiments were carried out to observe the effect of using a mixed media on the standardisation of the cultivation. This was based on the notion that we could allow the cells to make a less harsh change of environment, allowing for a smoother transition into the utilisation of glucose. The cells would have more time to acclimatise to the loss of their preferred substrate and begin to use the readily available glucose that will have been accumulating in the media during the depletion of gluconate.

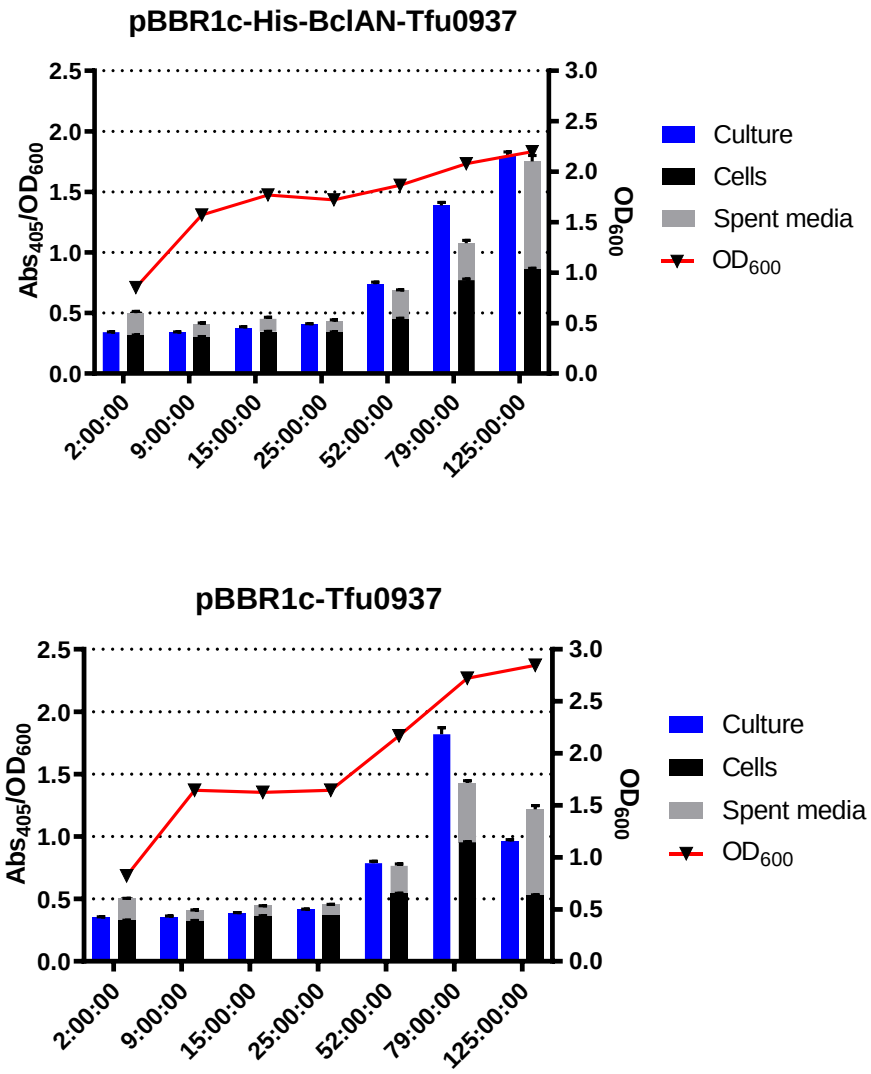

Figure 63 *Dual carbon source growth curves of pBBR1c-Tfu0937 and pBBR1c-His-BclaN-Tfu0937*

The system appeared to have worked to some extent as is made clear by the biphasic growth curve for both systems, however in these systems, the secondary exponential phase appeared to facilitate an abnormal increase in both extracellular and cell associated activity. This was the case for both strains illustrating the effect was not specific to the way the Tfu0937 was to interact with the media. The high incidence of extracellular activity however, only worked to make this data harder to decipher. It was clear that the higher extracellular activity began even earlier in the cellobiose metabolism. For this reason, it was concluded that this was probably not conducive to obtaining a growth profile that can give more insight into how the localisation of Tfu097 affects the glucose metabolism.

4.3.5. Utilisation of a constitutive promoter for display of Tfu0937 in

At this time, work developing the pJ5 promoter system had come into play and we now had an alternate method for the expression of pBBR1c-Tfu0937. Having seen the positive changes in the activity profiles seen in the standard expression, it was an interesting idea to see how these characteristics were going to translate to the cellobiose cultivation system.

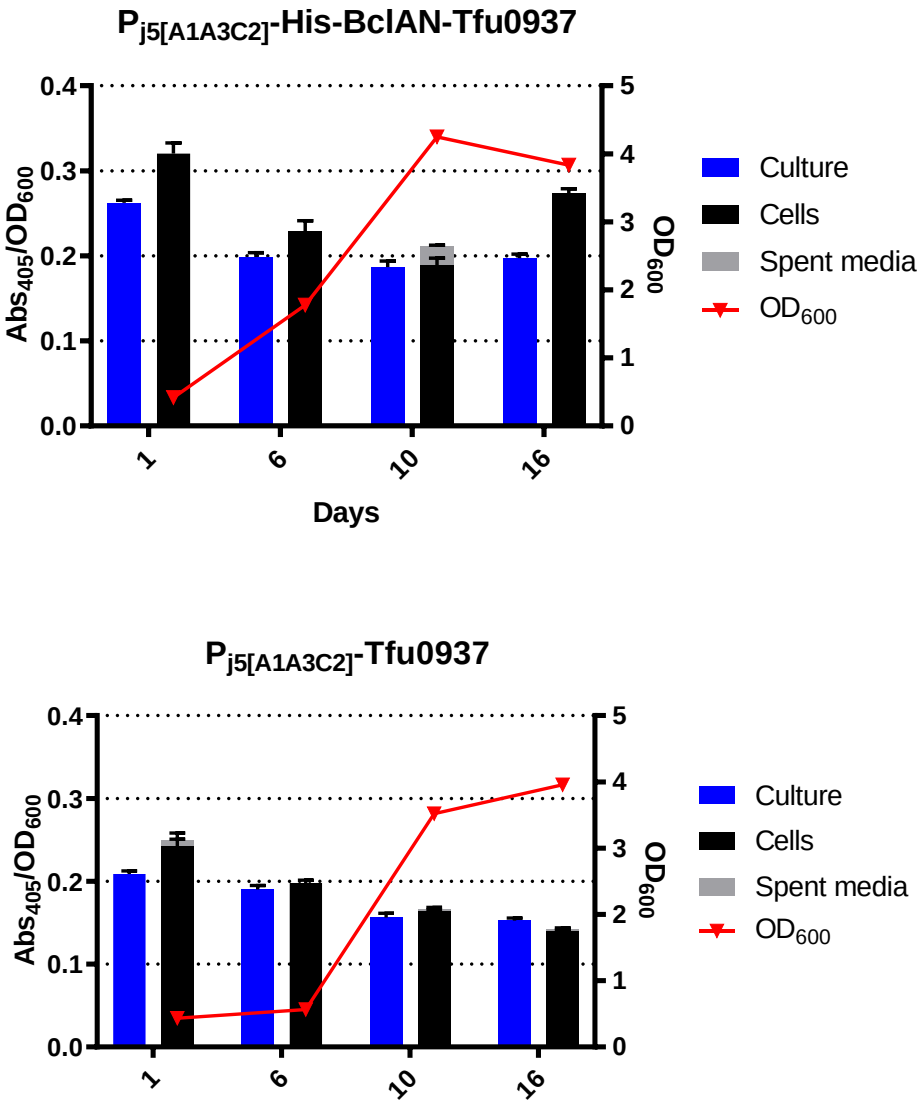

Figure 64 *Using the* $P_{J5[A1A3C2]}$ *constitutive system in a cellobiose cultivation. Both Tfu0937 and BclAN-Tfu0937 were measured.*

Using the pJ5 promoter system had immediate and obvious effects on the growth profile of the cells. The constitutive expression of the protein leads to significantly less protein being expressed. The reduction in Tfu0937 availability leads to low amounts of glucose being produced during the cultivation of the cells.

Prior to this, there had been postulations that the Tfu0937 being produced was so high that the glucose availability was not a bottleneck affecting the growth rate of the cells, but in this instance, the activity profile of both systems is reflective of the amount of growth being seen in each system.

This data set led us to believe that the using these induction conditions, we were able to see the effect of tfu0937 availability on the growth of the cells, while simultaneously providing more support for the hypothesis that Tfu0937 produced by cells in the inducible system were significantly less pertinent to producing comparative data due to excessive activity in the pBBR1c-Tfu0937 strain. This idea is further pushed forward by the fact that these systems lead to similar maximum ODs, and also take significantly longer to grow. The pBBR1c system showed saturation over the course of 4-5 days, whereas the pj5 system took nearly 2 weeks to grow. This was also thought to make sense in the context of relative activities shown. Here, the activity was on average 2-5 times less than the pBBR1c counter parts.

There was also a distinct lack of extracellular activity being shown in the system. This is extremely beneficial to clarifying exactly what kind of activity is allowing the growth to happen. It also potentially suggested that bound Tfu0937 has a lower activity than non-bound Tfu0937 which could contribute to the cell's slower growth.

4.3.6. Utilisation of the improved beta glucosidase assay on cells cultured in cellobiose

It was around this point that the discovery regarding the enzyme kinetics and further optimisations regarding the beta glucosidase assay had been made. While the data that had been gathered so far was now shown to be inaccurate, the trends in the data were still representative of what was going on. Not only that, many of the optimisations that had been made up until this point were still valid as is shown in what will be shown here.

The main changes that were implanted were the protocol adjustments which changed the working concentration of pNPG, and the protocol that gave us the fraction to be sampled. These changes allowed us to get higher resolution of the differences between the two systems specifically pertaining to the activity. This way, we are able to paint a better picture explaining the relationship between activity and growth in the cellobiose media.

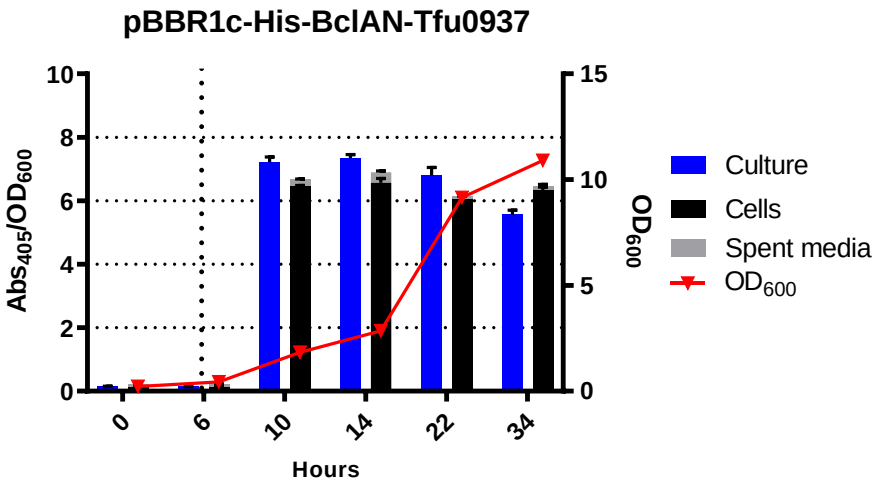
pBBR1c-His-BclAN-Tfu0937
Abs405/OD600
OD600
Hours
0
6
10
14
22
34
Culture
Cells
Spent media
OD600

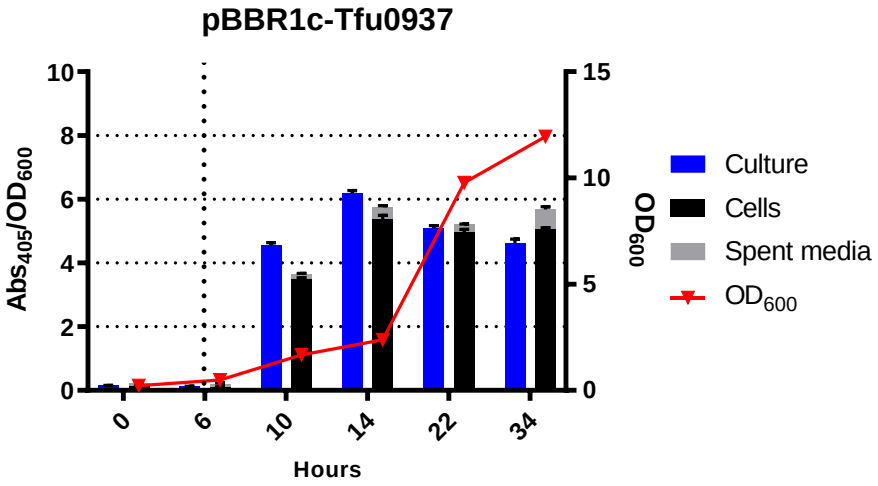
pBBR1c-Tfu0937
Abs405/OD600
OD600
Hours
0
6
10
14
22
34
Culture
Cells
Spent media
OD600

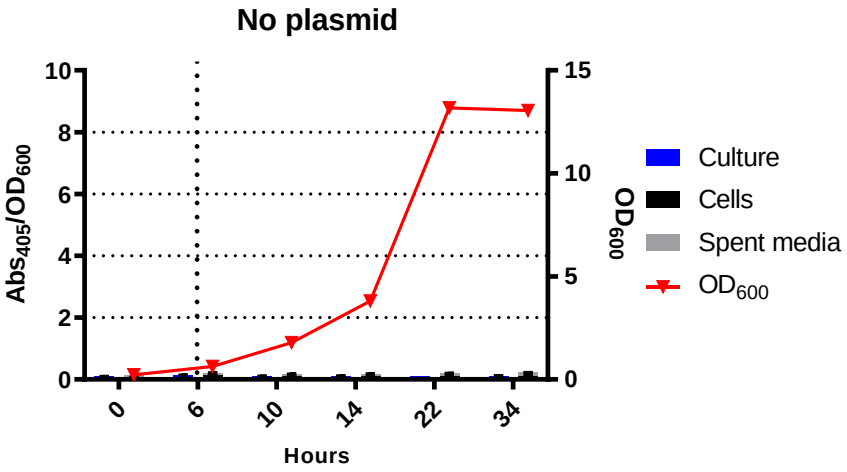
No plasmid
Abs405/OD600
OD600
Hours
0
6
10
14
22
34
Culture
Cells
Spent media
OD600

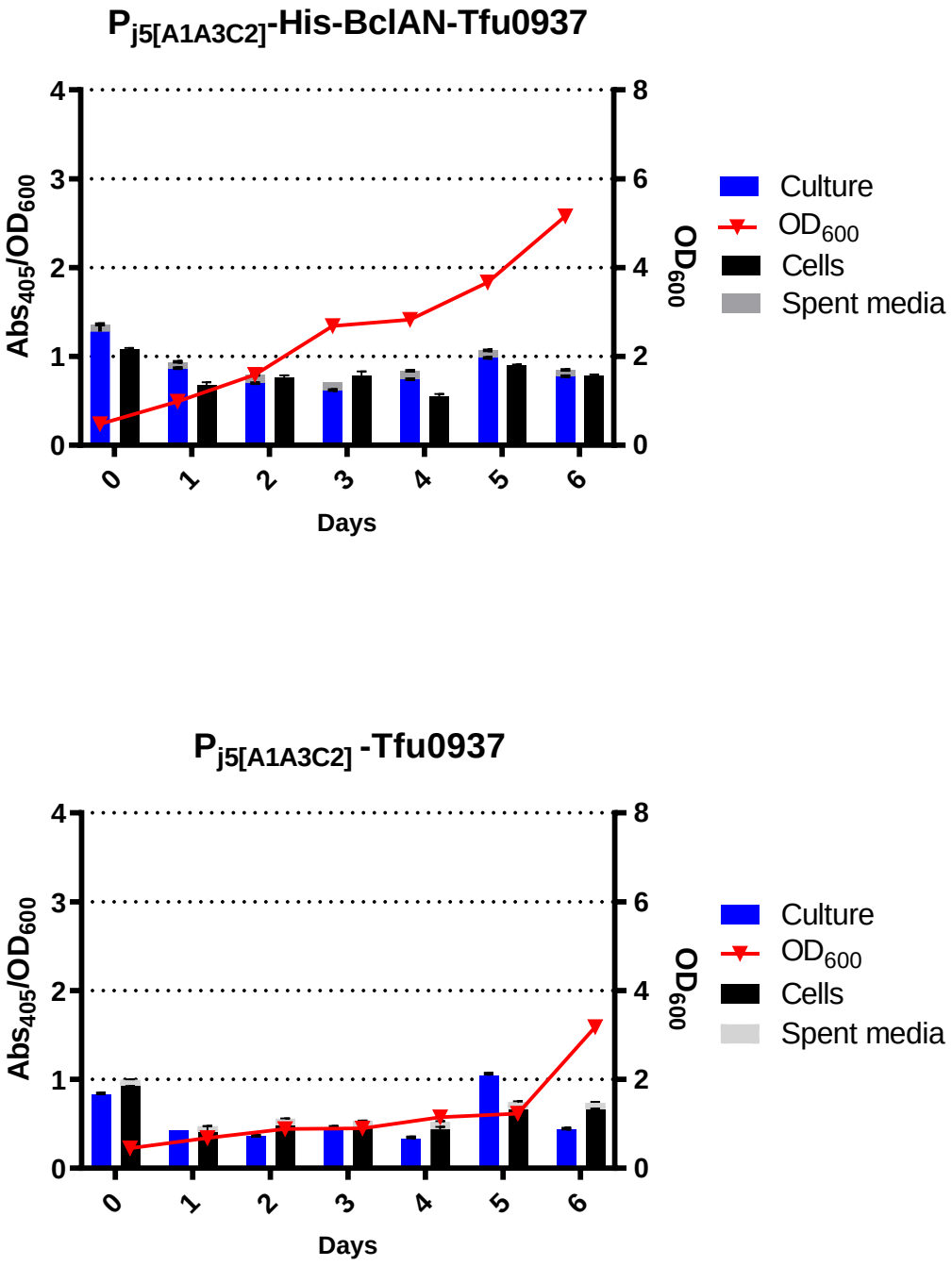

Figure 65 *Activity and growth profile of cells expressing BclaN-Tfu0937 and Tfu0937 using the constitutive system and the most accurate beta glucosidase assay method. Cells were induced with 0.1% arabinose.*

This is the last iteration of the pJ5 system that was used to illustrate the growth of the constitutive promoter system in cellobiose media. This is the most accurate representation of the activity. We can see that the cells follow a similar growth pattern as we have seen before seeing as the culture conditions have not really changed.

We can see that the activity does not really change over the course of the cultivation for both of these systems. The pJ5-Tfu0937 has significantly higher activity early on in the cultivation, but as the cultivation persists, the lack of carbon probably leads to the lowered amount of Tfu0937 present in the cells.

What is interesting here is that despite the measured activity between both systems being relatively close to one another, the growth is different. This is similar to previous observations which showed that even when activities were similar, growth patterns were different. Here, the same is true, but it appears to follow a different trend, with the pJ5-Tfu0937 showing less growth relative to its activity while the pJ5-BclAN system shows more growth with the same low amount of activity. What this highlight is that at low levels of expression, the activity appears to be more related to growth. This also shows us that the way in which the Tfu0937 is facilitating growth is different between the two systems.

Tfu0937 can interface with the cellobiose in a number of different ways given the parameters of the experiment, however the most obvious systems are via secretion into the media (lysis or auto secretion) or through display. There are other methodologies that could be at work such as the hypothesised periplasmic interface as discussed earlier, however, these two systems are the most likely to be responsible.

If secretion is playing a major role in the viability of the cells in cellobiose media, then we might have expected to see similar amounts of extracellular activity in the system, yet, despite increasing the sensitivity of the assay and the accuracy, we still are unable to see much extracellular activity. This weakens the hypothesis that secreted Tfu0937 that comes about via lysis and secretion can support growth. While not impossible, it is far more likely that the growth seen in the pJ5-Tfu0937 strain is likely only a result of the large amounts of periplasmic tfu0937 being able to interact with the cellobiose in the media.

However, if this were the case, we may also expect that some of this incidental periplasmic tfu0937 would also be present in the pJ5-BclAN system and would skew the growth patterns, but what we see instead is that there is consistently earlier growth in the BclAN system. This consistency is what

supports the idea that the BclAN system is actually supported by the display and earlier and more apparent activity of the Tfu0937. This is also clearly shown by the fact that the activity of all pJ5-BclAN systems is always consistently higher than that of the pJ5-Tfu0937 system. This clear correlation between activity and growth heavily suggest that the activity is in this system has a linear relationship.

The data gathered using a much lower induction concentration yielded similar trends in activity profiles as well as growth profiles. This further suggests that the high concentration of Tfu0937 present in the other systems was causing the amount of available Tfu0937 to not be the primary limiter of growth.

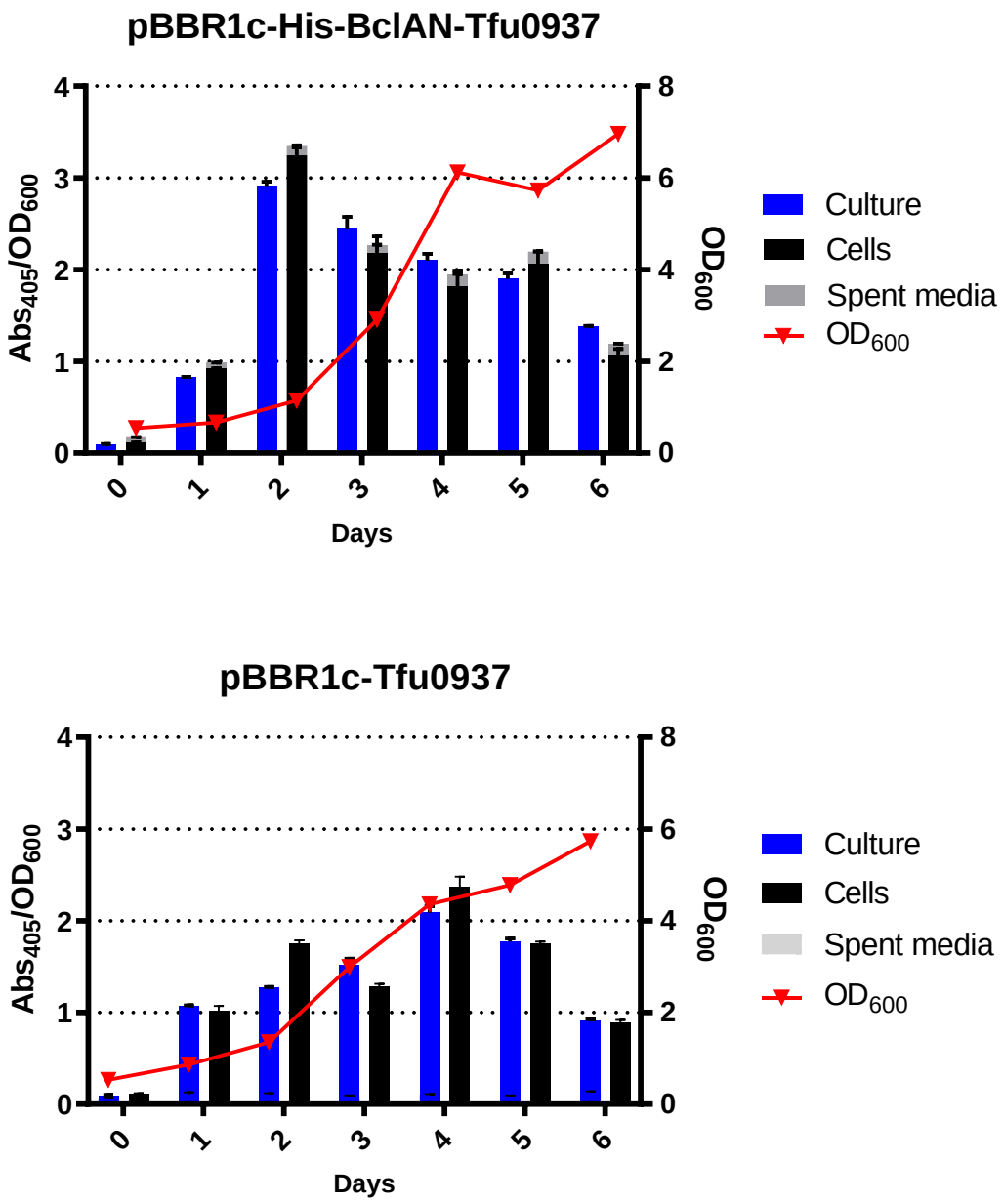

Figure 66 *Using optimized assay conditions and expression conditions to get a clear picture of the activity profile of cells expressing Tfu0937 both intracellularly and extracellularly and correlating these values to visualise the relationship between grown and activity.*

Because the pj5 system had produced such good results in clarifying the relationship between activity and growth, the results were attempted to be replicated by reducing the strength of the inducer. Here we see the gradual changes in the way the similarities between the two systems become more apparent. The trends in growth and activity show us that when the expression conditions are made to imitate those of the constitutive system, we create an environment in which we can see that the activity becomes the most important factor in determining the growth of the cells.

Despite this, the most important finding here is the illustration cell growth in cellobiose using displayed Tfu0937.

4.3.7. Conclusions

One of the key goals of this work was to develop an anchoring system to facilitate the modification of *C. necator* H16. The anchored protein was intended to demonstrate how display of a catabolic enzyme like Tfu0937 can be used to support growth in a medium containing a carbon source that does not support growth ordinarily. The simple answer to this is yes. The expression of membrane bound Tfu0937 appears to be able to facilitate growth in cellobiose media. However, these finding don't come without some important caveats.

One of the unusual things that we can take away from this section of work is the newfound understanding of how sensitive the system appears to be in regard to the way you choose to introduce the cells to the cellobiose system. Significant differences in growth and activity can be measured here illustrating the fact that while introducing the cells to the media after they have been induced can be valuable, the potential high metabolic stress on the cells caused by the media change while in the middle of high protein output can leave the cells rendered incapable of dealing with the environment. The lack of available carbon then has an unpredictable and adverse effect on growth as the available Tfu0937 interfacing with the media, be it membrane bound, periplasmic or cytosolic, is drastically changed by the amount of cell lysis that is generated by this effect. However, this change in available Tfu0937 could also potentially be attributed to PHB availability in the cells and the effect this has on carbon flux.

The other unusual finding here is that the relationship between growth and activity is not as obvious as one might think. This is something that can be clearly observed in many of the cultivations and could potentially be explained by the fact that we have not quantified what amount of carbon availability (in [glucose]) is responsible for what rate of growth. If we knew this, we could then work backwards and ascertain what amount of Tfu0937 activity is required in order to support growth within this system.

Finally, the most problematic issue with this data set is a downstream knock-on effect of not understanding the mechanism in which Tfu0937 is able to interface with the extracellular substrate cellobiose. Because of this, it becomes increasingly difficult to know how much of the activity we are seeing is attributed to this unknown mechanism in cells utilising the anchoring system. Despite this,

while it may appear a problem in the context of the BclAN system, in isolation, this is actually an incredibly novel finding. This work has demonstrated that *C. necator* H16 G+ cells expressing Tfu0937, can be cultivated in media where cellobiose is the only carbon source.

In summary, we were able to show that BclAN is able to support and increase the efficacy of Tfu0937 as a key enzyme in the acquisition of carbon from cellobiose.

5. Summary of thesis and future prospects

As was clearly stated at the beginning of this work, the main aim of this project was to develop a cell surface display system for *C. necator* H16, specifically to display Tfu0937, the beta glucosidase Tfu0937 of *T. fusca YX*. To do this, the N terminus sequence from the BclA protein was selected as the primary method of expediting this process.

On the surface, the binary nature of this question, means that we can comfortably say that the BclAN is capable of displaying Tfu0937.However, when we evaluate the success of the project in terms of the impact it has the main problem we were trying to solve. When we look at what this project contributes to allowing *C. necator* H16 to become a microbial biorefinery, the work done in this project has served to illuminate some of the shortcomings of trying to create a modular protein for protein display. The unpredictable and unreliable nature of the display of protein via BclAN means that it cannot work as means of reporting the expression of a protein. We can see this from the fact that it seems that Tfu0937 is not efficiently translocated to the outer membrane, as is made evident by the outer membrane fractionation experiments.

Regarding the display of Tfu0937 facilitating growth in the cellobiose media, the display of the Tfu0937 increases the amount of extracellular activity and in turn the rate of growth in the media when compared to the expression of cytosolic Tfu0937. However, this leads us onto one of the most prominent issues that underlies the reason a large proportion of this work is not as robust as it could be.

The extracellular activity of cells expressing only intracellular Tfu0937 with no motif is something that is fascinating as it defies all the paradigms of the way this enzymatic system should function. An important question we were unable to answer but would have been crucial to elucidating the true efficacy of display via BclAN, was why this system was not only able to have extracellular activity, but also facilitate growth in cellobiose media.

5.1. Future work

Utilisation of immunological assays are invaluable when looking at cell surface display. It is actually incredibly commonplace to see immunological assays such as western blots and ELISAs being used to check for the location of displayed proteins. I believe this is something that could be used to verify the subcellular location of Tfu0937 in both the pBBR1c-BclAN strain and the strain without the BclAN tag.

There is also something that could be said for potentially looking at using a different protein to verify the successful display of the protein. Even though experiments had been carried out prior to my arrival on this project that looked at the display of GFP and TGP via BclAN, I believe that more work could have been done to utilise the simplicity of those reporter proteins. The fact that we were using an enzyme made the complexity of these experiments significantly higher, because every time an adjustment is made to a protocol or an optimisation is made to a specific parameter, not only are you potentially changing the amount of protein but also potentially the activity. This increases the points of failure and increases the likelihood that variability in results begins to become an issue, which obviously in turn makes troubleshooting significantly more challenging. Working with a simpler reporter system may have been a way to circumvent these issues.

There is some argument to be made that a more rational approach could have been taken when picking a suitable anchoring motif. While BclAN is a novel anchor, since its publication in 2013, only 2 other publications have been shown to use this system as a means of cell surface display. This raises some concerns that other people may be finding it difficult to get BclAN to have efficient, stable display for their proteins. I believe that this system should have had a more significant impact on the space looking at cell surface display because one of its greatest merits is the fact that it was shown to display a large protein (135kDa) and that protein retained its activity. In addition to this, the tag is especially small. Meaning the likelihood that it interferes with the folding or activity of its passenger protein is significantly reduced. These two factors alone make it an excellent candidate for further study yet we there is a clear lack of interest in the system. Rational design of a display system by exploiting the

homologues of known functioning anchoring motifs could have had a positive impact on the workflow and viability of designing a cell surface display system and could have given insight into an important part of the optimization process that matches the passenger protein to the anchor.

I also believe that some of the analysis that was done could have been more concrete in verifying the data that had been collected. The most pertinent example is confirmation of the OmpA and OmpC proteins present in the sarkosyl membrane extraction that "proved" it was a membrane fraction. Mass spectroscopy analysis of these bands could have given us a much more robust set of evidence that that was the case. Instead, we had to only assume based on rational conjecture. Systems like this could also have been used to increase the fidelity of the data gathered from other experiments such as the lysozyme membrane extraction.

I also think that there is value in the information we learnt about the pBBR1c-Tfu0937 system. The fact that this system was able to function when all logic says it shouldn't be a testament to the novelty of that work. There is potential in understanding new ways the extracellular space and intracellular proteins are able to interface, or if this phenomenon was specific to the relationship between Tfu0937 and *C. necator* H16. Regardless, there appears to be some unknown mechanism at work that would be an exciting prospect to uncover.

6. References

Akinosho, H. *et al.* (2014) 'The emergence of Clostridium thermocellum as a high utility candidate for consolidated bioprocessing applications', *Frontiers in Chemistry*, 2(AUG). doi: 10.3389/fchem.2014.00066.

Alagesan, S., Minton, N. P. and Malys, N. (2018) '13C-assisted metabolic flux analysis to investigate heterotrophic and mixotrophic metabolism in Cupriavidus necator H16', *Metabolomics*, 14(1), p. 9. doi: 10.1007/s11306-017-1302-z.

Antoni, D., Zverlov, V. v. and Schwarz, W. H. (2007) 'Biofuels from microbes', *Applied Microbiology and Biotechnology*, 77(1), pp. 23–35. doi: 10.1007/s00253-007-1163-x.

Bae, W. *et al.* (2000) 'Enhanced bioaccumulation of heavy metals by bacterial cells displaying synthetic phytochelatins', *Biotechnology and Bioengineering*, 70(5), pp. 518–524. doi: 10.1002/1097-0290(20001205)70:5<518::AID-BIT6>3.0.CO;2-5.

Beckwith, J. (2013) 'The Sec-dependent pathway', *Research in Microbiology*, 164(6), pp. 497–504. doi: 10.1016/j.resmic.2013.03.007.

Besingi, R. N. and Clark, P. L. (2015) 'Extracellular protease digestion to evaluate membrane protein cell surface localization', *Nature Protocols*, 10(12), pp. 2074–2080. doi: 10.1038/nprot.2015.131.

Binder, U. *et al.* (2010) 'High-throughput Sorting of an Anticalin Library via EspP-mediated Functional Display on the Escherichia coli Cell Surface', *Journal of Molecular Biology*, 400(4), pp. 783–802. doi: 10.1016/j.jmb.2010.05.049.

van Bloois, E. *et al.* (2011) 'Decorating microbes: surface display of proteins on Escherichia coli', *Trends in Biotechnology*, 29(2), pp. 79–86. doi: 10.1016/j.tibtech.2010.11.003.

Chafee, M., Maignien, L. and Simmons, S. L. (2015) 'The effects of variable sample biomass on comparative metagenomics', *Environmental Microbiology*, 17(7), pp. 2239–2253. doi: 10.1111/1462-2920.12668.

Chang, D. *et al.* (2018) 'Proteomic and metabolomic analysis of the cellular biomarkers related to inhibitors tolerance in Zymomonas mobilis ZM4', *Biotechnology for Biofuels*, 11(1), p. 283. doi: 10.1186/s13068-018-1287-5.

Chen, X. (2017) 'Yeast cell surface display: An efficient strategy for improvement of bioethanol fermentation performance', *Bioengineered*, 8(2), pp. 115–119. doi: 10.1080/21655979.2016.1212135.

Chungjatupornchai, W. and Fa-aroonsawat, S. (2009) 'Translocation of green fluorescent protein to cyanobacterial periplasm using ice nucleation protein', *The Journal of Microbiology*, 47(2), pp. 187–192. doi: 10.1007/s12275-008-0188-x.

Davis, D. H. *et al.* (1969) 'Proposal to reject the genus Hydrogenomonas: Taxonomic implications', *International Journal of Systematic Bacteriology*, 19(4), pp. 375–390. doi: 10.1099/00207713-19-4-375.

Driks, A. (2009) 'The Bacillus anthracis spore', *Molecular Aspects of Medicine*, 30(6), pp. 368–373. doi: 10.1016/j.mam.2009.08.001.

Ebeling, W. *et al.* (1974) 'Proteinase K from Tritirachium album Limber', *European Journal of Biochemistry*, 47(1), pp. 91–97. doi: 10.1111/j.1432-1033.1974.tb03671.x.

Etz, H. *et al.* (2001) 'Bacterial Phage Receptors, Versatile Tools for Display of Polypeptides on the Cell Surface', *Journal of Bacteriology*, 183(23), pp. 6924–6935. doi: 10.1128/JB.183.23.6924-6935.2001.

Fan, L.-H. *et al.* (2011) 'Cell surface display of carbonic anhydrase on Escherichia coli using ice nucleation protein for CO2 sequestration', *Biotechnology and Bioengineering*, 108(12), pp. 2853–2864. doi: 10.1002/bit.23251.

Fedeson, D. T. and Ducat, D. C. (2017) 'Cyanobacterial Surface Display System Mediates Engineered Interspecies and Abiotic Binding', *ACS Synthetic Biology*, 6(2), pp. 367–374. doi: 10.1021/acssynbio.6b00254.

Fishilevich, S. *et al.* (2009) 'Surface Display of Redox Enzymes in Microbial Fuel Cells', *Journal of the American Chemical Society*, 131(34), pp. 12052–12053. doi: 10.1021/ja9042017.

Gaseous Carbon Waste Streams Utilization (2019) *Gaseous Carbon Waste Streams Utilization*. Washington, D.C.: National Academies Press. doi: 10.17226/25232.

Georgiou, G. *et al.* (1996) 'Display of β-lactamase on the *Escherichia coli* surface: outer membrane phenotypes conferred by Lpp′–OmpA′–β-lactamase fusions', *'Protein Engineering, Design and Selection'*, 9(2), pp. 239–247. doi: 10.1093/protein/9.2.239.

Haas, R., Jin, B. and Zepf, F. T. (2008) 'Production of Poly(3-hydroxybutyrate) from Waste Potato Starch', *Bioscience, Biotechnology, and Biochemistry*, 72(1), pp. 253–256. doi: 10.1271/bbb.70503.

Harshvardhan, K. and Jha, B. (2013) 'Biodegradation of low-density polyethylene by marine bacteria from pelagic waters, Arabian Sea, India', *Marine Pollution Bulletin*, 77(1–2), pp. 100–106. doi: 10.1016/j.marpolbul.2013.10.025.

Hobb, R. I. *et al.* (2009) 'Evaluation of procedures for outer membrane isolation from Campylobacter jejuni', *Microbiology*, 155(3), pp. 979–988. doi: 10.1099/mic.0.024539-0.

Jambeck, J. R. *et al.* (2015) 'Plastic waste inputs from land into the ocean', *Science*, 347(6223), pp. 768–771. doi: 10.1126/science.1260352.

Jeong, H.-S., Yoo, S.-K. and Kim, E.-J. (2001) 'Cell surface display of salmobin, a thrombin-like enzyme from Agkistrodon halys venom on Escherichia coli using ice nucleation protein', *Enzyme and Microbial Technology*, 28(2–3), pp. 155–160. doi: 10.1016/S0141-0229(00)00315-X.

Jönsson, L. J., Alriksson, B. and Nilvebrant, N.-O. (2013) 'Bioconversion of lignocellulose: inhibitors and detoxification', *Biotechnology for Biofuels*, 6(1), p. 16. doi: 10.1186/1754-6834-6-16.

Jung, H.-C. *et al.* (1998) 'Expression of Carboxymethylcellulase on the Surface of Escherichia Coli Using Pseudomonas Syringae Ice Nucleation Protein', *Enzyme and Microbial Technology*, 22(5), pp. 348–354. doi: 10.1016/S0141-0229(97)00224-X.

Jung, H.-C., Lebeault, J.-M. and Pan, J.-G. (1998) 'Surface display of Zymomonas mobilis levansucrase by using the ice-nucleation protein of Pseudomonas syringae', *Nature Biotechnology*, 16(6), pp. 576–580. doi: 10.1038/nbt0698-576.

Kannuchamy, S., Mukund, N. and Saleena, L. M. (2016) 'Genetic engineering of Clostridium thermocellum DSM1313 for enhanced ethanol production', *BMC Biotechnology*, 16(S1), p. 34. doi: 10.1186/s12896-016-0260-2.

Kotrba, P. *et al.* (1999) 'Enhanced Metallosorption of *Escherichia Coli* Cells Due to Surface Display of β- and α-Domains of Mammalian Metallothionein as a Fusion to Lamb Protein', *Journal of Receptors and Signal Transduction*, 19(1–4), pp. 703–715. doi: 10.3109/10799899909036681.

Kuroda, A. and Sekiguchi, J. (1991) 'Molecular cloning and sequencing of a major Bacillus subtilis autolysin gene', *Journal of Bacteriology*, 173(22), pp. 7304–7312. doi: 10.1128/jb.173.22.7304-7312.1991.

Lång, H. *et al.* (2000) 'Characterization of adhesive epitopes with the OmpS display system', *European Journal of Biochemistry*, 267(1), pp. 163–170. doi: 10.1046/j.1432-1327.2000.00981.x.

Lattemann, C. T. *et al.* (2000) 'Autodisplay: Functional Display of Active β-Lactamase on the Surface of *Escherichia coli* by the AIDA-I Autotransporter', *Journal of Bacteriology*, 182(13), pp. 3726–3733. doi: 10.1128/JB.182.13.3726-3733.2000.

Lee, J.-S. *et al.* (2000) 'Surface-displayed viral antigens on Salmonella carrier vaccine', *Nature Biotechnology*, 18(6), pp. 645–648. doi: 10.1038/76494.

Lee, K. *et al.* (2010) 'The genome-scale metabolic network analysis of Zymomonas mobilis ZM4 explains physiological features and suggests ethanol and succinic acid production strategies', *Microbial Cell Factories*, 9(1), p. 94. doi: 10.1186/1475-2859-9-94.

Lee, S. H. *et al.* (2004) 'Display of Bacterial Lipase on the *Escherichia coli* Cell Surface by Using FadL as an Anchoring Motif and Use of the Enzyme in Enantioselective Biocatalysis', *Applied and Environmental Microbiology*, 70(9), pp. 5074–5080. doi: 10.1128/AEM.70.9.5074-5080.2004.

Lee, S. H., Lee, S. Y. and Park, B. C. (2005) 'Cell Surface Display of Lipase in *Pseudomonas putida* KT2442 Using OprF as an Anchoring Motif and Its Biocatalytic Applications', *Applied and Environmental Microbiology*, 71(12), pp. 8581–8586. doi: 10.1128/AEM.71.12.8581-8586.2005.

Lee, S. Y., Choi, J. H. and Xu, Z. (2003) 'Microbial cell-surface display', *Trends in Biotechnology*, 21(1), pp. 45–52. doi: 10.1016/S0167-7799(02)00006-9.

Lequette, Y. *et al.* (2011) 'Domains of BclA, the major surface glycoprotein of the *B. cereus* exosporium: glycosylation patterns and role in spore surface properties', *Biofouling*, 27(7), pp. 751–761. doi: 10.1080/08927014.2011.599842.

Li, L., Gyun Kang, D. and Joon Cha, H. (2004) 'Functional display of foreign protein on surface ofEscherichia coli using N-terminal domain of ice nucleation protein', *Biotechnology and Bioengineering*, 85(2), pp. 214–221. doi: 10.1002/bit.10892.

Li, Q. *et al.* (2009) 'Improved phosphate biosorption by bacterial surface display of phosphate-binding protein utilizing ice nucleation protein', *FEMS Microbiology Letters*, 299(1), pp. 44–52. doi: 10.1111/j.1574-6968.2009.01724.x.

Li, Q. *et al.* (2012) 'Molecular Characterization of an Ice Nucleation Protein Variant (InaQ) from *Pseudomonas syringae* and the Analysis of Its Transmembrane Transport Activity in *Escherichia coli*', *International Journal of Biological Sciences*, 8(8), pp. 1097–1108. doi: 10.7150/ijbs.4524.

Li, Z. *et al.* (2020) 'Engineering the Calvin–Benson–Bassham cycle and hydrogen utilization pathway of Ralstonia eutropha for improved autotrophic growth and polyhydroxybutyrate production', *Microbial Cell Factories*, 19(1), p. 228. doi: 10.1186/s12934-020-01494-y.

Liu, H. *et al.* (2004) 'Formation and Composition of the Bacillus anthracis Endospore', *Journal of Bacteriology*, 186(1). doi: 10.1128/JB.186.1.164-178.2004.

Mohd Azhar, S. H. *et al.* (2017) 'Yeasts in sustainable bioethanol production: A review', *Biochemistry and Biophysics Reports*, 10, pp. 52–61. doi: 10.1016/j.bbrep.2017.03.003.

Mori, H. and Ito, K. (2001) 'The Sec protein-translocation pathway', *Trends in Microbiology*, 9(10), pp. 494–500. doi: 10.1016/S0966-842X(01)02174-6.

Mravec, F. *et al.* (2016) 'Accumulation of PHA granules in *Cupriavidus necator* as seen by confocal fluorescence microscopy', *FEMS Microbiology Letters*. Edited by A. Steinbüchel, 363(10), p. fnw094. doi: 10.1093/femsle/fnw094.

Müller, J. *et al.* (2013) 'Engineering of Ralstonia eutropha H16 for Autotrophic and Heterotrophic Production of Methyl Ketones', *Applied and Environmental Microbiology*, 79(14), pp. 4433–4439. doi: 10.1128/AEM.00973-13.

Narita, J. *et al.* (2006) 'Display of active enzymes on the cell surface of Escherichia coli using PgsA anchor protein and their application to bioconversion.', *Applied microbiology and biotechnology*, 70(5), pp. 564–72. doi: 10.1007/s00253-005-0111-x.

Nicchi, S. *et al.* (2021) 'Decorating the surface of Escherichia coli with bacterial lipoproteins: a comparative analysis of different display systems', *Microbial Cell Factories*, 20(1), p. 33. doi: 10.1186/s12934-021-01528-z.

Orita, I. *et al.* (2012) 'Identification of mutation points in Cupriavidus necator NCIMB 11599 and genetic reconstitution of glucose-utilization ability in wild strain H16 for polyhydroxyalkanoate production', *Journal of Bioscience and Bioengineering*, 113(1), pp. 63–69. doi: 10.1016/j.jbiosc.2011.09.014.

Orr, I. G., Hadar, Y. and Sivan, A. (2004) 'Colonization, biofilm formation and biodegradation of polyethylene by a strain of Rhodococcus ruber', *Applied Microbiology and Biotechnology*, 65(1). doi: 10.1007/s00253-004-1584-8.

Pal, A. and Paul, A. K. (2008) 'Microbial extracellular polymeric substances: central elements in heavy metal bioremediation', *Indian Journal of Microbiology*, 48(1), pp. 49–64. doi: 10.1007/s12088-008-0006-5.

Pallesen, L. *et al.* (1995) 'Chimeric FimH adhesin of type 1 fimbriae: a bacterial surface display system for heterologous sequences', *Microbiology*, 141(11), pp. 2839–2848. doi: 10.1099/13500872-141-11-2839.

Park, T. J. *et al.* (2013) 'Surface display of recombinant proteins on Escherichia coli by BclA exosporium of Bacillus anthracis', *Microbial Cell Factories*, 12(1), p. 81. doi: 10.1186/1475-2859-12-81.

Priefert, H. and Steinbüchel, A. (1992) 'Identification and molecular characterization of the acetyl coenzyme A synthetase gene (acoE) of Alcaligenes eutrophus', *Journal of Bacteriology*, 174(20), pp. 6590–6599. doi: 10.1128/jb.174.20.6590-6599.1992.

Repaske, R. (1962) 'NUTRITIONAL REQUIREMENTS FOR *HYDROGENOMONAS EUTROPHA*', *Journal of Bacteriology*, 83(2), pp. 418–422. doi: 10.1128/jb.83.2.418-422.1962.

Rice, J. J. (2006) 'Bacterial display using circularly permuted outer membrane protein OmpX yields high affinity peptide ligands', *Protein Science*, 15(4), pp. 825–836. doi: 10.1110/ps.051897806.

Riedel, S. L. *et al.* (2014) 'Lipid and fatty acid metabolism in Ralstonia eutropha: relevance for the biotechnological production of value-added products', *Applied Microbiology and Biotechnology*, 98(4), pp. 1469–1483. doi: 10.1007/s00253-013-5430-8.

Rutherford, N. and Mourez, M. (2006) 'Surface display of proteins by gram-negative bacterial autotransporters.', *Microbial cell factories*, 5, p. 22. doi: 10.1186/1475-2859-5-22.

Sarkar, P. *et al.* (2020) 'Adaptive laboratory evolution induced novel mutations in *Zymomonas mobilis* ATCC ZW658: a potential platform for co-utilization of glucose and xylose', *Journal of Industrial Microbiology and Biotechnology*, 47(3), pp. 329–341. doi: 10.1007/s10295-020-02270-y.

Shi and Wen Su W (2001) 'Display of green fluorescent protein on Escherichia coli cell surface.', *Enzyme and microbial technology*, 28(1), pp. 25–34. doi: 10.1016/s0141-0229(00)00281-7.

Shimazu, M., Mulchandani, A. and Chen, W. (2001) 'Cell Surface Display of Organophosphorus Hydrolase Using Ice Nucleation Protein', *Biotechnology Progress*, 17(1), pp. 76–80. doi: 10.1021/bp0001563.

Shimazu, Mark, Mulchandani, A. and Chen, W. (2001) 'Simultaneous degradation of organophosphorus pesticides and p-nitrophenol by a genetically engineered Moraxella sp. with surface-

expressed organophosphorus hydrolase', *Biotechnology and Bioengineering*, 76(4), pp. 318–324. doi: 10.1002/bit.10095.

Sichwart, S. *et al.* (2011) 'Extension of the Substrate Utilization Range of *Ralstonia eutropha* Strain H16 by Metabolic Engineering To Include Mannose and Glucose', *Applied and Environmental Microbiology*, 77(4), pp. 1325–1334. doi: 10.1128/AEM.01977-10.

Siegele, D. A. and Hu, J. C. (1997) 'Gene expression from plasmids containing the *araBAD* promoter at subsaturating inducer concentrations represents mixed populations', *Proceedings of the National Academy of Sciences*, 94(15), pp. 8168–8172. doi: 10.1073/pnas.94.15.8168.

Silhavy, T. J., Kahne, D. and Walker, S. (2010) 'The Bacterial Cell Envelope', *Cold Spring Harbor Perspectives in Biology*, 2(5), pp. a000414–a000414. doi: 10.1101/cshperspect.a000414.

Souzu, H. (1982) 'Escherichia coli B membrane stability related to cell growth phase', *Biochimica et Biophysica Acta (BBA) - Biomembranes*, 691(1), pp. 161–170. doi: 10.1016/0005-2736(82)90225-5.

Spigarelli, B. P. and Kawatra, S. K. (2013) 'Opportunities and challenges in carbon dioxide capture', *Journal of CO2 Utilization*, 1, pp. 69–87. doi: 10.1016/j.jcou.2013.03.002.

Spiridonov, N. A. and Wilson, D. B. (2001) 'Cloning and Biochemical Characterization of BglC, a β-Glucosidase from the Cellulolytic Actinomycete Thermobifida fusca', *Current Microbiology*, 42(4), pp. 295–301. doi: 10.1007/s002840110220.

Strauss, A. and Götz, F. (1996) 'In vivo immobilization of enzymatically active polypeptides on the cell surface of Staphylococcus carnosus', *Molecular Microbiology*, 21(3), pp. 491–500. doi: 10.1111/j.1365-2958.1996.tb02558.x.

Sylvestre, P., Couture-Tosi, E. and Mock, M. (2002) 'A collagen-like surface glycoprotein is a structural component of the Bacillus anthracis exosporium', *Molecular Microbiology*, 45(1), pp. 169–178. doi: 10.1046/j.1365-2958.2000.03000.x.

Sylvestre, P., Couture-Tosi, E. and Mock, M. (2005) 'Contribution of ExsFA and ExsFB Proteins to the Localization of BclA on the Spore Surface and to the Stability of the *Bacillus anthracis*

Exosporium', *Journal of Bacteriology*, 187(15), pp. 5122–5128. doi: 10.1128/JB.187.15.5122-5128.2005.

Tanaka, M. *et al.* (2008) 'Development of a Cell Surface Display System in a Magnetotactic Bacterium, " *Magnetospirillum magneticum* " AMB-1', *Applied and Environmental Microbiology*, 74(11), pp. 3342–3348. doi: 10.1128/AEM.02276-07.

Tanaka, T. *et al.* (2011) 'Creation of a Cellooligosaccharide-Assimilating Escherichia coli Strain by Displaying Active Beta-Glucosidase on the Cell Surface via a Novel Anchor Protein', *Applied and Environmental Microbiology*, 77(17), pp. 6265–6270. doi: 10.1128/AEM.00459-11.

Thomas, J. D. *et al.* (2001) 'Export of active green fluorescent protein to the periplasm by the twin-arginine translocase (Tat) pathway in Escherichia coli', *Molecular Microbiology*, 39(1), pp. 47–53. doi: 10.1046/j.1365-2958.2001.02253.x.

Thompson, B. M. and Stewart, G. C. (2008) 'Targeting of the BclA and BclB proteins to the *Bacillus anthracis* spore surface', *Molecular Microbiology*, 70(2), pp. 421–434. doi: 10.1111/j.1365-2958.2008.06420.x.

Tian, L. *et al.* (2019) 'A mutation in the AdhE alcohol dehydrogenase of Clostridium thermocellum increases tolerance to several primary alcohols, including isobutanol, n-butanol and ethanol', *Scientific Reports*, 9(1), p. 1736. doi: 10.1038/s41598-018-37979-5.

Tommassen, J. (2010) 'Assembly of outer-membrane proteins in bacteria and mitochondria', *Microbiology*, 156(9), pp. 2587–2596. doi: 10.1099/mic.0.042689-0.

Valls, M. and Delorenzo, V. (2002) 'Exploiting the genetic and biochemical capacities of bacteria for the remediation of heavy metal pollution', *FEMS Microbiology Reviews*, 26(4), pp. 327–338. doi: 10.1016/S0168-6445(02)00114-6.

Vinet, L. and Zhedanov, A. (2010a) 'A "missing" family of classical orthogonal polynomials', *Plastics Europe*. doi: 10.1088/1751-8113/44/8/085201.

Vinet, L. and Zhedanov, A. (2010b) ‘A “missing” family of classical orthogonal polynomials’, *Bioresource technology*. doi: 10.1088/1751-8113/44/8/085201.

Wagner, S. *et al.* (2007) ‘Consequences of membrane protein overexpression in Escherichia coli’, *Molecular and Cellular Proteomics*. doi: 10.1074/mcp.M600431-MCP200.

Wang, X. *et al.* (2018) ‘Advances and prospects in metabolic engineering of Zymomonas mobilis’, *Metabolic Engineering*, 50, pp. 57–73. doi: 10.1016/j.ymben.2018.04.001.

Westerlund-Wikström, B. (2000) ‘Peptide display on bacterial flagella: principles and applications.’, *International journal of medical microbiology : IJMM*, 290(3), pp. 223–30. doi: 10.1016/S1438-4221(00)80119-8.

Wimley, W. C. (2003) ‘The versatile β-barrel membrane protein’, *Current Opinion in Structural Biology*, 13(4), pp. 404–411. doi: 10.1016/S0959-440X(03)00099-X.

Wu, M. L., Tsai, C. Y. and Chen, T. H. (2006) ‘Cell surface display of Chi92 on *Escherichia coli* using ice nucleation protein for improved catalytic and antifungal activity’, *FEMS Microbiology Letters*, 256(1), pp. 119–125. doi: 10.1111/j.1574-6968.2006.00115.x.

Xu, Y. *et al.* (2008) ‘Surface Display of GFP by Pseudomonas Syringae Truncated Ice Nucleation Protein in Attenuated Vibrio Anguillarum Strain’, *Marine Biotechnology*, 10(6), pp. 701–708. doi: 10.1007/s10126-008-9108-7.

Xu, Z. and Lee, S. Y. (1999) ‘Display of polyhistidine peptides on the Escherichia coli cell surface by using outer membrane protein C as an anchoring motif.’, *Applied and environmental microbiology*, 65(11), pp. 5142–7. doi: 10.1128/AEM.65.11.5142-5147.1999.

Yabuuchi, E. *et al.* (1995) ‘Transfer of Two *Burkholderia* and An *Alcaligenes* Species to *Ralstonia* Gen. Nov.’, *Microbiology and Immunology*, 39(11), pp. 897–904. doi: 10.1111/j.1348-0421.1995.tb03275.x.

Yang, Y. *et al.* (2015) 'Complete genome sequence of Bacillus sp. YP1, a polyethylene-degrading bacterium from waxworm's gut', *Journal of Biotechnology*, 200, pp. 77–78. doi: 10.1016/j.jbiotec.2015.02.034.

Yang, Z. *et al.* (2008) 'Novel Bacterial Surface Display Systems Based on Outer Membrane Anchoring Elements from the Marine Bacterium *Vibrio anguillarum*', *Applied and Environmental Microbiology*, 74(14), pp. 4359–4365. doi: 10.1128/AEM.02499-07.

Zhang, K. *et al.* (2019) 'New technologies provide more metabolic engineering strategies for bioethanol production in Zymomonas mobilis', *Applied Microbiology and Biotechnology*, 103(5), pp. 2087–2099. doi: 10.1007/s00253-019-09620-6.

Zhang, Z. *et al.* (2016) 'Surface Immobilization of Human Arginase-1 with an Engineered Ice Nucleation Protein Display System in E. coli', *PLOS ONE*. Edited by M. Isalan, 11(8), p. e0160367. doi: 10.1371/journal.pone.0160367.